Villanova University

Department of Civil and Environmental Engineering

Graduate School

WATER QUANTITY STUDY OF A POROUS CONCRETE INFILTRATION BASIN BEST MANAGEMENT PRACTICE

A Thesis in

Civil Engineering

by

Tyler C. Ladd

Submitted in partial fulfillment

of the requirements

for the degree of

Master of Science in Water Resources

and Environmental Engineering

June 2004

WATER QUANTITY STUDY OF A POROUS CONCRETE INFILTRATION BASIN BEST MANAGEMENT PRACTICE

By

Tyler C. Ladd

June 2004

Robert G. Traver, Ph.D., P.E. Associate Professor of Civil and Environmental Engineering	Date
Andrea L. Welker, Ph.D., P.E. Assistant Professor of Civil and Environmental Engineering	Date
Ronald A. Chadderton, Ph.D., P.E. Professor and Chairman, Department of Civil and Environmental Engineering	Date
Barry C. Johnson, Ph.D. Dean, College of Engineering	Date

Acknowledgements

First and foremost I would like to thank my Mom for her love and support and for believing in me. I'd like to thank my brother and sister for letting me be the smartest one of us. Thanks to Dad and Shirley for always listening and giving me advice about the real world. Thank you to Grandma and Grandpa for always being there. Thanks to Waldo for remembering me whenever I go home and to Gizmo for clawing my arms and legs and eating my food whenever I go in the other room.

A tremendous thank you to my advisor, Dr. Robert Traver, for giving me this great opportunity and to Dr. Andrea Welker for helping me with this thesis and also to the rest of the faculty for letting me hang around for two more years.

Thanks to my roommate Adrian for playing loud music when I was trying to write this and for the Jesus action figure. A huge thanks goes out to Mike Kwiatkowski for putting up with me over the past two years and carrying the bike pump. Don't worry; someday you'll lift the heavy weights. A big thanks to Clay Emerson for the belief and drive to do things right the first time, despite what we said, and for always winning the beard of the week award, except that one time we had that guest speaker. A big thanks to Matt, Jordan, Erica, Greg, CJ, Mike, and Ryan for putting up with me pretty much since you met me.

Thank you to Linda and Margie who were always there telling me to do the right thing and letting me hang out in the office instead of doing work and to George Pappas for always being there to help build something or kill time when we should have been working.

Abstract

The focus of this research is to evaluate the hydrologic effectiveness of a Porous Concrete Infiltration Basin Best Management Practice (BMP) and to develop and assess the modeling techniques used in this evaluation. The effectiveness of the BMP is measured by determining the amount of runoff captured and infiltrated on a storm event basis.

Increased stormwater runoff from changing land use and its adverse effects on the environment has become a growing concern over the past few years. The traditional practice of mitigating the peak flow solely through detention has proved to be an ineffective means of stormwater management (Traver and Chadderton 1983; McCuen and Moglen 1988; EPA 2002). To help remedy this situation, new practices and techniques, termed BMPs, are being developed which use innovative approaches when dealing with stormwater. Approaches such as infiltration, in addition to more effective use of conventional detention designs, are helping to mitigate the problems caused by stormwater.

In the summer of 2002, the common area between two dormitories on the campus of Villanova University was retrofitted to create a Porous Concrete Infiltration Basin BMP. The area previously consisted of an asphalt roadway with curbs and concrete walkways for pedestrians. The retrofit consisted of three infiltration beds overlain with porous and standard concrete and ringed by stone paving stones. The site is designed to collect and infiltrate stormwater runoff from the surrounding buildings, grass areas, and walkways. The building rooftops are connected directly to the infiltration beds through pipes. Runoff from the standard concrete walkways or grass areas is directed onto the

porous concrete where it passes through to the infiltration beds. Runoff leaves the site either through infiltration or overflow. When the water level in the lower infiltration bed reaches a height of 18 inches, the water exits through an overflow pipe into a catch basin. The site is instrumented to record rainfall, water elevation in the infiltration beds, and outflow from the site. Data from these instruments were used to evaluate the effectiveness of the site and the accuracy of the model.

Two computer models of the site were developed, one for small storm events and one for larger events, using HEC-HMS, a hydrologic modeling program developed by the Army Corps of Engineers (HEC 2001). Results from the models were compared to a set of recorded storm event measurements for calibration. Another group of storms was then used to validate the models' accuracy. The effectiveness and accuracy of the models were measured by comparing the model outputs with observed water surface elevation data. It was found that smaller storm events could not be modeled accurately due to questionable applicability of SCS Methods and initial losses occurring in the infiltration beds. The model results for larger events became more accurate as each storm event progressed, further emphasizing the impact of initial losses.

Recommendations regarding the proper installation and use of porous concrete as well as future research possibilities are included at the end of this study. The initial loss rate from the BMP was identified as a primary direction for future research. The lessons learned from this study will hopefully encourage the proper use of porous concrete and the implementation of similar types of BMPs.

Table of Contents

List of Figures

List of Tables

Chapter 1: Project Overview

Introduction

The focus of this research is to evaluate the hydrologic effectiveness of a Porous Concrete Infiltration Basin Best Management Practice (BMP) and to develop and assess the modeling techniques used in this evaluation. The companion to this thesis is Kwiatkowski (2004), which looks at the study site from a water quantity aspect. The site is a pedestrian area in the middle of Villanova University's campus. The site design includes three underground infiltration beds overlain with porous concrete, regular concrete, and paving stones. The rooftop gutter collection system is directly connected to the three beds through underground pipes. The infiltration beds were designed to capture and infiltrate the first 2 inches of all rainfall events. Excess runoff exceeding the capacity of the infiltration beds exits the site through the original storm sewer system. Sixteen storm events were recorded using a tipping bucket rain gage over a nine-month period. Thirteen of these events were used to create and calibrate the hydrologic model of the site and three were used for verification. The success of the calibration was based on how well the model reproduced the water surface elevations obtained from instrumentation located in the lower infiltration bed. One storm event overflowed from the site during the course of this study. This event included significant snowmelt and was therefore not used. Aside from that one event, the site was successfully able to store and infiltrate all storm events that occurred throughout the duration of this study. The outcome of the modeling was not as successful, though it did identify a direction for future research possibilities.

Model Development

Based on the physical and hydrologic characteristics of the site, computer models were created to mimic what was occurring in the infiltration beds. These models helped to better understand how the site captured and infiltrated surface runoff. The models also emphasize the need for more accurate information from a greater variety of locations throughout the site. The Villanova Porous Concrete Infiltration Basin BMP is the result of years of establishing guidelines and refining techniques for the proper design and use of large scale infiltration basins for managing stormwater runoff. Through the use of new materials and proven methods, the BMP accomplishes its goal of capturing and infiltrating the first 2 inches of rainfall events. This is close to 80% of the total rainfall volume for this region (Prokop 2003). Another valuable purpose of the BMP is its use as a demonstration site. It helps to educate and further peoples' understanding of these systems and how they operate.

Background

The urbanization of natural areas has been a major environmental problem for a long time. Urbanization destroys the natural wooded and grass areas and replaces them with buildings, parking lots, and roadways, thus increasing the amount of impervious coverage in a watershed and changing the hydrology of the site. Lee and Heaney (2003) state that impervious cover has serious impacts on the health of a watershed and taxes the storm water system designed to handle it. Impervious cover prevents water from infiltrating into the ground (Lawrence et al.1996), thereby decreasing baseflow to streams and rivers (Barbosa and Hvitved-Jacobsen 2001). This lack of baseflow lowers the normal flow and elevation of the stream.

Runoff makes its way quickly through impervious collection systems such as gutters, along curbs, and through storm sewers channels. During storm events, runoff velocity of flow and peak flows are increased. These increased flow rates and volumes cause erosion in the streambed and banks. This erosion not only has an adverse effect on the stream where it is occurring, making it deeper and wider, but downstream as well. The eroded particles travel downstream, getting deposited in slow moving areas of the stream (Moglen and McCuen 1988). This causes these slow moving areas, such as pools or bends in the stream, to become filled with sediment. This not only affects the health of the stream but also the wildlife living in the stream. Flows running off of heated impervious areas increase the temperature in streams, decreasing the quantity and diversity of organisms in the stream habitat. Increased volumes and flows to streams also increases the occurrence and severity of flash flooding. Beighley and Moglen (2002) prove that with an increase in urbanization, there is an increase in the flood frequency. Because there are no longer any natural barriers to slow the flow of runoff and decrease its volume, large quantities of water are rapidly introduced into stream and storm sewer systems, exceeding their design capacity. Since the streams are already at capacity and the water cannot infiltrate, flooding becomes an ever-increasing problem when upstream areas are urbanized.

Throughout the 1960's and early 1970's, increased public concern and awareness over the control of water pollution led to the Federal Water Pollution Control Act Amendments of 1972, more commonly known as the Clean Water Act. These amendments completely changed the original law enacted in 1948. That law was based on the River and Harbor Acts of 1890 and 1899, which focused on the unauthorized

alteration of navigable waters (FEMA 2004). Although the original Clean Water Act of 1972 dealt primarily with pollutant discharge and municipal sewage treatment plant construction, the Act laid the groundwork for the legislation that would follow. In 1978, the state of Pennsylvania passed the Storm Water Management Act, known as Act 167 (Lathia 2004). The purpose of the act was to address stormwater-flooding concerns and to address solutions and stormwater planning from a watershed management basis, not through the conventional method of county or municipal boundaries. The two major requirements of Act 167 were that individual counties develop their own Watershed Stormwater Plans. These plans would require a watershed hydrologic and hydraulic evaluation. These evaluations would take into account existing problems as well as the impact of future watershed conditions and changes. The plans would also include any obstructions to waterways or drainage problems within the watershed. Criteria for the control of stormwater runoff as well as any existing or proposed stormwater collection systems would also have to be included in the watershed plan (Lathia 2004). The Act also required that developers, not municipalities, implement stormwater controls and BMPs as part of their stormwater management plan. The Act states that the maximum rate of runoff (peak flow) following development can be no greater than the runoff rate prior to development. It also says that the stormwater runoff must be managed in such a way that health and property are adequately protected from injury.

Conventional methods of stormwater management in this period involved capturing and temporarily storing runoff from storm events. Runoff from entire sites was collected in a single detention basin, generally located at the lowest elevation on the site, through pipes or over land through grass channels or swales (Traver and Chadderton

1983). The stored runoff was then allowed to outflow from the basin at a controlled rate, typically to receiving waters such as streams, or it was occasionally discharged as overland flow. As time passed and more studies and research were done into the effects of these approaches, it was realized that these methods were not the most effective at dealing with stormwater (McCuen and Moglen 1988). These traditional methods did not consider a number of factors that are crucial to stormwater management today. These methods dealt with attenuating the peak flow of the hydrograph to recreate the pre-construction peak flows. Very little attention was paid to the increase in total volume of runoff or duration of peak flow that was entering the receiving waters and what impact it would have on the morphology of the stream. There was a tremendous loss in the amount of infiltration that was occurring on the newly developed site, thus decreasing groundwater recharge. If infiltration was occurring in the detention basins, it was usually coincidental and not part of the basin design. Evapotranspiration is also reduced as the amount of vegetated areas decreased (USEPA 2002), further impacting the natural hydrologic cycle.

Another component of the 1972 Clean Water Act is the National Pollutant Discharge Elimination System (NPDES). This system is a permitting program that regulates point source pollutant discharge into surface waters. Phase I of the program was established in 1990. Phase I focuses on stormwater runoff from medium to large municipal separate storm sewer systems (MS4's), construction activity disturbing five or more acres, and certain industrial activities. With the success of Phase I, Phase II was enacted in late 1999. It was the next step in expanding the existing program to protect the nation's water resources. Phase II focused on addressing stormwater discharges from

small MS4's and on construction sites that disturbed over one acre (USEPA 2003). Sites over five acres already required permits from Phase I. Phase II also required the use of structural and non-structural Best Management Practices for new construction in populated areas. It also required the use of BMPs as volume and quality controls.

To help remedy the continued effects of urbanization as well as the ineffectiveness of conventional stormwater treatment facilities, innovative stormwater management practices are being developed. Through the use of new and innovative designs and BMPs, watersheds are dealing with stormwater management more efficiently and in environmentally friendlier ways than ever before. The passage of the Clean Water Act and its subsequent amendments, along with Act 167 in Pennsylvania, brought the use of BMPs to the forefront of thinking when dealing with stormwater runoff problems. The need to use infiltration to control stormwater runoff has been recognized since at least 1991 (Whipple 1991). Mikkelesen et al. (1996) further studied the developments in infiltrating stormwater runoff infiltration. Based on this and other work, the EPA now encourages recharge of groundwater through infiltration. It recognizes many types of infiltration BMPs that have different advantages and disadvantages (USEPA 2002). Large-scale infiltration basins can serve large areas, but must be maintained. Smaller infiltration trenches can be placed in medians or other unused areas of a development site, but also require maintenance and need permeable soil. Porous pavements provide runoff control without the need for extra land. They are best suited for lightly trafficked areas and also require maintenance to keep flow pathways clear. The two major types of porous pavement are porous asphalt and porous concrete. Porous asphalt was developed in the 1970's at the Franklin Institute in Philadelphia, PA (Adams 2003). The use of

porous concrete has been around for quite some time as well. Research into the material has been underway since the early 1980's (Field et al. 1982). Studies are underway to see if these new methods are successful at mitigating the peaks flows and total volume of high frequency storm events. One investigation by Nehrke and Roesner (2004), studied the effects of flood control design and the use of BMPs on the flow-frequency curve. It found that, for the two cases studied, traditional detention storm design development does not produce a post development flow-frequency curve that matches the predevelopment for storms smaller than the 2-year storm.

The effectiveness of a BMP can vary greatly. It can depend on how well the BMP was designed and for what purpose. The condition of the watershed surrounding the BMP and the need for any maintenance on the BMP itself can also affect its performance. Studies into the effectiveness of various BMPs have been going on for years. Strecker et al. (2001) state that the effectiveness of a BMP cannot only be measured, but that the data gathered from a particular site can be applied to similarly designed BMP systems.

Stormwater management systems need to be designed for a certain range of storm events. They also need to focus on the volume produced from smaller storms. Because the majority of storms, approximately 80%, have precipitation of 1 inch or less, systems are being designed to focus on these smaller storms. Konrad and Burges (2001) contend that single-purpose systems with small reservoirs can be effective for a variety of flows. Judgment is still out on the effectiveness of BMPs while research studies are being conducted. In some cases, improperly designed BMPs can harm waterways as much as conventional stormwater treatment (Roesner et al. 2001).

As with any new technology or change in thinking, some resistance will be encountered. Many land developers and engineers are hesitant to use BMPs in their designs and on their properties for a variety of reasons. Slowly, people are coming around to the fact that BMPs do in fact work. This has been shown through the increase in the variety of designs and the more widespread usage of BMPs. There have been many approaches recently to lower the perceived cost of these systems. One approach is to offer stormwater credits. A credit system gives developers and designers' incentive to implement better site design that has less impact on the surrounding water resources. The advantage to developers is that the use of credits translates directly to a savings in cost by reducing the size of stormwater storage and conveyance systems (Stormwater Manager's Resource Center 2003). Because cost is a major factor in deciding whether to implement BMPs, another method of controlling stormwater runoff is through the use of tradable allowances within watershed boundaries (Thurston et al. 2003). However, the situation is improving. The East Clayton Stormwater Infiltration System, for example, was designed using many of these techniques and approaches (Dumont 2003).

Chapter 2: Study Site

Site Description

The Porous Concrete Infiltration Basin BMP is located on the east end of Villanova University's main campus. Villanova University is located approximately 20 miles west of the city of Philadelphia in southeast Pennsylvania. The BMP is located in a heavily traveled common area of the campus situated between two dormitories, Sheehan and Sullivan Halls. The watershed consists of concrete walkways, patios, green spaces, and building rooftops as shown in Figure 1.

Figure 1: Overhead photo of site

Traffic on the site is predominantly pedestrian. This area acts as the main corridor for campus for students going to class or their dormitories. The site does experience some light vehicle traffic at the beginning and end of each semester as

students move in and out of the adjacent dormitories. University maintenance and grounds keeping vehicles as well as campus security and emergency vehicles are also periodically seen in and around the site.

The drainage area for the BMP is 57,700 square feet, and 35,850 square feet, or 62% of that is impervious. The impervious areas consist of portions of the dormitory rooftops, concrete walkways, part of an asphalt driveway at the upper end of the watershed, the paving stone border around the porous concrete, and the traditional concrete areas surrounded by the porous concrete as shown in Figure 2. Of the remaining area, 34%, or 19,700 square feet is pervious. This consists of the grass areas located in front of and along the sides of Sheehan and Sullivan Halls. Porous concrete comprises the remaining 2,150 square feet.

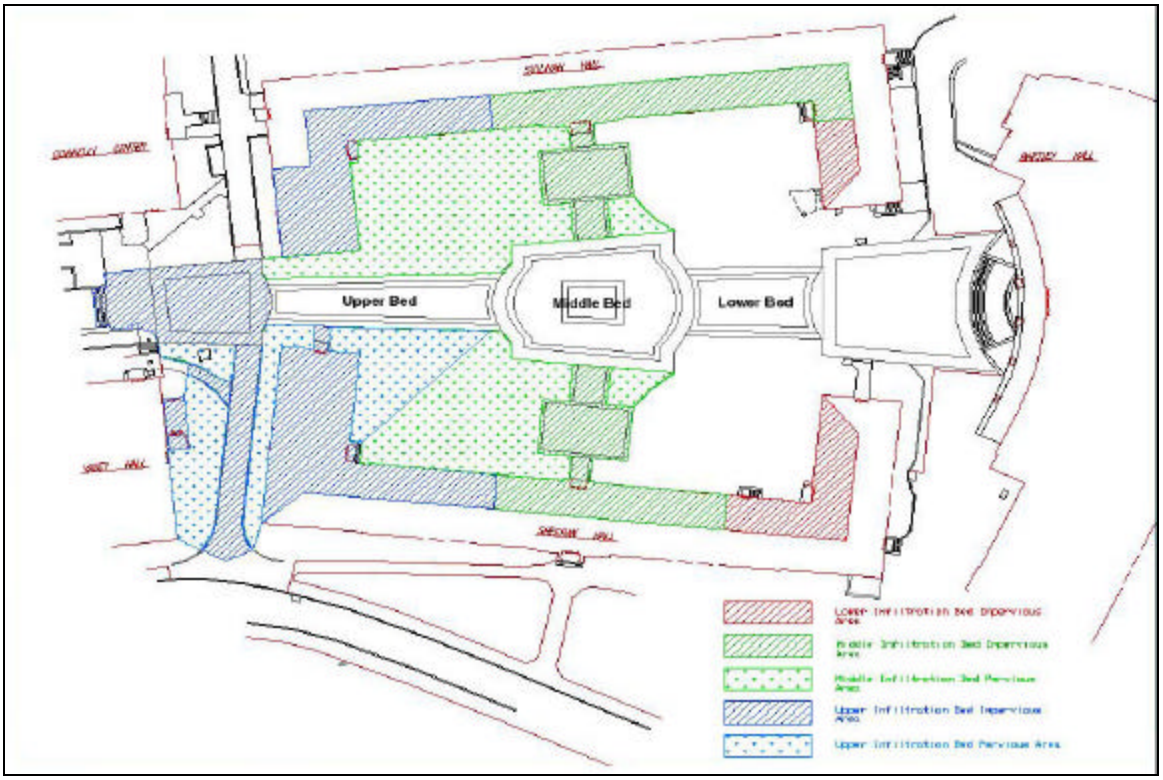

Figure 2: Layout sketch of the site

Site Design

Cahill Associates of West Chester, PA (Cahill 2003) completed the hydrologic design for this site in 2001. Cahill conducted percolation tests in mid-September with a finalized design being completed shortly thereafter.

The Porous Concrete BMP consists of three large rock infiltration beds arranged in a cascading structure down the center of the site (Figure 3). The beds are overlain with areas of traditional concrete ringed by porous concrete and non-porous paving stones. The porous concrete itself primarily acts as a transportation medium, allowing runoff on the surface to find its way into the infiltration beds underneath. The rooftop gutters of the adjacent dormitories also drain to the infiltration beds. The downspouts from these gutters are connected to 4-inch High Density Polyethylene (HDPE) pipes which are in turn connected directly to the three infiltration beds.

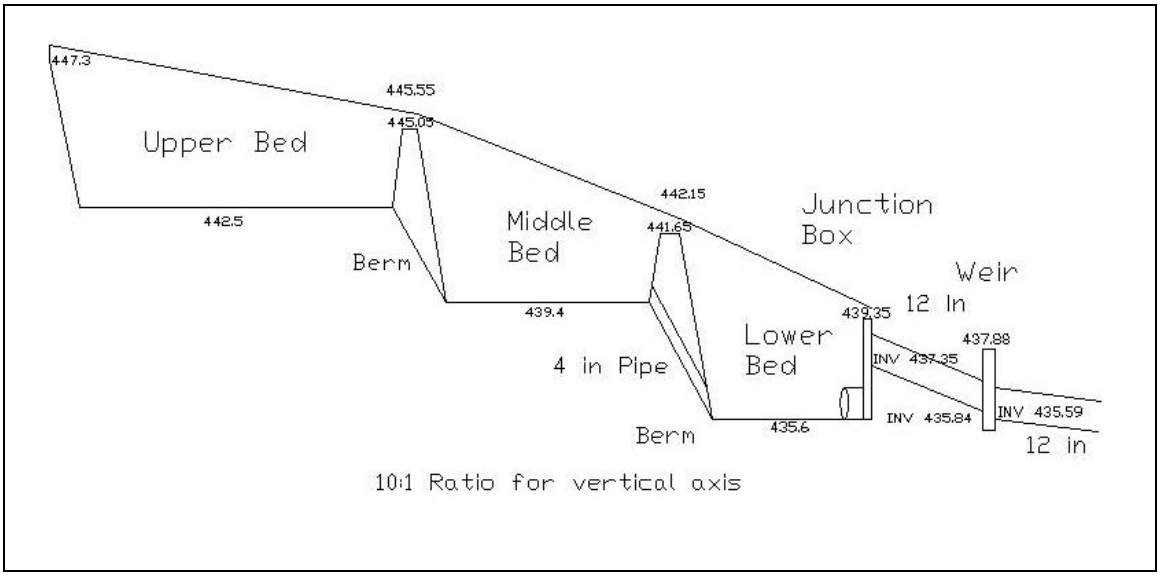

Figure 3: Water surface profile of infiltration beds

A slot drain located near the top of the site and a storm drain inlet near Sheehan Hall connects to the upper infiltration bed through a series of 8-inch HDPE pipes. The slot drain captures runoff from the concrete area at the top of the site while the storm drain inlet was designed to capture runoff from the driveway and areas next to the building. The grate of the inlet is currently too high, causing runoff to bypass the inlet.

Each bed is between 3 and 4 feet deep and is composed of a number of different layers and materials. Directly above the undisturbed native soil is a layer of geotextile filter fabric. This layer provides separation between the stones and soil to prevent any upward migration of the soil. Above the filter fabric is 3 feet of American Association of State Highway and Transportation Officials (AASHTO) No. 2 course aggregate stone. These stones have a diameter of 3 to 4 inches. Figure 4 shows the course aggregate stones on top of the filter fabric for the middle infiltration bed.

Figure 4: Infiltration bed under construction

Located on top of the course aggregate are one to 3 inches of AASHTO No. 57 choker stone. These smaller diameter (2 to 4 inches) stones provide a solid base for the porous concrete and prevent the porous concrete from falling into the void spaces of the larger stones during pouring. The uppermost visible layer consists of 6 inches of porous concrete. A 4-inch HDPE pipe connects the bottoms of the lower two infiltration beds. This allows water to travel down from the middle bed to the lower bed. There are also two 6-inch HDPE pipes, which run along the top of all three beds, directly below the choker course. These pipes allow excess water, once bed capacity is reached, to travel down to the bottom of the site and into the existing storm sewer system. This reduces the

risk of water popping up through the porous concrete. Figure 5 shows a cross section sketch of an infiltration bed.

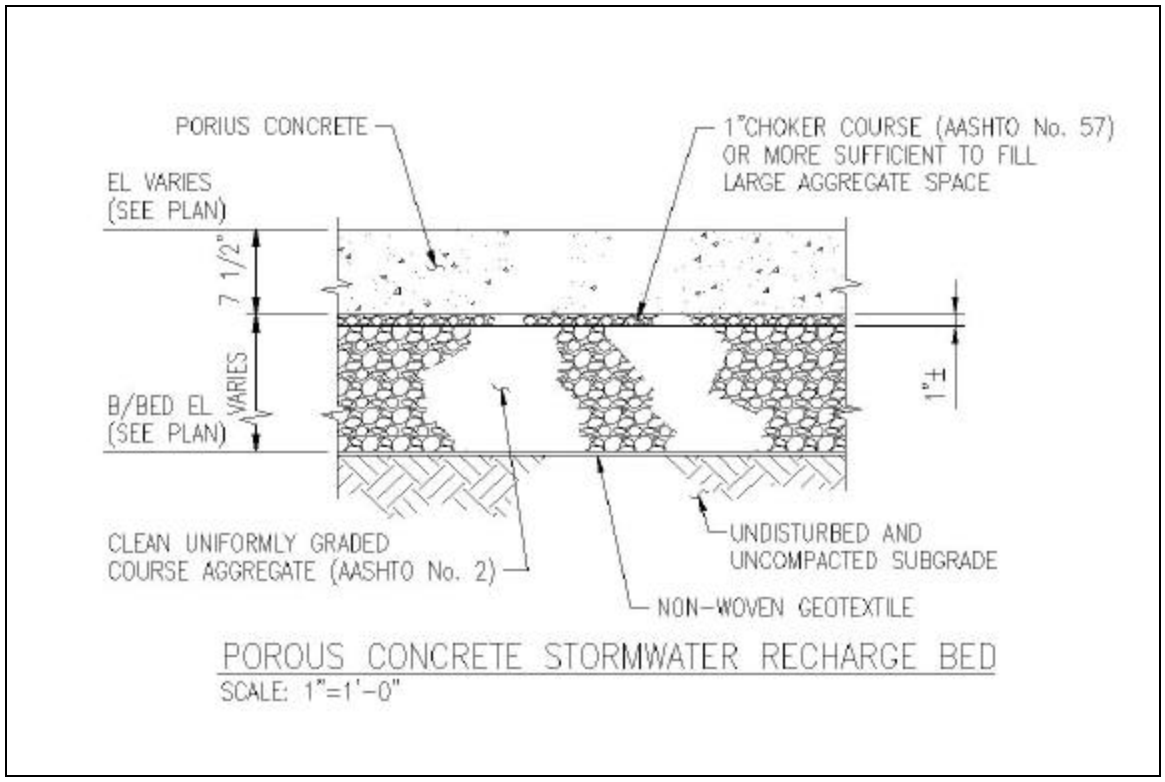

Figure 5: Cross section of an infiltration bed

The original design of the site called for the entire area above the infiltration beds between the paving stones to be porous concrete. The redesign, which will be discussed further in the section on reconstruction, called for a smaller area of porous concrete. A strip of porous concrete between 3 and 4 feet wide inside the paving stone border was determined to be sufficient. This was because the flow rate of water through the porous concrete was high enough that this smaller area could be used to capture the runoff.

The site was designed to store and infiltrate runoff the first 2 inches of a storm event through the use of the three infiltration beds. Storms of this size represent

approximately 80% of the annual storm events for this region (Prokop 2003). Storms with a volume of runoff greater than the beds were designed for would still have the first portion captured during the storm event. Excess water would leave the site through the existing storm sewer system by means of an overflow pipe. This pipe is located in a junction box that is directly adjacent to the lower infiltration bed in the bottom corner. The junction box serves as an intersecting point for pipes coming from the rooftop gutters and the lower infiltration bed (Figure 6). Overflow from the beds leaves through the overflow pipe that discharge the water into the existing storm sewer system.

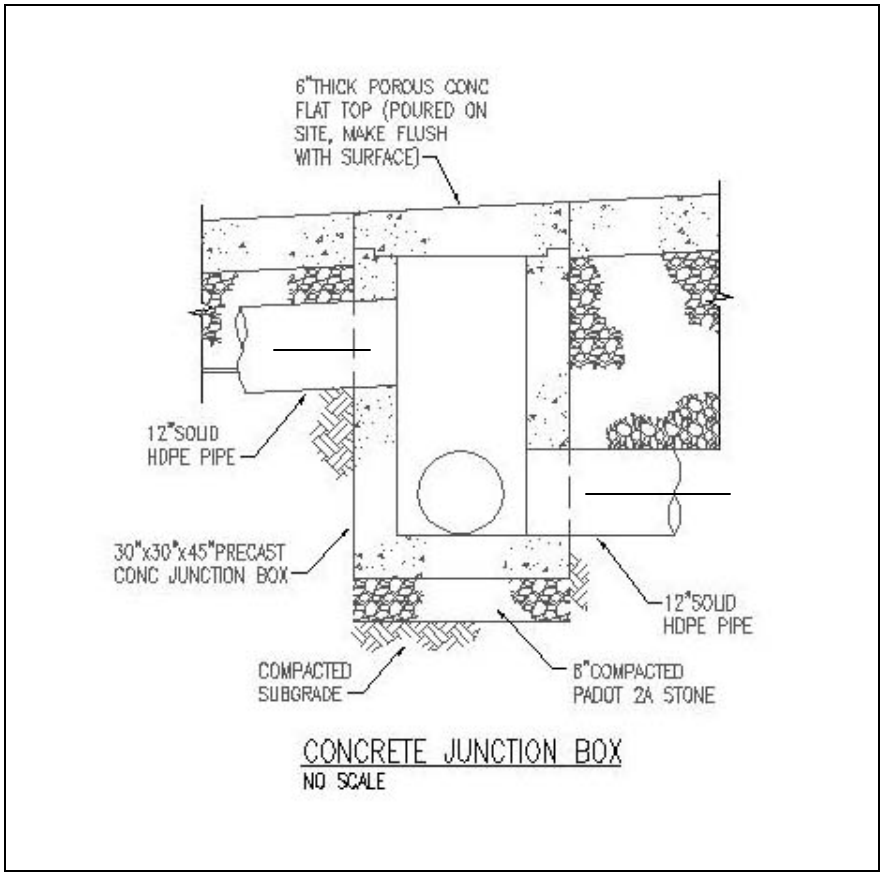

Figure 6: Sketch of junction box

Chapter 3: Construction

Construction on the site began on May 20th, 2002, immediately following Villanova University's graduation ceremonies. N. Abbonizio Contractors, Inc. of Conshohocken, PA were the contractors. The first phase of the construction process involved removing the existing asphalt pavement roadway, curbing, and concrete sidewalks and entrance walkways (Figure 7).

Figure 7: Original site before construction

This work was completed during the first week of June. The boundaries of the infiltration bed closest to Bartley Hall were marked out and the bed was excavated to the required depth and dimensions. This process was repeated for the middle infiltration bed during the second week of June. A 4-inch HDPE pipe was run through the berm

connecting the two infiltration beds and the geotextile filter fabric was then laid across the bottom and sides of the lower bed. The junction boxes, as mentioned in the previous section, were installed in the lower corners of the bottom infiltration bed as shown in Figure 3 and Figure 8.

Figure 8: Junction box

These boxes provide a junction for the pipes from the gutter downspouts, pipes inside the lower bed, and outflow pipe from the BMP to the existing storm sewer system. Inside the bed, two 12-inch HDPE pipes were laid along the bottom of the lower bed and connected to the junction boxes. These are used to disperse the water across the whole area of the bed. The bed was then filled with the AASHTO No. 2 stones to a depth of approximately four feet. The geotextile filter fabric was then placed in the middle infiltration bed and

two 10-inch HDPE pipes were placed on top of that. The bed was then filled with AASHTO No. 2 stones to the same depth of approximately 4 feet. Figure 9 shows the middle infiltration bed during construction. The construction of the beds was sequenced so that no heavy equipment came in contact with the undisturbed soil, thus protecting it and preserving its infiltration capacity. The beds were excavated from the sides and no equipment passed over the bottom until each bed had been filled with the AASHTO No. 2 stone. These stones absorbed and dispersed the weight of the vehicles in such a way that no compaction of the underlying soil occurred.

Figure 9: Middle infiltration bed under construction

The upper infiltration bed was excavated and filled in the same manner. The only major difference in the construction of the bed was there was no pipe placed in the berm

connecting the upper and middle beds. The pipes laid along the bottom of the bed were 8- inch HDPE and had connectors for the pipes coming from the gutter downspouts (Figure 10).

Figure 10: Upper infiltration bed mid-way through construction

At the same time as the three infiltration beds were being constructed, work was underway to connect all of the building's downspouts to the infiltration beds. Trenches were dug in front of the two dormitories and HDPE pipes were laid. Four-inch pipes were connected directly to all of the downspouts and ran the length of the buildings as shown in Figure 11. Six-inch and 8-inch pipes connected the 4-inch pipes directly to the larger pipes already covered by stone in the infiltration beds. A 4-inch pipe was used to

connect the downspout from part of the Sullivan Hall roof near Bartley Hall directly to the junction box in the lower bed that allows overflow from the site.

Figure 11: HDPE pipes connecting downspouts

Once the three infiltration beds were filled with the No. 2 stones, a one to three inch layer of AASHTO No. 57 choker stone was laid over the three beds and the two earthen berms. These smaller diameter stones provide a stable base for the porous concrete and prevent it from falling into the large void spaces of the AASHTO No. 2 stones.

A steel rebar reinforced concrete base for the paving stones was laid around the outer edges of the infiltration beds and in the center of the middle infiltration bed. This

base was poured on top of the choker stone layer. The base gives a solid, flat surface for the paving stones to rest on and to prevent the stones from moving in the event the rocks below settle.

Figure 12: Overflow pipes being installed

An 8-inch deep trench was dug into the choker stone layer and two 6-inch HDPE overflow pipes were laid and then covered (Figure 12). These pipes collect water when the beds are full and transport it to the lower portion of the site where it is discharged through the existing storm sewer system.

Pouring of the porous concrete began on the last day in June 2002. Wooden bracing was laid to act as a framework for the concrete. The original design called for the entire area between the paving stones to be porous concrete. To help strengthen the

concrete, an additive called Eco-Creto (Eco-Creto 2004) was used. The Eco-Creto was mixed with the porous concrete while it was still in the truck. Approximately 3 gallons of Eco-Creto was added to each yard of concrete. A traveling vibratory screed was used to spread and compact the concrete. It proved to be too cumbersome and ineffective at achieving the level of compactness required. A hand tamper was then used to compact the concrete, which worked, but proved to be too slow.

Figure 13: Plastic sheets covering the porous concrete

The workers were unable to keep pace with the concrete being poured. Finally, a vibrating push tamper was modified with a larger bottom plate. This tamper followed the screed and finished the concrete. This provided an adequate surface and was able to keep pace with the rate of pouring. At the end of the day of pouring, after the concrete was

compacted, large sheets of plastic were laid over the surface (Figure 13). These sheets were used to allow the porous concrete to properly hydrate while it was curing. The sheets were held down with stones, pieces of wood, buckets, and pieces of steel rebar found lying around the site. This proved insufficient as some areas were left exposed and were not able to set properly. Pouring of the other two beds progressed in much the same fashion. There were delays throughout the pour due to problems with the porous concrete material. On some days there were minor problems and work progressed satisfactorily. On others, bad truckloads meant that only a small area could be successfully poured. Pouring of all the porous concrete areas was completed by the middle of August. Patching was required for areas that did not cure properly (Figure 14). These areas were removed and replaced with a fresh batch of porous concrete.

While the pouring of the porous concrete was progressing down the site, work had begun on laying the paving stone border. The traditional concrete area at the top of the site had already been poured and was ringed with the paving stones first. The stone border was then begun around the porous concrete, which was already dry. The paving stone installers were two days behind the workers pouring the concrete. This allowed time for the concrete to set as to not interfere with the placement of the paving stones.

Figure 14: Patching of failed areas

The traditional concrete walkways leading up to the two dormitories had been partially poured before work with the porous concrete began. The large pads directly in front of each building were framed and poured approximately three weeks prior to the porous concrete. Because the pads were relatively out of the way, this allowed the contractors to focus on the porous concrete. The sections of concrete connecting the larger pads to the paving stone border were poured after work with the porous concrete was finished.

After all the traditional concrete areas had been poured, final touches to the site were completed. The most extensive of these was the final landscaping of the area. Small trees were planted and sod was placed over the exposed soil. The sod helped control erosion of the bare soil. Chain link construction fences were taken down and the entire site was washed to remove any remaining debris. Filter fabric collection devices were placed under storm drain grates to collect the debris that would have otherwise made its way into the storm sewer system. Blue plastic fencing was placed around the newly planted areas to prevent students from walking on them. The landscaping and fencing are shown in Figure 15. The protective fence remained in place for another two months until the end of October.

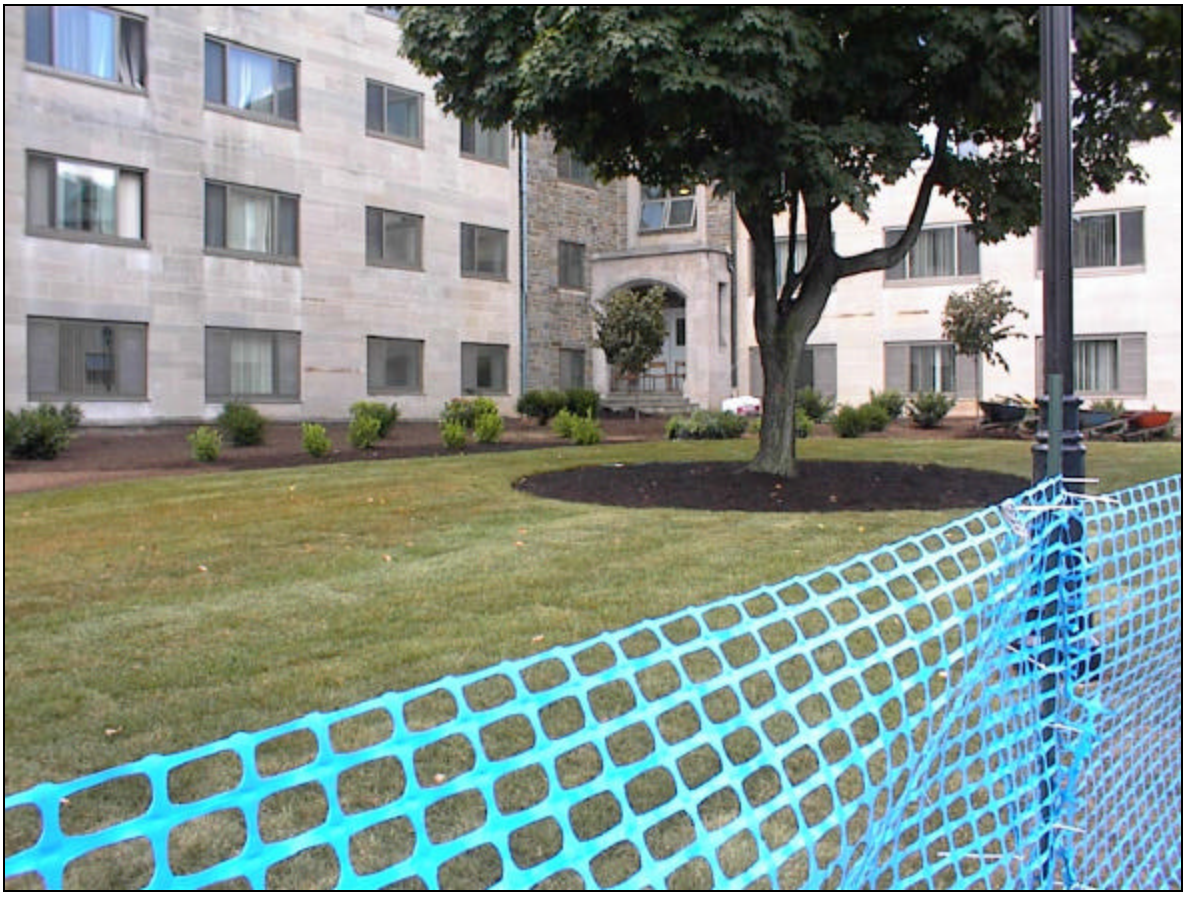

Figure 15: Fencing and landscaping following construction

Re-Construction

Due to large-scale failure of the initial pour, re-construction of the porous concrete was required by the following summer. Within a month of completion of the original construction, the porous concrete surface had already begun to fail in numerous spots. In fact, spalling was occurring in some spots immediately following construction. By the time the problem was bad enough to require attention, classes had already begun so there was little that could be done to immediately rectify the situation. Within six or seven months of the completion of construction, the entire surface had failed and was little more than loose gravel for the first few inches of depth (Figure 16).

Figure 16: Failed porous concrete surface

There are believed to be many reasons why the concrete failed after the initial construction attempt. The major reason for the failure was the lack of knowledge and understanding about the porous concrete material itself and how to successfully work with it. Environmental factors also contributed to the failure. When pouring began on the original construction, at the end of July, this region was in the middle of a severe heat wave. The increased temperatures caused the concrete to set faster than anticipated. There was also variation in the material from truck to truck. In some instances, the material sat in the trucks for almost 2 hours before being poured. In others, it was mixed and poured right away. To combat the high temperatures, the concrete plant added a retardant to the loads to slow the reaction time. The contractors were not aware of this and therefore could not adjust accordingly. It was also found after construction that the stone aggregate used was not washed correctly, leaving fine particles that absorbed water, changing the water cement ratio. The concrete was originally supposed to be spread and compacted using a traveling vibratory screed. This proved to be cumbersome and ineffective. It was determined later that the concrete could be rolled to improve the desired appearance. The curing of the concrete was ineffective. Large sheets of plastic were laid 15 to 20 minutes after compaction. The sheets were poorly secured, which led to large exposed areas. This prevented the concrete from properly hydrating. The overlying theme in the failure of the original construction was that the workers involved in the concrete installation process were unfamiliar with the material, and variations in the material prevented the corrective action from taking place.

One fact that was learned from the original construction was that the porous concrete was extremely porous. Based on the results of a flow rate test and field

observations, the rate of water intake was extraordinary. An apparatus was devised, Figure 17, which mimicked extreme rainfall. When water began to pond on the porous concrete surface, the flow rate was recorded at 12 ft/sec.

Figure 17: Flow rate test apparatus

Based on this data, it was determined for the new pour; a smaller area of porous concrete would be sufficient. A three to four foot wide strip around each of the beds, just inside the paving stone border would be adequate. The remaining area inside these porous concrete areas was filled with traditional concrete. This concrete would be crowned to direct runoff onto the porous concrete strips. It was also learned that rolling the concrete would provide the best compaction and surface appearance. To accomplish this, a 50 gallon drum roller was used that when filled with water, gave the desired finish. The

roller also worked well because the new pour was narrow enough to allow the roller to compact the entire strip at once (Figure 18). The strips also made it much easier for the concrete to be covered effectively with the plastic sheets.

Figure 18: Drum roller on porous concrete strip

The re-construction began on May 19, 2004. The upper bed was re-constructed first. Leaving the other two beds intact allowed the contractors to move equipment in and out of the site. The first stage of the process involved removing the old, failed porous concrete. This was done while leaving the paving stone border intact. Although the top few inches of the porous concrete had turned to gravel, the bottom few inches remained solid. A backhoe with a jackhammer attachment was therefore needed to completely break-up the concrete (Figure 19).

Figure 19: Broken concrete prior to removal

The failed concrete was then removed and the choker stone layer was re-leveled for the new pour. Wooden framework for the pour was laid first. This acted not only as a mold for the porous concrete but also as a rail for the drum roller. On the day of the actual pour, the weather was favorable. It was cloudy, around 70 degrees, with a light rain falling at times. This turned out to be advantageous because the rain kept the roller wet, preventing the concrete from sticking to it. Water and the Eco-Creto additive, which was again used to add strength to the material, were added on-site. This allowed complete control over the consistency of the material. Every worker had an assigned job that they were responsible for before pouring began. This allowed the pouring to proceed quickly

before the material had a chance to set. Immediately after the concrete was poured and hand-leveled, it was compacted by the drum roller to the desired thickness (Figure 20).

Figure 20: Porous concrete being poured and rolled

The concrete was then immediately covered and properly secured. Three sides of the upper bed were poured on the first day. The remaining side was purposely left open so that the concrete trucks could get in to pour the traditional concrete, without having to drive over the porous concrete. This fourth side became the first part of the middle bed pour. The traditional concrete was poured while the porous concrete from the middle bed was being removed. The porous concrete pouring process was repeated for the middle bed over a two-day period. The weather was again favorable so everything proceeded as planned. One truckload of porous concrete during the middle bed pour was

unsatisfactory. It was speculated that the concrete plant failed to add cement to the truck so the aggregate was not binding together. The problem was recognized and the load was not used.

The re-construction continued in this manner for the next week. It was completed on May 30, 2003. There were no sections which needed to be re-poured or patched. The final surface met expectations for compaction and appearance (Figure 21). General feelings were that the re-construction was a success.

Figure 21: Completed re-construction

One year later, some areas of the new pour are in need of repair. It is speculated that the freeze and thaw process had an effect on some of the areas that were not as porous as hoped. Some of these non-porous areas may have held water, which froze,

causing the stones to break apart. This is currently under review by the contractors and Villanova University's Facilities Management Department.

Chapter 4: Modeling Overview

Introduction

Water quantity instruments were installed to support the development of a hydrologic computer model of the site. Due to the layout of the runoff collection system, there were many monitoring challenges present at the beginning of the project. The inflow pathways include a slot drain, a storm drain at the top of the site, fourteen downspout connections, and the porous concrete surface itself. Runoff exits the infiltration beds through both infiltration through the bed bottom and, if the storm event is large enough, overflow into the storm sewer system. Overflow occurs when the water surface elevation in the lowest infiltration bed reaches 18 inches in the junction box (Figure 6). Once the water reaches this height, it exits through a pipe into a catch basin located directly downstream from the infiltration beds. Based on experience and observations, only large storm events over two inches or multiple storm events occurring successively causes the water surface elevation to reach the 18 inch height. Because of the multiple flow pathways entering the BMP, obtaining a directly measured inflow was not feasible. Instead, it was decided to create a hydrologic computer model of the site. This model, once calibrated and verified approximates the amount of runoff entering and exiting the infiltration beds during a storm event.

The hydrologic computer model of the BMP was developed using HEC-HMS, a program designed to model watershed systems (HEC 2001). Hydrologic site characteristics and a number of different size storm events were used to calibrate and verify the model. Included in the output are the water surface elevations for each infiltration bed. The model elevation of water in the lower bed was compared to the

water surface depths recorded. It was through this method that the model was verified to ensure it accurately modeled the site.

Instrumentation[1]

To collect data for modeling, the study site was instrumented with a variety of measuring devices, located as shown in Figure 22. The first of these was a tipping bucket rain gage located on the roof of Bartley Hall. The rain gage was originally located on the roof of neighboring Sullivan Hall. After a few weeks of operation, it was discovered that the rain gage was not accurately reflecting the rainfall over the watershed. The results where compared to two other rain gages, located near the site on other research projects, for the same storm events. Based on those comparisons and a variety of tests and calibrations, it was determined that the location of the gage was the problem. It was theorized that because the gage was located on the outer side of the building, away from the study site, that prevailing wind currents caused inaccurate readings. To remedy this problem, a suitable location was found through experimenting with portable rain gages in different locations over the course of a series of storms. The best location turned out to be the roof of Bartley Hall where the gage was relocated.

To monitor what was taking place in the infiltration beds, a pressure transducer probe was installed in the junction box located in the lowest infiltration bed following reconstruction. This new probe measures the depth of water in the bed. By observing the drop in water surface elevation after the rainfall ceases, infiltration rates are determined for each storm event. A second pressure transducer, in conjunction with a V-Notch weir, is located in the catch basin at the downstream end of the lower infiltration beds overflow

[1] Portions of this section are taken from the Villanova Stormwater Porous Concrete Demonstration Site Quality Assurance Quality Control Project Plan (Traver et al. 2003).

pipe. It measures the height of water in the chamber and from that, flow and volume of water overflowing the weir and exiting the system are calculated. During some storm events, minimal flows were recorded flowing over the weir in the catch basin where the depth had not yet reached the overflow pipe. This minor flow was attributed to perforations or leaks in the pipe connecting the two structures and was deemed insignificant to this study. Complete technical information for the instruments used can be found in Appendix A.

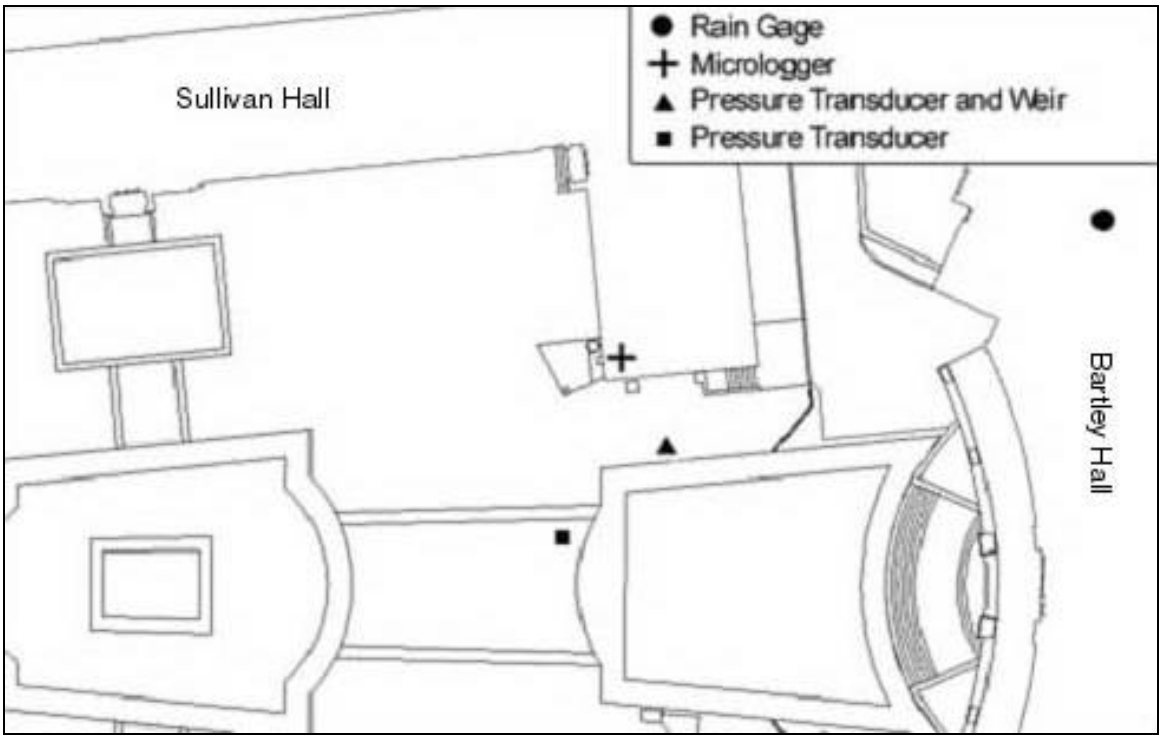

Figure 22: Instrument locations

Hydrologic Computer Model

The computer software program HEC-HMS Version 2.2.2 (HEC 2001) was used to create the model of this site. HEC-HMS, or Hydrologic Engineering Center –

Hydrologic Modeling System, was developed by the US Army Corps of Engineers to "simulate the precipitation-runoff processes of dendritic watershed systems" (HEC 2001). The program allows users to enter the specific hydrologic characteristics of their site and analyze them under a variety of environmental and flow conditions. HEC-HMS is organized into three data input and control components entitled Basin Models, Meteorological Models, and Control Specifications.

The first component is the Basin Model. This is where the network of elements being analyzed is created and where the hydrologic characteristics of the site are entered. For the computer model of this site, the study area was broken down into three areas based on which infiltration bed the areas drained to. The areas were then separated into pervious and impervious sections to allow better control over the properties associated with each. For the study site, each infiltration bed has both an impervious and a pervious area draining to them as seen in Figure 23.

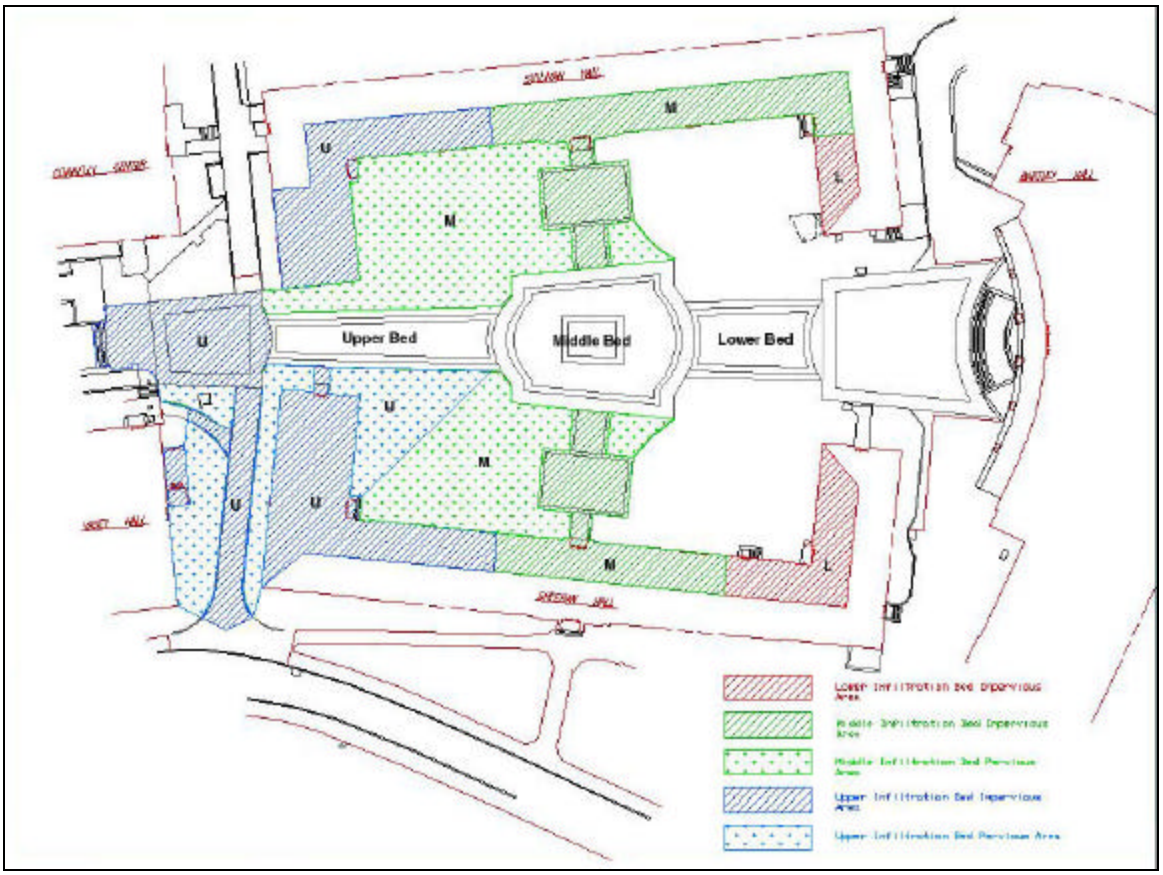

Figure 23: Drainage area breakdown

Subbasins were used to represent each drainage area in the study site. The upper two subbasins are the pervious and impervious areas that drain to the upper infiltration bed. The two areas are then connected by a junction element, which is in turn connected to a reservoir. The reservoir element is representative of the upper infiltration bed because the bed can be seen as essentially an underground reservoir. A diversion element was used to separate out the infiltration that was occurring in the reservoir from the rest of the basin outflow moving through the system. The impervious rooftop area and the middle infiltration bed were connected next, and the lower portion of the site was modeled in the same manner, using a subbasin, reservoir, and a diversion. The resulting Basin Model, as represented in HEC-HMS, is shown in Figure 24.

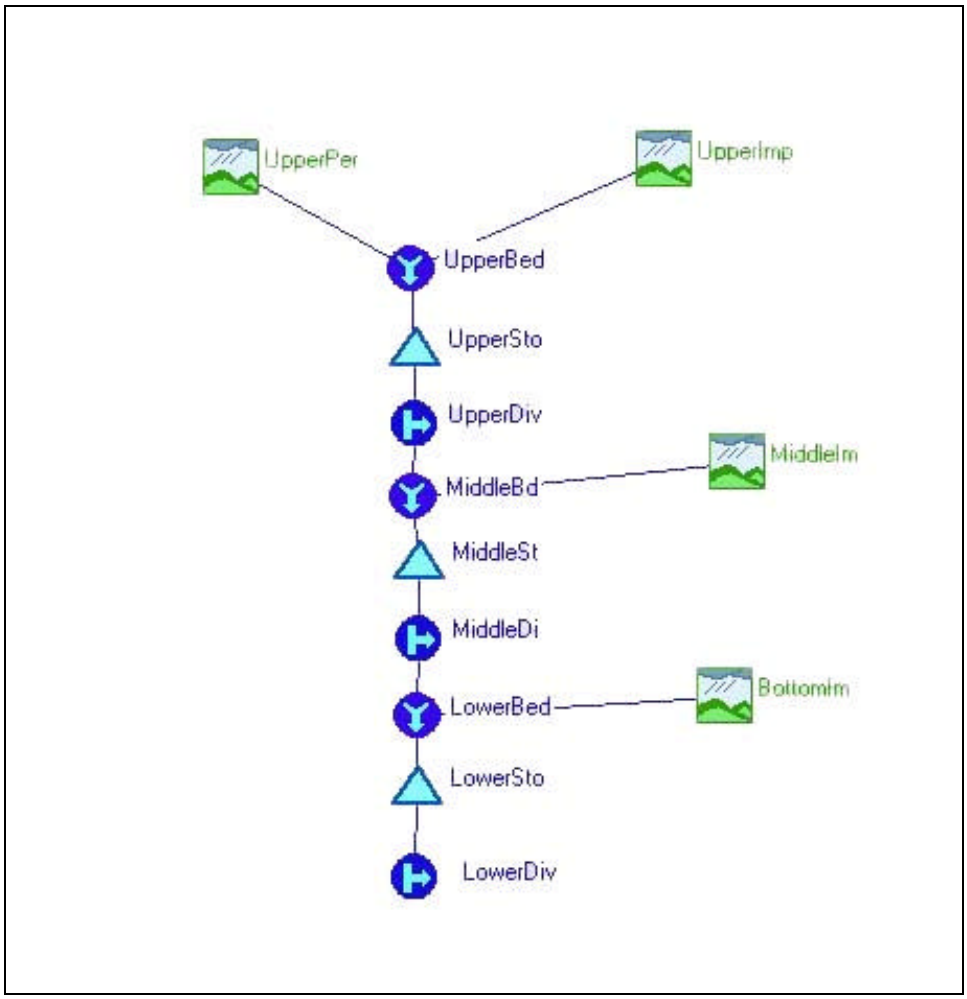

Figure 24: Basin model layout

The first information needed for each subbasin was the area, in square miles, that the subbasin represented. Based on the AutoCAD drawings (STV 2002) and from observations made of the site during storm events, the site was broken down into subbasins based on which infiltration bed the areas drained to. Once the sub areas were determined, the site plans were used to obtain accurate area measurements. The porous concrete areas were treated as impervious areas, as most of the rainfall landing on the

porous concrete would permeate through into the infiltration beds. The same effect is mimicked in the model by routing the impervious flows directly to the reservoir.

For each subbasin, a Loss Rate Method was selected. For this study, the Soil Conservation Service (SCS) Curve Number Method was chosen (Equation 1). The SCS Curve Number Method estimates precipitation excess as a function of cumulative precipitation, soil cover, land use, and antecedent moisture (Rallison 1980, Mays 2001).

$$P_e = \frac{(P - I_a)^2}{P - I_a + S} \quad (1)$$

$$I_a = 0.2 * S \quad (2)$$

$$S = \frac{1000}{CN} - 10 \quad (3)$$

Where:

P_e = Accumulated precipitation excess at time t (in)

P = Accumulated rainfall depth at time t (in)

I_a = Initial abstractions (in)

S = Potential maximum retention (in)

The first parameter used by HEC-HMS is the amount of initial losses, in inches. This field was left blank, allowing the default of the method, 0.2 times the storage, to be used. The percent impervious was set at 0.0%. Imperviousness would be accounted for in the Curve Number. The Curve Number is a value, which ranges from 100 for bodies of water, to 30 for permeable soils with high infiltration rates (Mays 2001). Based on the type and condition of the soil in the study site, a Curve Number of 75 was chosen for the pervious areas and sidewalks. This corresponds with a light residential land use with a

Hydrologic Soil Group type B. The impervious areas were assigned a Curve Number of 98; a value typically associated with parking and paved surfaces such as driveways and rooftops.

The SCS Unit Hydrograph Method (Viesmann and Lewis 1995), Equation 4, was chosen due to its overwhelming use in this area. For the impervious areas, the longest time of travel was calculated based on the furthest distance runoff had to travel and the slopes encountered along the way. It was determined that from the farthest point, it would take runoff five minutes to flow into the nearest infiltration bed. This was verified based on when the water elevation in the infiltration beds began to rise after the start of a rain event. A travel time of twenty minutes was used for the pervious areas. This was based on observations made during storm events. Because there are no natural streams or springs in the study area, no Baseflow Method was required.

$$Q_P = \frac{484 * A}{t_{peak}} \tag{4}$$

Where:

Q_p = Peak discharge (cfs)

A = Drainage area (mi^2)

t_{peak} = Time to peak (hr)

Reservoir elements were used to represent the infiltration beds. There are five different methods HEC-HMS can use when calculating storage for the reservoir. The method used for this study was the Storage Indication Method (Viesmann and Lewis 1995). Data for this method is inputted through the use of the Elevation-Storage-Outflow

Method in HEC-HMS. The dimensions and locations of outflow pipes of each bed were known so outflow from the reservoirs, as a function of depth, were determined. The initial conditions were set to an elevation of 0 feet which was the bottom of the infiltration bed.

Based on the AutoCAD drawings of the three infiltration beds, storage capacities for different elevations were able to be determined. The known information was the surface area of the bottom of the beds, the slopes of the sides, and the area of the top of the bed. Each bed was broken into slices, starting at the bottom of the bed and increasing 0.1 feet until the top of the bed, at 4 feet, was reached. By knowing the areas of the top and bottom slices, a relationship was found which approximated the size of each slice as the elevation increased. By comparing two slices, a volume was found. This volume, when added to the volume of the previous two slices, gives the volume of the bed to that point. Once the volume-depth relationship of each bed was found, the volume of pore spaced available for water storage was determined. This was based on the fact that the AASHTO No. 2 stones had a void space of 40%, so 40% of the total bed volume could be used to store water (Appendix B).

The outflow component of the Elevation-Storage-Outflow table is comprised of the water that leaves each bed through pipes as well as the water that leaves through infiltration. The infiltration component is then separated out using diversions as will be discussed in the next section. The only overflow pipes for the uppermost infiltration bed are the two pipes located just beneath the concrete surface. The flow through these pipes was calculated using the modified weir equation, Equation 5 shown below (Emerson 2003).

$$Q = 3.6 * (0.785 * D) * H^{1.5} \quad (5)$$

Where:

Q = Flow over the weir (cfs)

D = Diameter of the pipe (ft)

H = Height of water over the weir (ft)

For the middle infiltration bed, the same two overflow pipes were present but there was also a 4-inch HDPE pipe connecting the bed with the bottom infiltration bed. This 4-inch pipe was modeled using the modified weir flow equation until the water surface elevation in the bed reached a depth higher than 4 inches. The pipe then functioned as an orifice, as represented by Equation 6 (Emerson 2003).

$$Q = 0.6 * (p * \frac{D^2}{2}) * \sqrt{(2 * g * (H - \frac{D}{2})} \quad (6)$$

In the event the water surface elevation reached the two overflow pipes, the flow from the bed would be a mixture of the infiltration, the orifice flow from the bottom pipe, and weir flow from the two overflow pipes. The bottom infiltration bed outflow functions in much the same way. An overflow pipe, leading to the catch basin where the V-Notch weir is located, is located at a height of 18 inches from the bed floor. Until the water surface reaches that height, the only water leaving the bed is through infiltration. Once the water surface reaches 18 inches, the modified weir flow equation (Equation 5) is used to measure the amount of water leaving the bed.

An outflow, including the water that was infiltrating, was calculated for every tenth of a foot increase in elevation within each of the three beds. This information was

entered into the corresponding Elevation-Storage-Outflow table Appendix C). Figure 25 shows a graph of the information for the lower infiltration bed. The outflow curve is only the infiltration component, starting at 0.0022 cfs, until the water surface elevation reaches 1.6 feet.

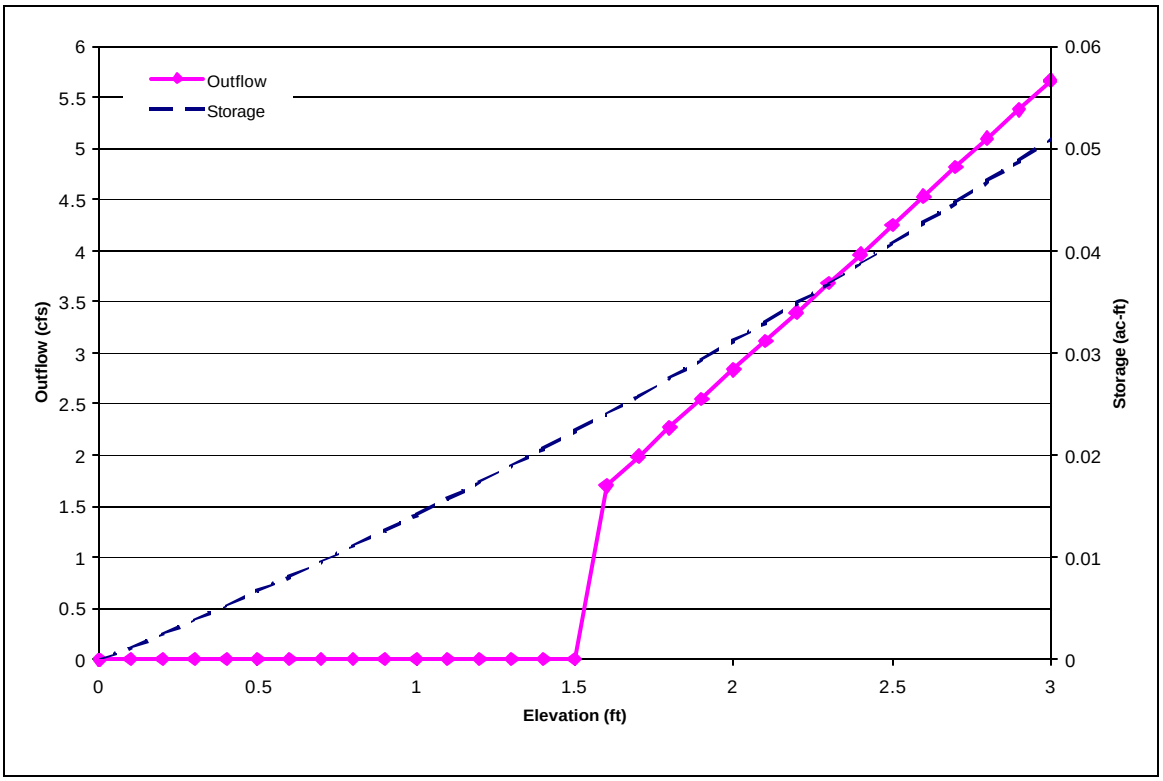

Figure 25: Elevation-Storage-Outflow Curve graph

The Elevation-Storage-Outflow table for middle infiltration bed used the same value for the infiltration rate as the lower infiltration bed. Based on the elevation of the middle bed in relation to the lower bed, the middle infiltration bed will rarely fill with water because the majority of water would exit into the lower bed. Because of that, there is little change in storage or surface area to affect the infiltration rate.

Diversions were then used in the model to separate the infiltration component of the outflow leaving from the reservoirs from the water that is leaving through pipes.

Diversions work by taking a portion of the flow and diverting it to another location. The remaining flow then moves down the system to the next element. For this model, there is no final location for diverted flow; it is simply subtracted from the system.

During the initial calibration, a constant infiltration rate was estimated and inputted into the diversion and Elevation-Storage-Outflow tables. For inflows of all magnitudes, a constant diverted flow of 0.005 cfs was used. This rate was based on the infiltration rates of the recession limbs from the five storm events that occurred early in the study listed below in Table 1. The highest value was used for this initial run because the model was still overestimating runoff from the site.

Table 1: Initial storm events for diversions and infiltration rates

Storm Event	Rainfall (in.)	Starting Depth (in)	Ending Depth (in)	Elapsed Time (hrs)	Reservoir Infiltration (in/hr)	Reservoir Infiltration Rate x 10^{-3}(cfs)
9/28	0.70	2.83	0.01	30.33	0.093	2.3
9/23	0.93	5.80	0.06	47.75	0.120	2.9
9/19	1.27	11.89	0.01	52.25	0.227	5.5
10/15	1.35	8.21	0.32	62.25	0.127	3.1
9/15	2.30	9.81	0.01	49.42	0.198	4.9

HEC-HMS uses Control Specifications to tell the model the date and time to start and end the computations being performed on the system. A time interval of 5 minutes was also set to specify the amount of time between each time step. For this study, the start date and time of the computations were set at when the first tip of the rain gage was recorded. The end date and time are when the water surface elevation in the port, as measured by the pressure transducer, reaches zero, meaning the beds have emptied. In some cases, precipitation from another storm event began before the beds had an opportunity to completely infiltrate. In these cases, the end date and time were set to

when the water surface elevation began to increase again and therefore recorded as a multiple storm event.

Observed rainfall measurements can be entered into HEC-HMS through one of two ways. It can be entered manually when creating a Precipitation Gage or it can be accessed through a single external Data Storage System file, or DSS file. The DSS file approach was chosen for this study due to ease of file management. The DSS file was created using the program HEC-DSS Vue, which stand for HEC-Data Storage System Visual Utility Engine (HEC 2003). HEC-DSS Vue is a Java based utility also developed by the US Army Corps of Engineers that allows users to input and edit HEC database files. Rainfall data in five-minute increments was entered into the program, creating a file called "RainGage.dss." It is this file that HEC-HMS will access later to obtain the rainfall information.

A Precipitation Gage was created for each storm event using the external DSS file. The time interval for each gage was set from the Control Specification for the corresponding storm. The tables pulled from the DSS file were checked and graphed to ensure all the data points were imported correctly. The Precipitation Gages are used by the Meteorological Model to provide rainfall for the model runs. No evapotranspiration was used for this study because the program uses a Monthly Average Method and that data was not recorded or available.

A spreadsheet of storm events was created to maintain a record of storm events that took place on the site. Storm events are defined as periods of measurable rainfall with an associated flow or rise in bed water surface elevation. The date and time of the beginning and end of the rainfall is recorded along with the total amount of precipitation,

the maximum one-hour precipitation, and the average intensity of the rainfall. Additional characteristics of each storm event are also noted in the spreadsheet. These include the occurrence of flow over the weir, the maximum water surface elevation in the port, and the antecedent dry time since the last storm event. The complete storm list can be found in Appendix D.

Calibration and Verification

Preliminary Model Run

At the beginning of the modeling process, a few preliminary model runs were made to check the model. It was found the model overestimated the amount of runoff reaching the infiltration beds. This was determined based on the water surface elevation from the pressure transducer in the lower infiltration bed. The drainage areas were then reexamined to determine their effect on the system. By looking back through construction photographs, it was realized that there was no pipe (as specified) through the berm connecting the upper two beds. Based on this finding, it was decided that the upper bed was separated from the middle and lower beds. Next, the drainage areas were reexamined. The pervious areas that drain to the middle infiltration bed were removed from the model. This was done because it was observed that runoff from these areas ran down the side of the paving stones, thereby bypassing the infiltration beds altogether. This was not an intended purpose of the paving stones and this bypassing occurrence decreases the capture efficiency of the site. Another source of bypass for the system turned out to be the storm drain inlet located at the top of the site next to Sheehan Hall. During construction, the inlet was not installed properly. Instead of being level, it was placed two inches higher than the asphalt path. This caused runoff from the path to

bypass the inlet completely and continue flowing along the stone border and out of the watershed. This reduced the area for that subbasin that was originally thought to contribute to the upper infiltration bed but because the runoff remains in that bed, it was left in the model. It was further determined that because the dormitory rooftops were directly connected to the infiltration beds through pipes, the runoff from these areas had a direct impact on the water elevation in the beds.

Calibration - Constant Infiltration Rate

Initially, a separate basin model was created for each storm event using each storm's specific infiltration rate from its recession limb. This was done to determine the affect of each different rainfall event and to make sure the results were the same order of magnitude as the observed water surface elevation. Because the overflow pipe from the lower bed is located at an elevation of 18 inches it was determined from observations and measurements that the majority of storms would not cause the water surface elevation to reach this level, and there would be little to no flow exiting through that pipe. Therefore the only way to correlate what is taking place on the site with the results that the model is producing is through the use of the pressure transducer located in the observation port of the lower infiltration bed. This depth can be directly compared to the water surface elevation calculated by the model.

For the first series of model runs, a constant infiltration rate was added to the outflow column in the reservoirs Elevation-Storage-Outflow tables and in the diversion tables. A rate of 0.005 cfs was used, the largest of the values listed previously in Table 1 of storm events. This higher value was used because for some storms events, the model

was still allowing too much water to reach the lower infiltration bed. Each storm event was modeled using this constant infiltration rate and the results were compared to the observed port water surface elevation as shown in Figure 26.

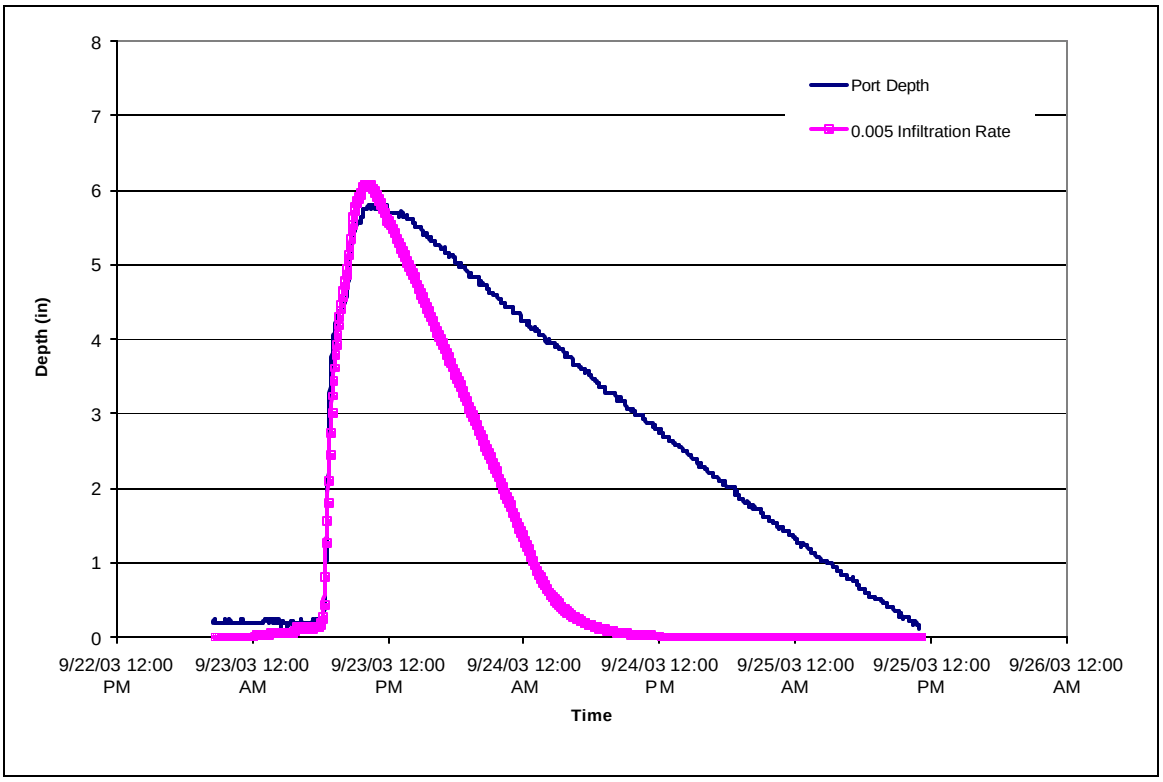

Figure 26: Small storm event with constant infiltration rate

For the small storm event shown in Figure 26, the model calculates a linear drop in water surface elevation. This was expected as a constant value was used. Based on the slope of the line, it appeared that the constant infiltration rate used was too high. For smaller storm events, the infiltration rate is linear, as observed from measured water surface elevation readings. However, for larger storms, the drop in water surface elevation is not linear; therefore a linear representation is not accurate for what is occurring on the site (Figure 27).

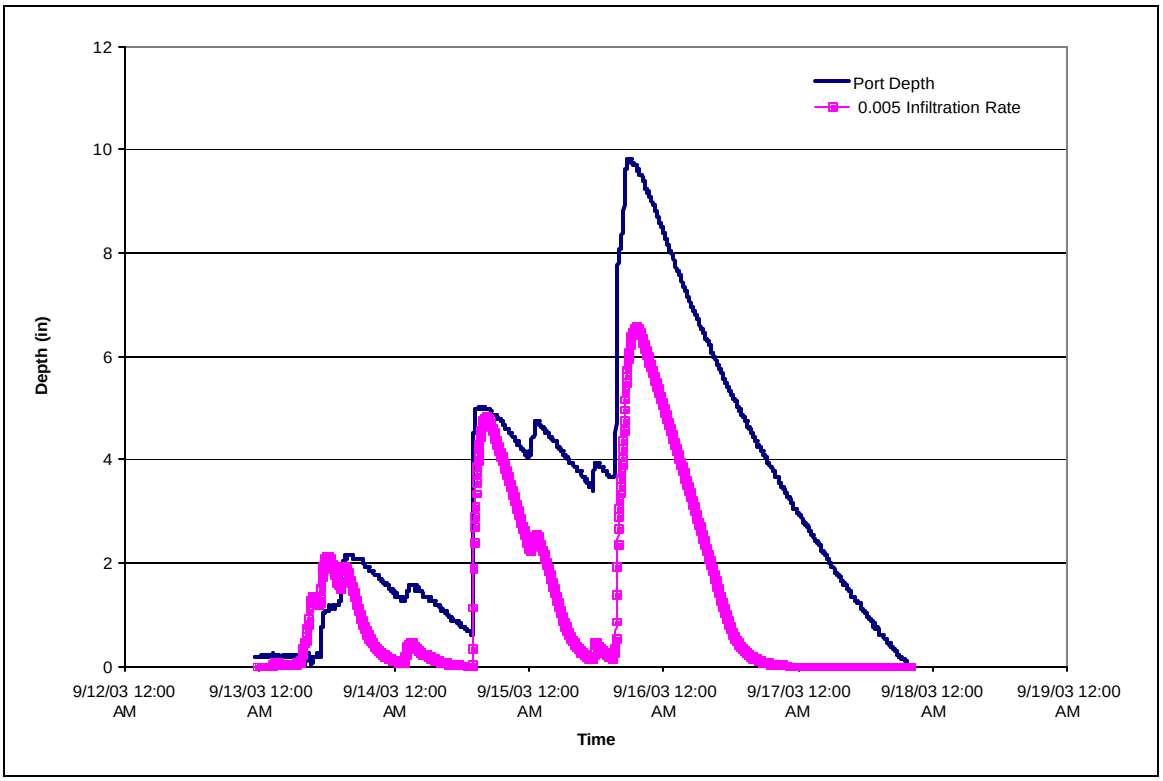

Figure 27: Large storm event with constant infiltration rate

This graph illustrates that the model results, as shown by the thicker line, too steep a drop in the water surface elevation. The observed water depth, the thinner line, is also not linear on the tailing end of the curve. To better match what was occurring on the site, it was determined that for larger storms, a non-linear infiltration rate was needed.

Calibration - Storm Specific Infiltration Rates

To determine a specific infiltration rate for each storm event, the receding limb of each observed port water elevation curve was used. The volume of water in the infiltration bed was then calculated for each time step of five minutes. Every time step was then subtracted from the one after it to obtain a change in volume every five minutes and multiplied by negative one, so that the decreasing depth would be shown as a

positively increasing line. This value was then converted to cubic feet per second to get an infiltration rate for each time step (Appendix E). The infiltration rates were then graphed as a scatter plot, with cubic feet per second on the y-axis versus the original observed depths, in feet, along the x-axis. A trend line was fit to the scatter plot showing the linear trend of the data points. The equation of this trend line was representative of the rate at which the recession limb of the observed port water depth curve was changing. This equation was then used to calculate the infiltration component of the outflow from the bottom infiltration bed for use in the Elevation-Storage-Outflow table. Figure 28 shows how the receding limb of the curve of each storm event was used to calculate the infiltration rate for the entire storm.

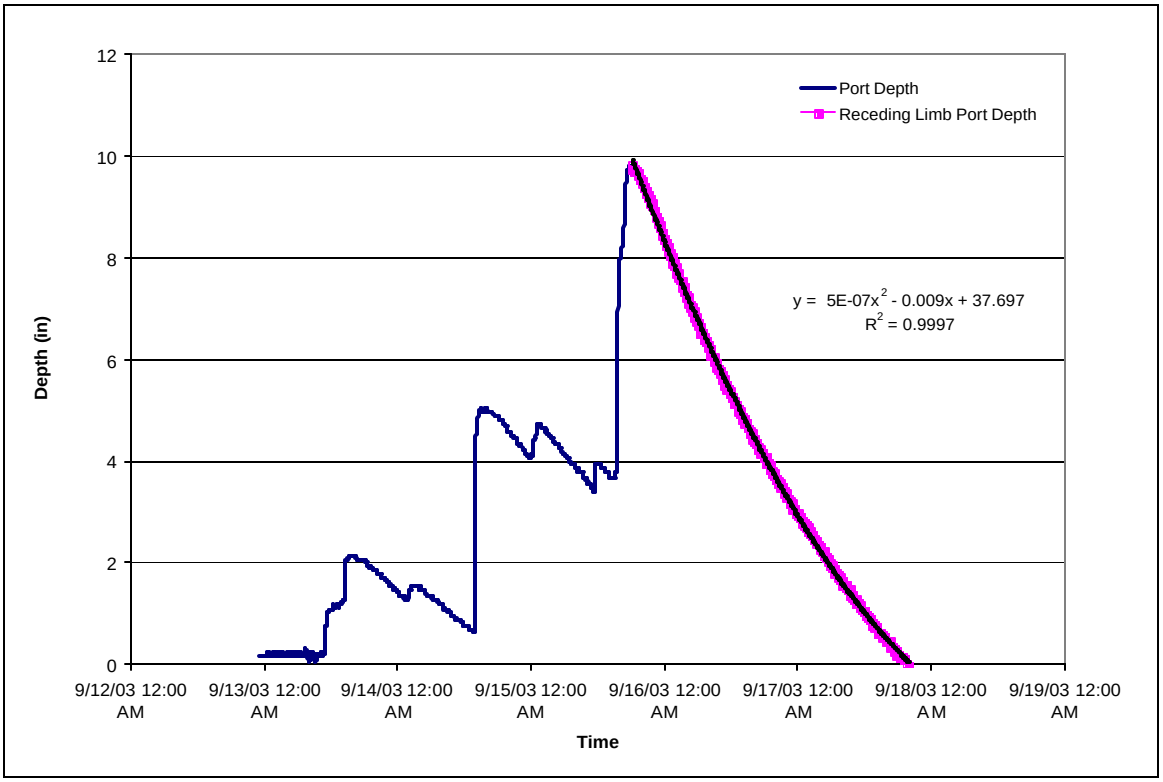

Figure 28: Receding limb used for specific infiltration rate

Once the specific infiltration rates for each storm event were determined in this manner and entered into the individual storm Basin Models, the models were re-run to observe the effects of the new values. As expected, the new storm specific infiltration rates provided a much better approximation of the water surface elevation (Figure 29). The dashed line represents the observed water surface elevation for the storm event from the pressure transducer. The straight line is the water surface elevation generated by the new computer model.

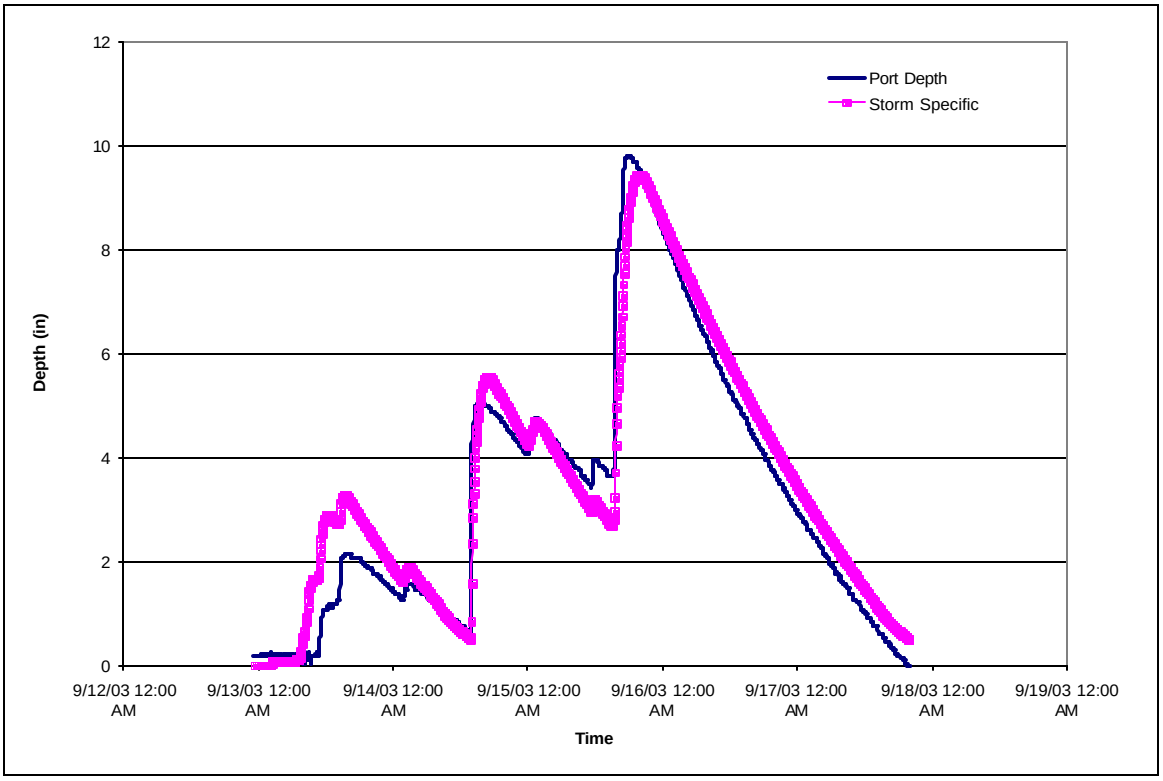

Figure 29: Comparison between observed water depth and model output

The percent error for the peak elevation of each curve was calculated. The error compared the peak of the observed water surface elevation with the peak from the curve that the model produced. The change in storage between the two curves was also found. To do this, the observed water surface elevation curve was subtracted from the curve the

model produced and the difference was summed across the duration of the storm event. After running all the storm events through their respective new models with infiltration rates specific to that storm event, the errors were compared and a relationship was found regarding the results. It was observed that for larger storms events, i.e. events with rainfall greater than 1.00 inches of precipitation and a maximum water surface elevation above 8 inches, the receding limb of the water surface elevation curve decreased in a nonlinear manner. For the smaller storm events, i.e. those less than 1.00 inches and belong inches, the decrease was linear (Figure 31). This relationship is shown in Table 2.

Table 2: List of storms and type of receding limb

Storm Event	Rainfall	Regression	Maximum Water Height (in.)	% Peak Error for observed vs. storm specific curves	Change in storage between observed and storm specific curves (ft)
11/12	0.44	Linear	0.92	-15.71	-0.02
1/4	0.55	Linear	1.08	-34.68	7.22
9/27	0.70	Linear	2.83	-52.86	119.93
11/4	0.78	Linear	1.97	35.75	-20.65
11/28	0.84	Linear	4.53	-33.32	43.24
9/22	0.93	Linear	5.80	-23.6	94.37
12/14	1.06	Polynomial	12.20	69.16	-341.96
9/18	1.27	Polynomial	11.89	20.55	-81.73
10/14	1.35	Polynomial	8.21	-37.78	312.77
12/9	1.56	Polynomial	15.86	55.09	-275.96
11/19	1.64	Polynomial	11.98	-9.42	82.19
12/24	1.81	Polynomial	15.17	9.06	-23.72
9/12	2.30	Polynomial	9.81	3.89	27.99

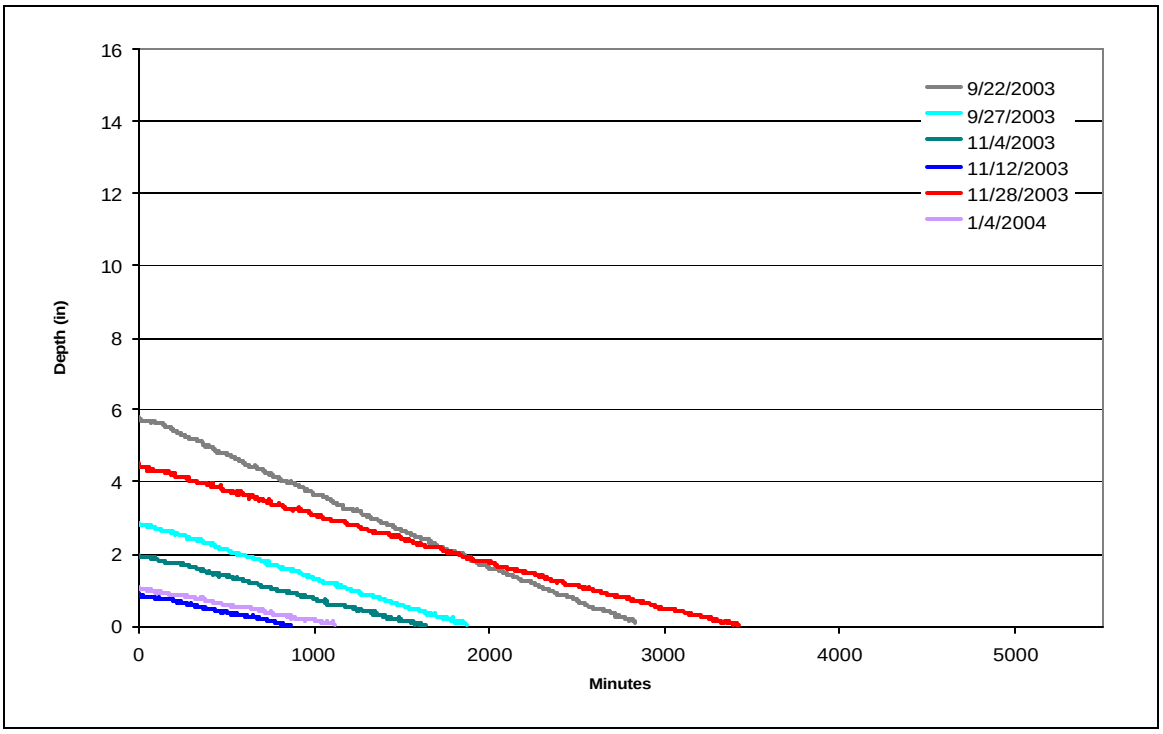

Figure 30: Linear curves

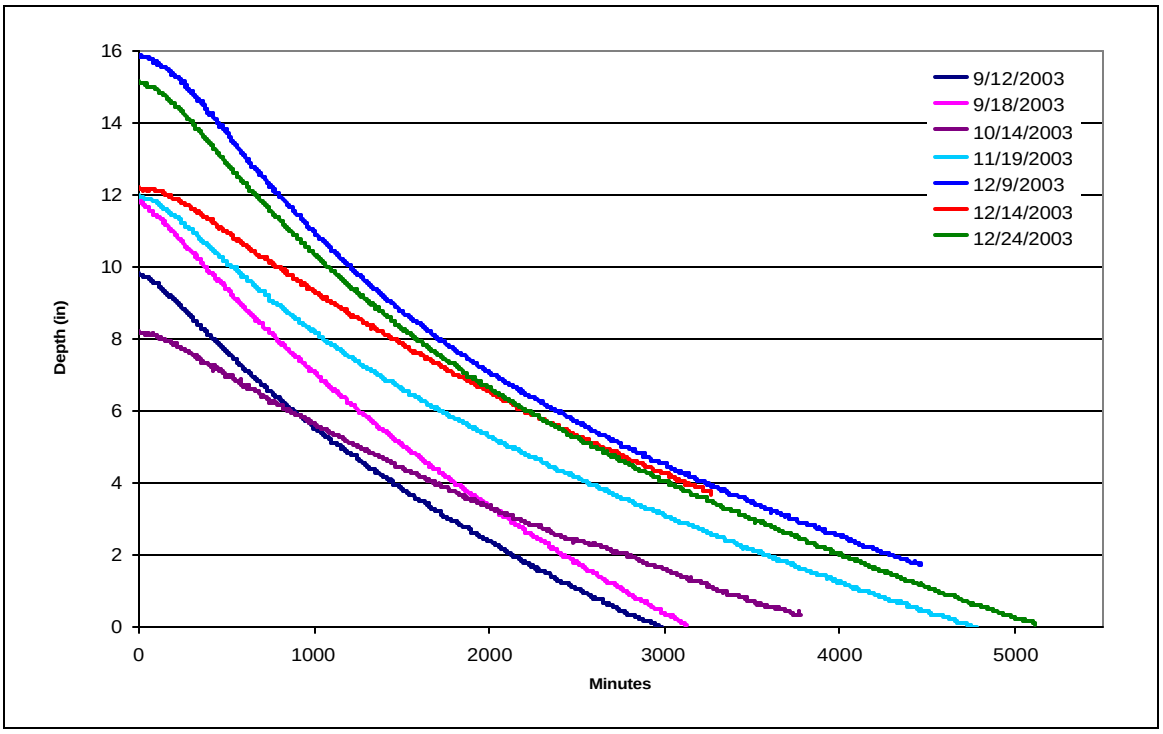

Figure 31: Polynomial curves

The relationship is based on the maximum height the water reaches in the lower infiltration bed. Because smaller storm events do not produce as much runoff as larger storm events, the infiltration bed does not fill up as much. These lower elevations translate to a constant infiltration rate. Because larger storms generate more runoff, a higher water surface elevation is reached. This causes an increased pressure force that causes the water to infiltrate more quickly, until it reaches an elevation where the pressure no longer has an effect and the curve becomes linear, like the smaller storm events. The slope of the sidewalls of the bed also contributes to the increase in infiltration rate. The greater surface area provides more contact for the water.

Based on this relationship, it was determined that two infiltration rate representations were needed to represent both the small, linear storms as well as the larger, polynomial storms. The first, for the smaller storms, uses a constant infiltration rate for each bed, based on an average of the infiltration rates following the cessation of rainfall for the smaller storm events. The second model, for the larger storms, uses a polynomial equation to represent the change in infiltration rate as the water depth decreases.

Calibration - Composite Models

Composite Linear Model

The initial attempt at creating a computer model used a constant infiltration rate of 0.005 cfs. This proved not to be very accurate, as seen previously in Figure 26. This value was based on the storm events from Table 1, which was calculated by using the highest point the water reached and the time it took for the bed to empty. For the

composite linear computer model, all of the storm events with a linearly decreasing observed water depth curve were used. The receding limb of each storm event curve, starting at the maximum water surface elevation reached, was graphed as a scatter plot and a trend line was fit to each individual storm event (Figure 32).

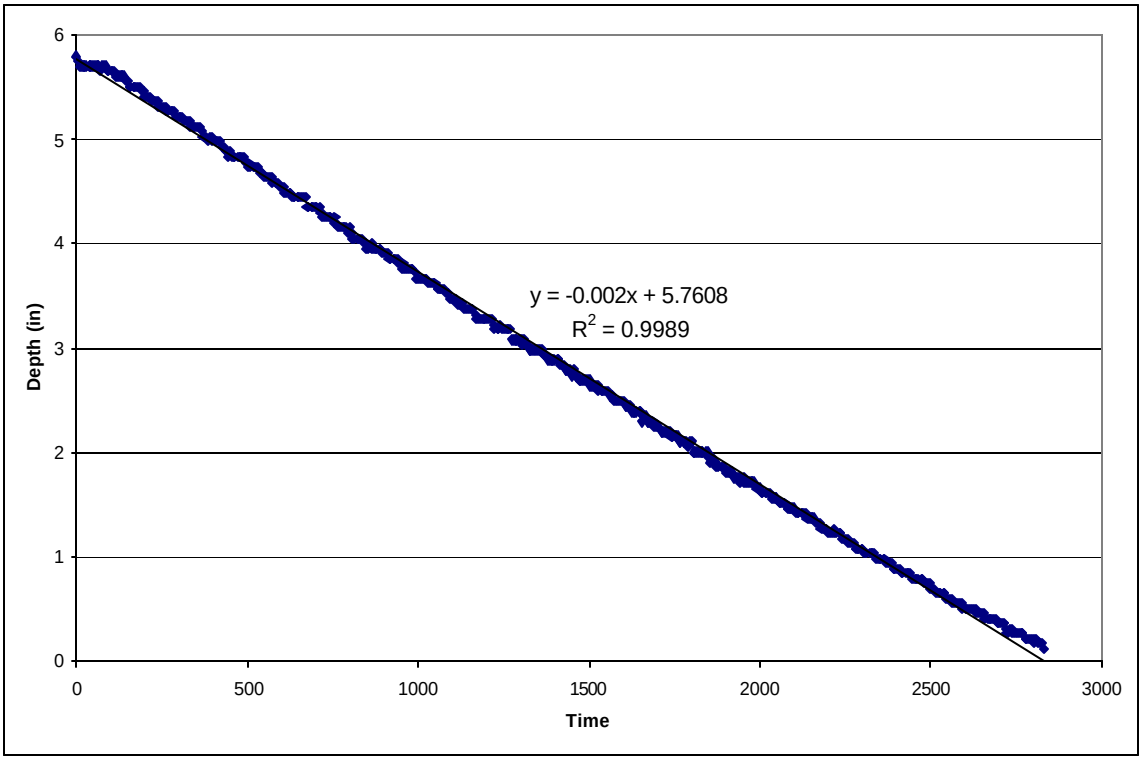

Figure 32: Receding limb scatter plot for linear storm event

The r^2 value of 0.9989 for this storm event shows that a line is extremely accurate representation of what is occurring. The slope of this trend line gave the infiltration rate for this specific storm. After all of the individual storm events were graphed in this manner and the equation of their receding limbs found the slopes were compared and the errors between the peaks and the storage difference between the curves were calculated Table 3).

Table 3: Storm events with linear equations

Storm Event	Rainfall	Maximum Water Height (in.)	Slope	% Peak Error for observed vs. composite linear model curves	Change in storage between observed and composite linear model curves (ft)
11/12	0.44	0.917	-0.001	-62.84	27.37
1/04	0.55	1.079	-0.0009	-62.77	39.97
9/27	0.70	2.831	-0.0015	-51.42	104.84
11/4	0.78	1.968	-0.0012	-40.09	67.50
11/28	0.84	4.526	-0.0013	-38.69	164.16
9/22	0.93	5.8	-0.002	-26.37	178.98

The "m" values, or slopes, are negative because the curve is decreasing. The initial attempt at creating the linear equation model averaged these "m" values to get an infiltration rate of 0.0013 cfs. This new infiltration rate was then applied to the tables in the diversion elements and added to the outflow column of the Elevation-Storage-Outflow table in each of the reservoirs to create a new Basin Model. The six storm events were run through the model again using this common infiltration rate and the individual results were graphed (Figure 33). It is important to note that all of the peak errors were negative although the change in storage was all positive, indicating the observed water surface elevation was lower than the model output for all six storms. This will be addressed further in the conclusions section.

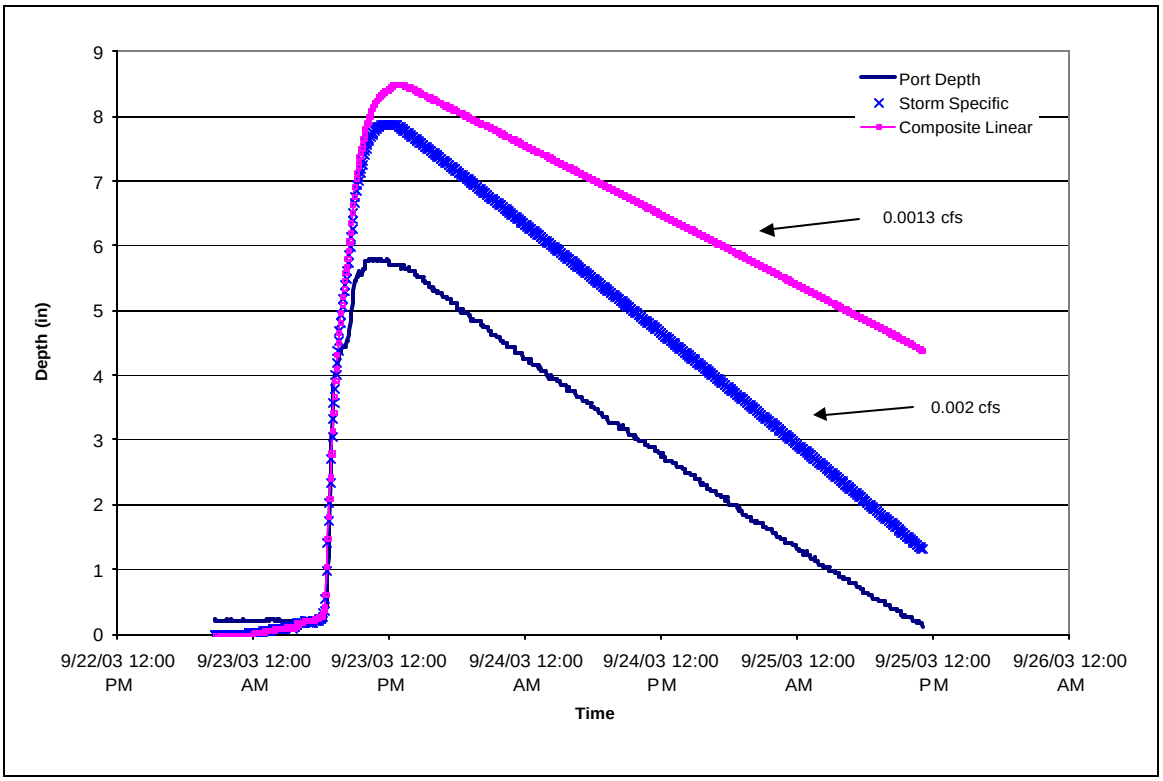

Figure 33: Linear Storm event showing different curves

The thin line shows the observed water surface in the lower infiltration bed. The thickest line shows the results using an average infiltration rate of 0.0013 cfs. Graphs for the storm events can be found in Appendix F. After analyzing these results, it was thought that a higher infiltration rate might lower the total volume by taking more runoff out of the system, thereby decreasing the water elevation that is reached in the model. The storm specific value of 0.002 cfs was then used from the September 22 storm event. The Basin Model was altered to reflect this new value and the model was re-run; these results are represented by the lighter blue line in the figure. While this higher infiltration rate of 0.002 cfs did decrease the maximum water surface elevation slightly, the slope of the line became too steep in most cases. It was found that as the infiltration rate increased from 0.0013 cfs to the original value of 0.005 cfs the maximum height the water reaches

decreased until it reached the observed height as seen previously in Figure 26. While the maximum depth reached decreased, the slope of the line increased sharply. This showed that the problem with the model was not with the infiltration rate. The average value of 0.0013 cfs worked well in most cases in mimicking the rate of decrease of the water in the bed. The problem was that the model was still over predicting the quantity of runoff that was entering the system for an infiltration rate of that magnitude. This means that there is variation in the system when dealing with small storm events that is not represented in the composite model and thus this linear representation is not valid.

Composite Polynomial Model

For the composite polynomial computer model, all of the storm events with exponential recession limb port water curves were used. As with the linearly regressing storm events, the receding limb of each observed storm event curve was graphed as a scatter plot. A polynomial trend line was then fit to each curve (Figure 34).

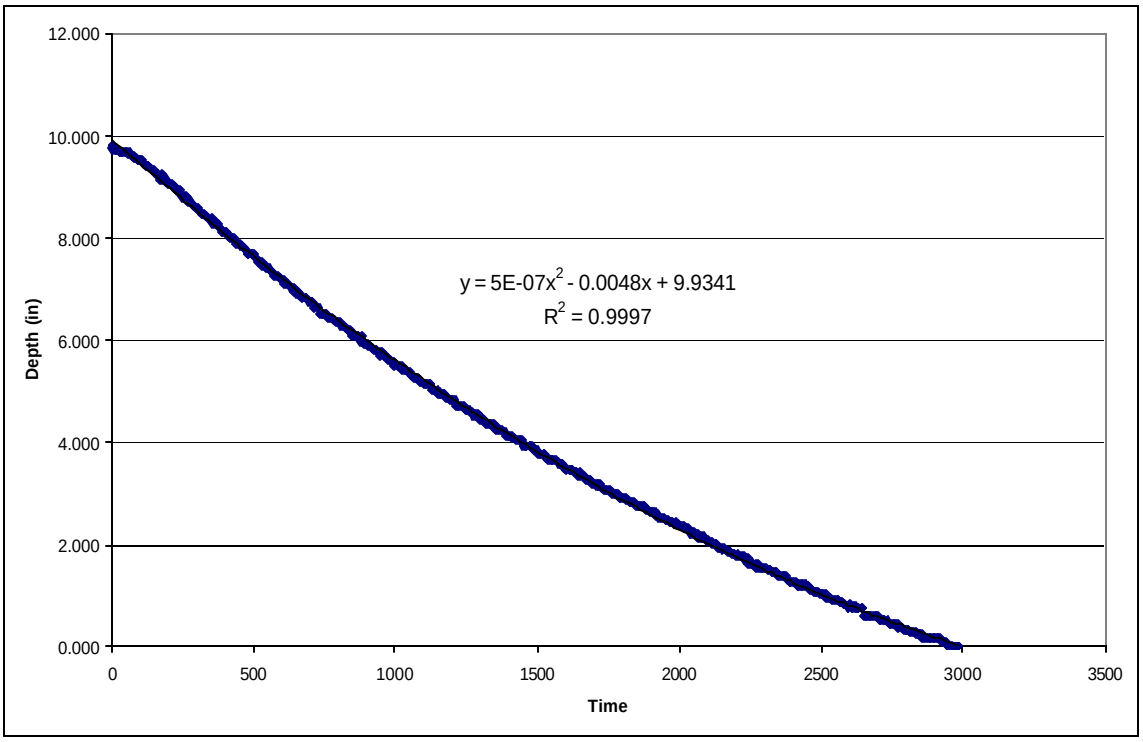

Figure 34: Receding limb scatter plot for polynomial storm event

The r^2 value for this curve was 0.9997, again indicating a very good fit. The equations of each of the storms' trend lines were compared (Table 4) and a composite equation was created (Equation 7).

$$y = 3.33x10^{-7}x^2 - 0.0044x + 12.26 \quad (7)$$

Table 4: Storm events with polynomial equations

Storm Event	Rainfall	Maximum Water Height (in.)	Equation $y = ax^2 + bx + c$			% Peak Error for observed vs. composite polynomial model curves	Change in storage between observed and composite polynomial model curves (ft)
			a	b	c		
12/14	1.06	12.2	4*10-7	-0.0035	12.564	64.6	-305.92
9/18	1.27	11.89	5*10-7	-0.0053	11.894	18.7	-27.69
10/14	1.35	8.21	2*10-7	-0.003	8.3699	-26.37	88.93
12/09	1.56	15.86	5*10-7	-0.0056	16.176	61.5	-332.24
11/19	1.64	11.98	3*10-7	-0.0039	11.946	-9.06	29.15
12/24	1.81	15.17	4*10-7	-0.005	15.141	9.95	-44.72
9/12	2.30	9.81	5*10-7	-0.0048	9.9341	-1.49	87.32

For the creation of the composite polynomial equation, the “a”, “b”, and “c” values were averaged to obtain representative values. Using the new composite polynomial equation, a curve was plotted. The curve was treated as if it were the recession limb of an actual storm event. A volume was found and an infiltration rate was calculated for each five-minute increment. The points were then graphed as a scatter plot. From that scatter plot, an exponential equation was obtained. As shown in Figure 35, the equation was only used up to one foot. After that, a linear equation was used for depths up to 4 feet.

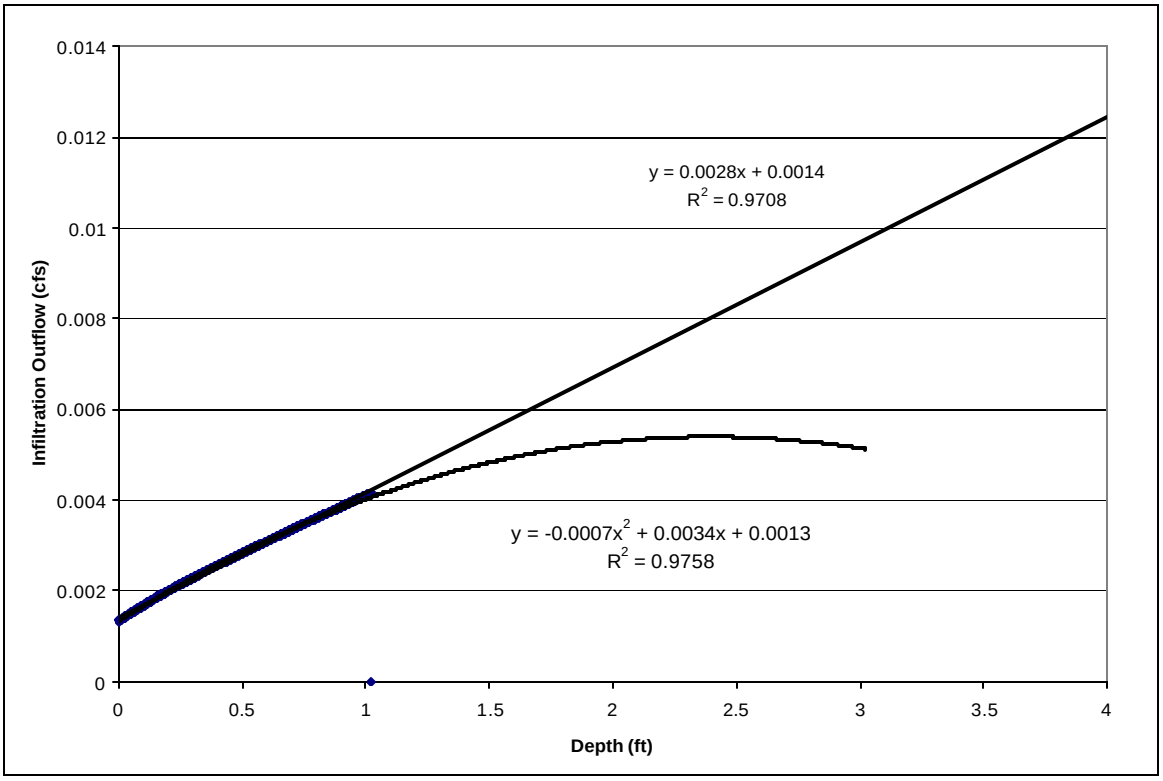

Figure 35: Trend lines for composite polynomial curve

This linear equation was needed because the polynomial equation created a parabolic curve that would not work once the water surface elevation reached higher water depths.

Each of the storm events were then run through the HEC-HMS model again using their own individual Meteorological Model and Control Specification but with a

single Basin Model which reflected the use of the composite polynomial infiltration equation. The results from each bed elevation table were plotted against the observed water depth and the storm specific infiltration rate (Figure 36).

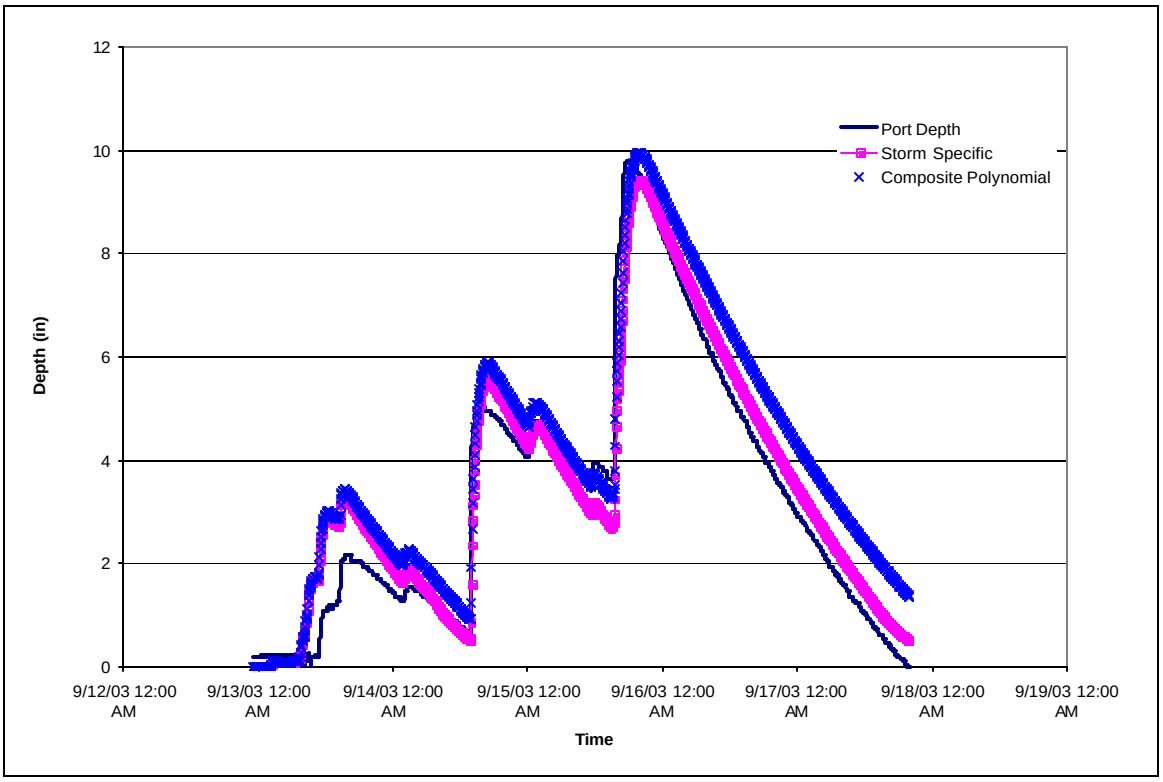

Figure 36: Curve comparison (9/12)

The thin represents the observed water depth from the port. The thickest line is the curve generated by the model using an infiltration rate specific to this storm. The line consisting of points shows the water depth using the single Basin Model and the new composite polynomial infiltration rate. The error between the peaks and the change in storage between the curves was calculated and recorded in Table 4. The error between the peaks on the curves lessened for larger storm events. This will be discussed further in the conclusions section. For this storm event, the composite polynomial model represented what happened on the site extremely well, giving slightly higher peaks and a

slower infiltration rate. The error in volume was higher at the beginning of the storm event than at the end. This further emphasizes the effect that initial losses of the infiltration basins have on the system. For some other storm events, the model did not mimic the observed water surface elevation as well (Figure 37). In this figure, the thin line represents the observed water surface elevation, the thickest the elevation using the storm specific infiltration rate, and the line of data points shows the curve from the composite polynomial equation. This figure shows that the equation did not allow the water surface to reach the maximum that it did during the actual storm event. This was most likely due to the high rainfall intensity associated with this storm event. The event occurred quickly, not allowing the proper infiltration and losses to occur. The slopes of the lines are very similar but the error between the peaks and the volume under each curve are considerably large.

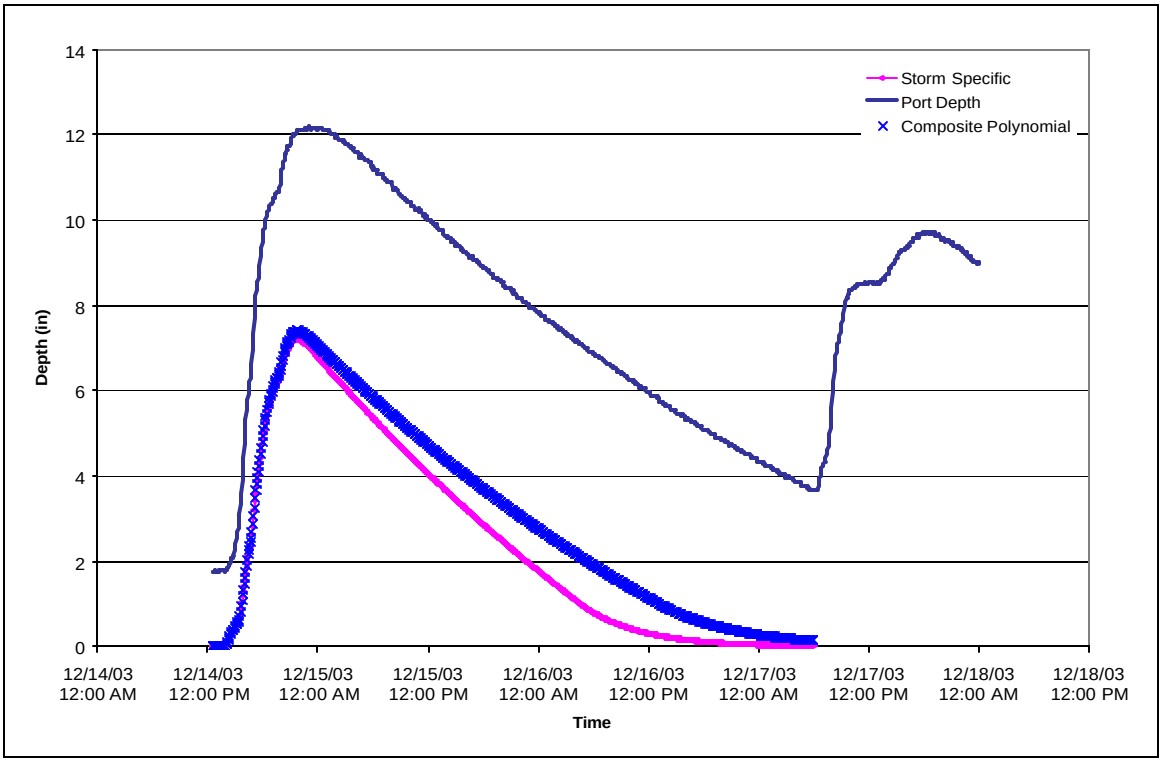

Figure 37: Curve comparison (12/14)

By using a composite polynomial equation to determine the infiltration rate, some storm events will be overestimated and some will be underestimated. The goal was to develop a model that would approximate the observed water surface elevation as closely as possible for the greatest number of storm events. For the complete set of graphs for these storm events, see Appendix G. In most cases, the composite polynomial model did an adequate job at matching the shape and curves of the observed water surface elevation but could not match peaks or volume.

It is interesting to note that another storm event was originally used for the calibration of the composite polynomial model. The storm event occurred on December 17, 2003 and had a precipitation of 0.75 inches. The maximum water surface elevation in the bed reached during this storm was 9.73 inches. For a storm event of comparable size, the event on November 4, 2003 had a rainfall of 0.78 inches. This event reached a maximum water surface elevation of only 1.9 inches. Upon further review, it was realized that this December 17th storm occurred slightly over two days after the storm event on December 14th (Figure 37). The water elevation in the bed was still at 3.8 inches when the new storm event occurred, thus adding to the water elevation already in the bed. This means that depending on the elevation of water reached in the infiltration bed, the bed might not be empty before another rainfall event begins.

Model Verification Runs

To verify that the two models were working properly, new storm events were run through each. Two storms were selected for the composite linear model and one was

chosen for the composite polynomial model based on available data. These three storms are listed in Table 5.

Table 5: Storm events used for model verification

Storm Event	Rainfall (in)	Calibration Method	Maximum Water Height (in.)	% Error in Peak for observed vs. verification storm curves	Change in storage between observed and verification storm curves (ft)
4/23	0.77	Linear	2.89	-51.04	80.27
4/02	0.84	Linear	8.11	86.87	-163.02
4/12	2.10	Polynomial	13.28	105.60	-478.95

Each of the three storm events was run through their respective models to verify their accuracy. The results for the linear storms (Figure 38 and Figure 39) and the polynomial storm (Figure 40) are shown in the following graphs.

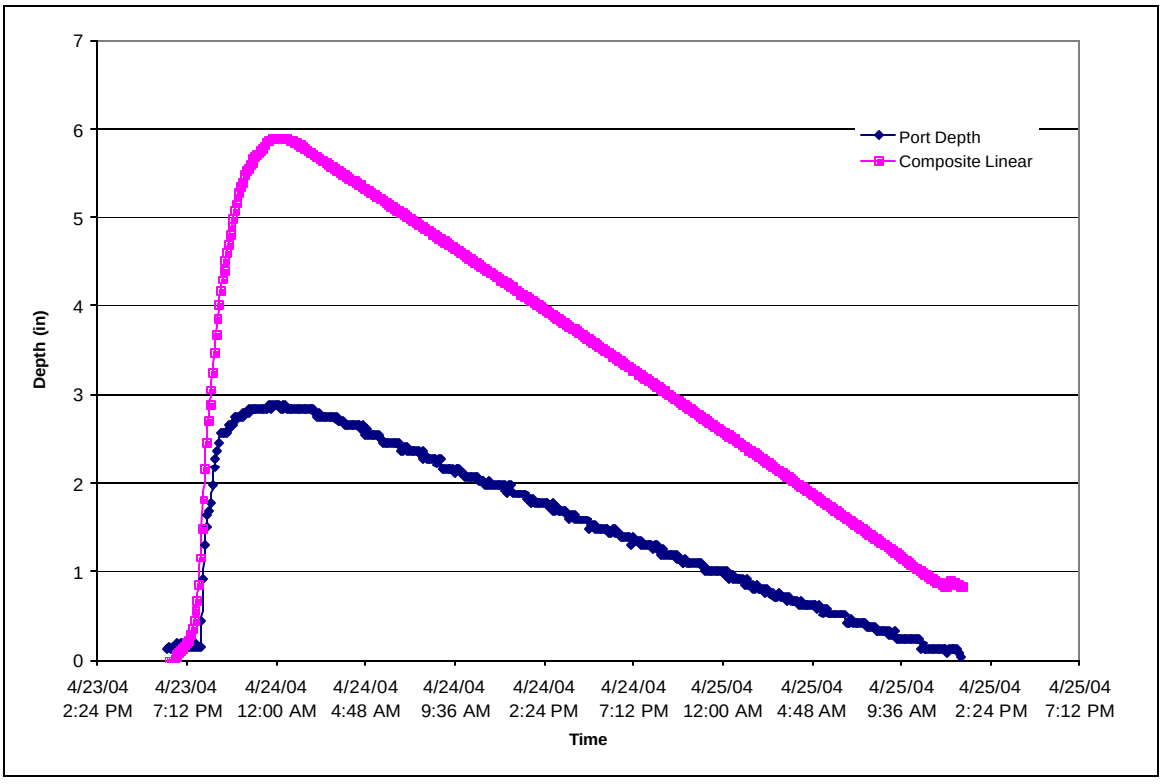

Figure 38: First verification storm event for linear model

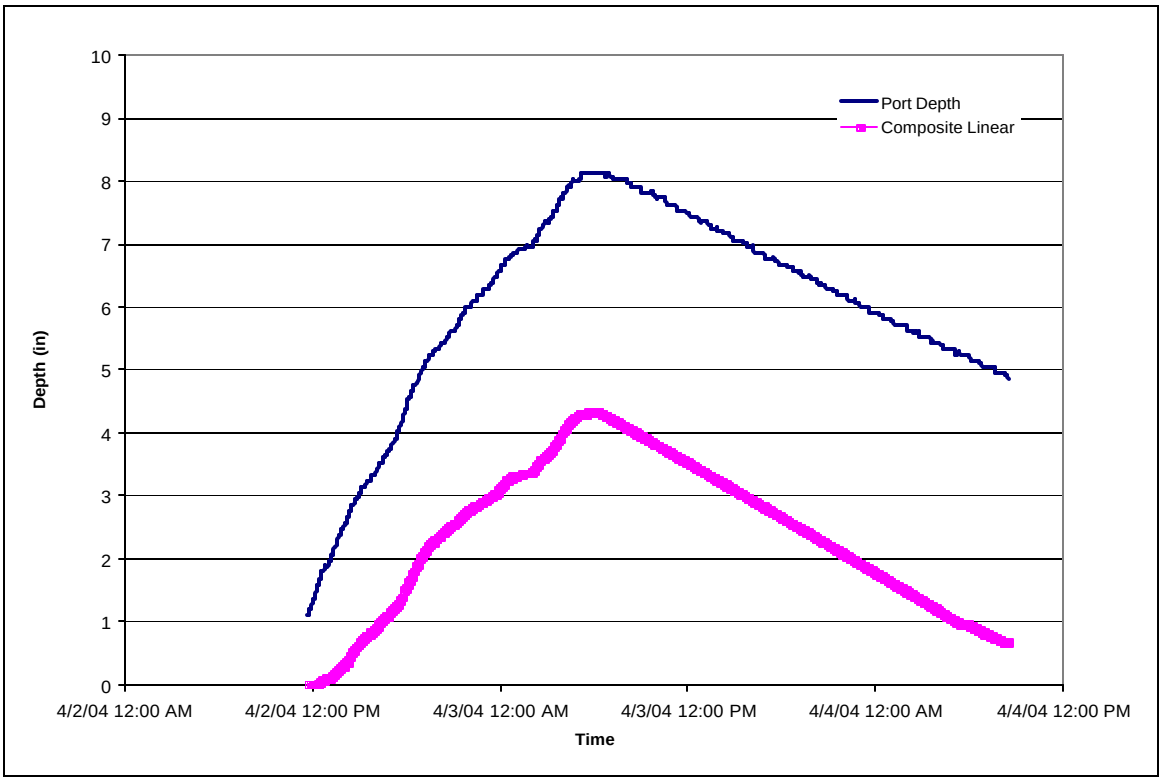

Figure 39: Second storm event for linear model

Due to the uncertainty associated with the linear model, one of the elevation curves for the storm events was above the observed water surface elevation and one was below. Both storms had comparable rainfalls. The slope in Figure 38 is slightly steeper than the observed water surface slope whereas in Figure 39, the slope is a good match to what occurred. This helps to illustrate the impact the variables have on the output of the system and the effect initial losses have, especially during small storm events.

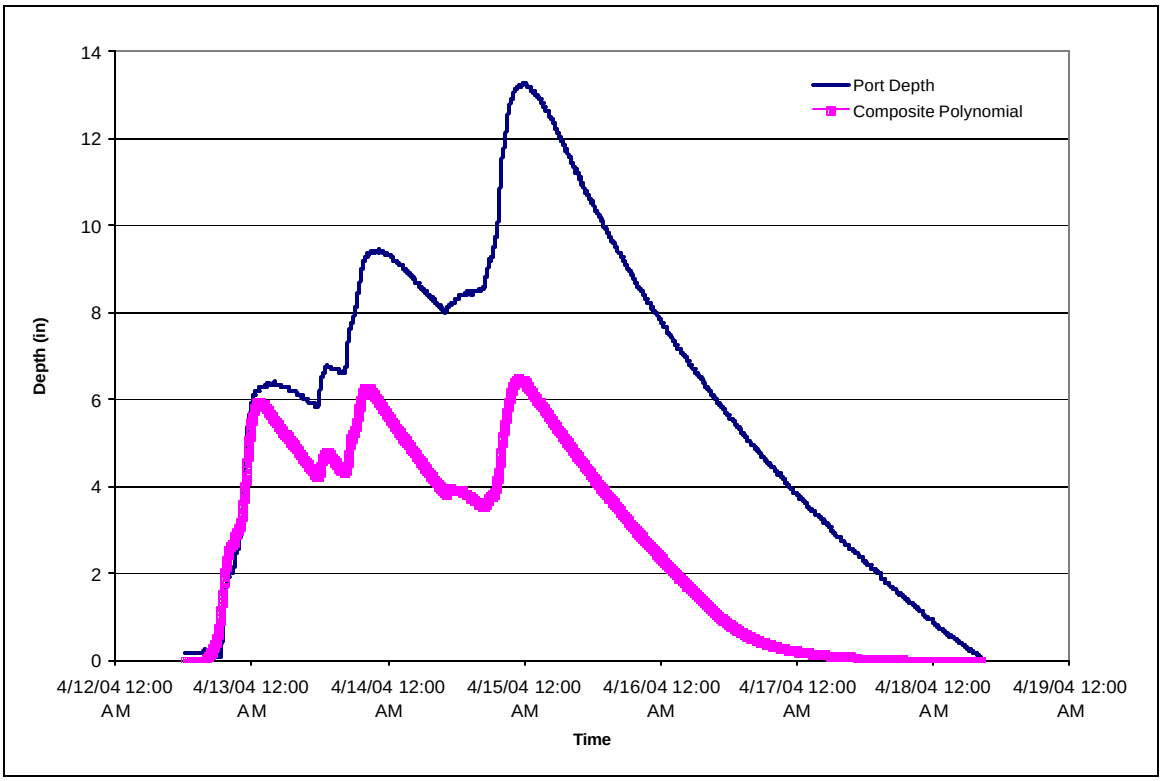

Figure 40: Verification storm event for polynomial model

The verification storm for the composite polynomial model (Figure 40) produced a closer approximation of the observed curve than the composite linear model did for its storm events. The model was able to mimic the timing of the multiple peaks of the storm but could not produce its maximum heights. The occurrence of smaller peaks means that there was not as much runoff calculated in the model as there was on the site. This is evident from the change in storage volume between the two curves (Table 5). This was most likely due to the composite infiltration rate and how the model used it through the duration of the storm event. The infiltration rate was developed using the receding limb of previous storm event curves. This meant that the infiltration beds had already filled before this relationship could be applied. What the model was doing was applying the composite rate to the system as the beds were filling. This infiltrated the maximum

amount, up to that rate, for each time step as the model ran, lessening the amount of water that made its way to the bottom infiltration bed. The slopes of the receding limbs of the second and third peaks demonstrate a close match with the observed. This shows that once the bed has reached its maximum elevation and there is no more rainfall, the model can do a successful job of modeling the infiltration rate.

Chapter 5 – Conclusions

After extensive study and observations, it was found that the site performed as designed, although most likely not in the manner it was expected to. Lessons were learned regarding what works and what does not dealing with the design and construction of a Porous Concrete Infiltration Basin BMP. The two-inch rainfall event was successfully captured and infiltrated with the exception of a small amount bypassing the infiltration beds. The infiltration rate from the receding limb of the infiltration bed curves varied between 0.1 and 0.3 inches per hour depending on the maximum surface water elevation in the beds. It was found that it is possible to create a hydrologic computer model of the site. The results from the models were encouraging. They show that, based on limited information and numerous assumptions, fairly accurate results can be obtained for storm events with greater than 1-inch of precipitation. The results also identified the importance of including the infiltration process in creating a successful model. The overall success and accuracy of the model however, are ultimately based on the variety and accuracy of the data available. More detailed information regarding the initial infiltration bed losses and the processes taking place in the other two infiltration beds are required for further model calibration. It was also realized that during the process of creating a composite model from a number of different storm events, tradeoffs needed to be made. Each storm event had its own specific behavior and properties that were not necessarily addressed or that had to be mitigated in the composite models.

There were many factors relating directly to the construction and layout of the site that caused the modeling process to be complex. One of the biggest factors was that there was no way to accurately measure the inflow into the infiltration beds. This was

due to the number and variety of inflow points. Assumptions needed to be made and inflows back calculated from observed and recorded data. Outflow was another factor that complicated modeling. Outflow from the site could either be measured over the V-Notch weir, which never occurred during this study, through infiltration and losses from the grass, or infiltration from the infiltration beds that could only be measured from the observation port in the lower bed.

To further complicate the process, the infiltration beds were not constructed to specifications and only one infiltration bed, the lower one, was instrumented. Based on the measurements from this one infiltration bed, assumptions needed to be made regarding the performance of the other two beds. It was assumed that because the upper infiltration bed was not directly connected to the middle bed, none of the runoff entering the bed would have any effect on the rest of the system. Based on the amount of runoff entering the bed and the slope of the site, some water probably did pass through the earthen berm connecting the two beds; however this is difficult to prove. Another assumption regarding the middle infiltration bed was that there was very little storage occurring, even though the bed had the largest available storage volume. This was based on the water profile of the site, Figure 3, which shows that the majority of the water would flow through the small pipe to the lower bed. Because the bottom of the bed was level, the middle bed was probably storing some water, but how much was unable to be determined without further instrumentation. Assumptions also needed to be made regarding the lower infiltration bed itself. It was assumed that the bottom of this bed was also level. If that was not the case, water would pool in the bottom end of the bed, where the pressure transducer was located, thereby showing a greater depth of water than what

was actually in the bed. This error could be further compounded by the use of the Storage Indication Method. One shortcoming of the method is its inability to successfully track the movement of water across the bottom of the bed. It assumes the bed will fill at an even rate, utilizing the entire area of the bottom of the infiltration bed. Again, whether any pooling was occurring in the infiltration bed or not is conjecture. To create a successful hydrologic computer model, more assumptions are required. Curve numbers and lag times for the subbasins were based on average conditions across the drainage areas. Some areas of the site could have had a greater impact on the system but their effects were mitigated in the modeling process.

Although modeling is possible, modeling small storm events in particular can be very difficult. One of the main reasons is due to greater sensitivity to changes of the variables entered into the model. It was found that a slight change in one of the many variables had an impact on the system and the output from the composite linear model. For example, the SCS Curve Number Method was specifically designed for use on larger storm events (Rallison 1980). In the development of the method, storm events of 2 inches or more were used to create the relationships. This means that the method itself is not geared toward successfully dealing with smaller events, which is indicated by the model results for the linear composite model. The composite polynomial model however, worked very well in most cases. Many of the reasons it worked so well are the same as why the linear model did not work. The impacts of the numerous variables and the assumptions that were made were minimized due to the higher volumes. The composite polynomial model was used to model larger storm events, i.e. events with around an 1-inch or more of precipitation and a maximum water surface elevation of 8 inches or more.

This greater precipitation and volume meant that the effects of error in the variables were minimized because more runoff was being produced throughout the site. For smaller storm events the amount of rainfall taken up by initial losses in the infiltration beds and depressions throughout the site could be a significant amount, for larger events that amount is not that significant when compared with the total precipitation.

There are two causes as to why the linear composite model over predicted the runoff. The first is that the site is not being hydrologically modeled correctly. The Basin Model layout of the site and the site's hydrologic characteristics were determined based on observations and recorded data. Some of that could have been wrong and the model is reflecting that as discussed previously regarding the SCS Curve Number Method and the Storage Indication Method. The second reason for the excess runoff could be due to initial losses within the infiltration beds, which are occurring on the site at the beginning of the rainfall event while the infiltration beds are filling. Initial losses are directly related to the antecedent moisture content (AMC) of the soil. When it has not rained in a while, the void spaces of the soil, as well as any depressions on the site, are empty. Because of this, more of the initial rainfall is soaked up or held, thereby allowing less to become runoff. Conversely, if a rainfall event had occurred a day or two before, there would be no place for the water to go except runoff from the site.

This occurrence also shows the importance of time when dealing with infiltration. Based on the results of this study and from observations from the recorded water surface elevation, it was found that the time between events is important not only in modeling the site but in the site design itself. It has been shown previously that the maximum elevation the water reaches in the bed determines how long it takes for the bed to empty.

In a number of observed cases, the lower infiltration bed had not completely emptied before the beginning of the next storm event. This addition of runoff not only complicates efforts to model the bed for the initial storm event, but it also changes the infiltration characteristics of the new storm. The starting elevation is now at some higher elevation instead of the bottom of the bed. The infiltration rate for both storm events is also changed due to the increase in pressure on the water that is already there and the fact that the soil is already saturated. In most case, it takes approximately three days for the infiltration beds to completely empty, based on the infiltration rates calculated for each storm. The likelihood of this occurring must be taken into account in the design when the infiltration beds are sized. It must be realized that the total volume for storage and infiltration may not always be available. Duration of the storm event itself is also an important factor. As seen previously in Figure 36, the initial losses had a greater effect at the beginning of the event but as the event continued; the losses played a much smaller role as seen by the peaks of the three curves getting closer. This is also reflected in the peak errors in Table 4. Large storm events had a smaller error between peaks later on during the event; peaks that occurred after it had been raining for a while. The errors for the larger storm events also varied between positive and negative. A truly calibrated model would have half of the events with positive error and half with negative. That is not the case with the linear composite model for the small storm events. For all six events, the model output was higher than the observed water surface elevation as shown by the negative numbers in Table 3. This further emphasizes the fact that there is some type of loss occurring at the beginning of rainfall events that the model is not accounting

for. This magnitude of the loss and the effect on the system decreased as the size of the storm event increased.

From a capture efficiency standpoint, the design of the site was good. The three infiltration beds provided adequate storage to capture and infiltrate the two-inch rainfall storm events that they were designed to hold. The overflow pipe located at 18 inches was sufficiently high enough to ensure the runoff from these storm events remained in the bed. The fact that the rooftop gutters and downspouts were directly connected to the infiltration beds helped to capture more of the total rainfall. The design of the infiltration beds to have pipes connecting them was good, if only the topography of the land cooperated. Due to the slope of the site and the manner in which the infiltration beds were constructed, there was no way the water would ever fill the lower bed and backflow into the middle bed, taking advantage of its extra storage capacity. Future design practices should take note of this occurrence and design accordingly. From a total capture standpoint, these losses increase the overall efficiency of the site. Although the runoff is not reaching the infiltration beds, the runoff is still remaining on site and either evaporating over time or infiltrating through the grass areas on the site.

Overall, the site was a success in terms of capturing and infiltrating the size rainfall event for which it was designed. The majority of the runoff that occurred on the site was collected in the infiltration beds and allowed to infiltrate. Another portion of the runoff was still kept on site through initial losses and abstractions. Modeling the site was difficult due to the numerous variables encountered both on the site and in the model, but two models were successfully created. These models, for the most part, represent the general functioning of the infiltration beds and offer acceptable approximations of each

storm event. Continued study and data collection are required to further calibrate the models.

Future Recommendations and Research

- Design
  - More runoff should be captured and infiltrated by the BMP. The inlet at the top of the site should be lowered to make it level with the drainage path. This would help to capture more runoff from the upper third of the site.
  - A sediment trap should be installed in the inlet to reduce the amount of leaves and sediment entering the BMP as discussed in Kwiatkowski (2004).
  - More comprehensive monitoring is needed. Pressure transducer probes or another type of water depth measuring device should be installed in the upper and middle infiltration beds. This would help understand what infiltration is occurring in them.
  - Low flow bypass piping between the infiltration beds do not need to be used in future designs to promote maximum storage and infiltration. If piping is required, values should be used to restrict flow between beds. Making use of the extra storage capacity available in each infiltration bed would increase the overall effectiveness of the site.
  - The use of multiple smaller beds with shallower slopes between them could promote the occurrence of backwater between the infiltration beds.

- Maintenance
    - Maintenance should be performed on a periodic basis, every six months to one year, to open up any flow pathways that may have become clogged.
- Research
    - This study identified the significant impact initial losses within the infiltration beds have on the system. That impact should be further examined.
        - The use of a diversion element in the hydrologic model before the reservoir element could help to model the initial losses occurring in each infiltration bed.
        - Multiple peaking rainfall events (Figure 28) can be used as the basis for future research.
        - The effect of time between storm events on the site should be further investigated. This would determine what effect the antecedent moisture content has on the performance of the infiltration beds.

Funding

Funding for this project was provided by the United States Environmental Protection Agency through Pennsylvania Department of Environmental Protection's 319 Non-Point Source Pollution Program and Villanova University through the Villanova Urban Stormwater Partnership.

Lessons Learned

An article discussing the lessons learned with the porous concrete material and installation will be published in the August edition of Stormwater Management Magazine (Traver et al. 2004)

List of References

American Society for Testing Materials (2001), "Standard Test Method for Open Channel Flow Measurement of Water with This-Plate Weirs (D 5242-92)," ASTM International.

Adams, M. C. (2003). "Porous Asphalt Pavement With Recharge Beds: 20 Years and Still Working." Stormwater Magazine, X(X), XXX-XXX.

Barbosa, A. E., and Hvitved-Jacobsen, T. (2001). "Infiltration Pond Design for Highway Runoff Treatment in Semiarid Climates." *Journal of Environmental Engineering*, 127(11), 1014-1022.

Beighley, R.E., and Moglen, G.E. (2002). "Trend Assessment in Rainfall-Runoff Behavior in Urbanizing Watersheds." *Journal of Hydrologic Engineering*, 7(1), 27-34.

Cahill Associates, Environmental Consultants (2003). http://www.thcahill.com

Campbell Scientific (2003). "CR200 Datalogger Operator's Manual." Campbell Scientific, Logan, UT.

Campbell Scientific (2000). "CR23X Micrologger Operator's Manual." Campbell Scientific, Logan, UT.

Campbell Scientific (2002). "LoggerNet User Manual Version 2.0." Campbell Scientific, Logan, UT.

Campbell Scientific (2003). "NL100/105 Network Link Interface Instruction Manual." Campbell Scientific, Logan, UT.

Campbell Scientific (2003). "TE525 Tipping Bucket Rain Gage." Campbell Scientific, Logan, UT.

Dumont, J. (2003). "East Clayton Stormwater Infiltration Systems Design and Predicted Operation." *2003 Georgia Basin/Puget Sound Research Conference*. Puget Sound Action Team, Westin Bayshore, Vancouver, British Columbia.

Eco-Creto of Texas, Inc. (2004). http://www.ecocreto.com

Emerson, C. (2003). "Evaluation of the Additive Effects of Stormwater Detention Basins at the Watershed Scale." *Masters Thesis*. Drexel University, Philadelphia, PA.

Federal Emergency Management Agency (FEMA) (2004). "Environmental and Historic Preservation and Cultural Resources Programs." http://www.fema.gov/ehp/cwa.shtm

Field, R., Masters, H., and Singer, M. (1982). "Porous Pavement: Research, Development, and Demonstration." *Transportation Engineering Journal*, 108(3), 244-258.

Instrumentation Northwest (2002). "PS-9805 Submersible Pressure/Temp. Transducer Instruction Manual." Instrumentation Northwest, Kirkland, WA.

Instrumentation Northwest (2002). "Submersible Pressure Transmitter PS9800 Instruction Manual." Instrumentation Northwest, Kirkland, WA.

Konrad, C. P., and Burges, S. J. (2001). "Hydrologic Mitigation Using On-Site Residential Storm-Water Detention." *Journal of Water Resources Planning and Management*, 127(2), 99-107.

Kwiatkowski, M. (2004). "Water Quality Study of a Porous Concrete Infiltration Best Management Practice." *Masters Thesis.* Villanova University, Villanova, PA.

Lathia, D. (2002). "Pennsylvania Act 167 Stormwater Management Planning Program." *New Directions in Stormwater Management*, Villanova University, Villanova, PA.

Lawrence, A. I., Marsalek, J., Ellis, J. B. and Urbonas, B. R. (1996). "Stormwater Detention & BMP's." *Journal of Hydraulic Research*, 34(6), 799-813.

Lee, J. G., and Heaney, J. P. (2003). "Estimation of Urban Imperviousness and its Impacts on Storm Water Systems." *Journal of Water Resources Planning and Management*, 129(5), 419-426.

Mays, L. W. (2001). Water Resources Engineering, 1st ed., (1), Wiley, New York, NY, 262-268.

McCuen, R.H. and Moglen, G. E. (1988). "Multicriterion Stormwater Management Methods." *Journal of Water Resources Planning and Management*, 114(4), 414-431.

Mikkelsen, P.S., Jacobsen, P., and Fujita, S. (1996). "Infiltration Practice for Control of Urban Stormwater." *Journal of Hydraulic Research*, 34(6), 827-840.

Moglen, G.E. and McCuen, R. H. (1988). "Effects of Detention Basins on In-Stream Sediment Movement." *Journal of Hydrology*, 104,129-139.

Nehrke, S. M., and Roesner, L. A. (2004). "Effects of Design Practice for Flood Control and Best Management Practices on the Flow-Frequency Curve." *Journal of Water Resources Planning and Management*, 130(2), 131-139.

Pennsylvania Department of Environmental Protection (2004). http://www.dep.state.pa.us/

Prokop, M. (2003). "Determining the Effectiveness of the Villanova Bio-Infiltration Traffic Island in Infiltrating Annual Runoff." *Masters Thesis.* Villanova University, Villanova, PA.

Rallison, R. E. (1980). "Origin and Evolution of the SCS Runoff Equation." *Symposium on Watershed Management 1980*. ASCE, Boise, ID.

Rosener, L., Bledsoe, B. P., and Brashear, R. W. (2001). "Are Best-Management-Practice Criteria Really Environmentally Friendly?" *Journal of Water Resources Planning and Management*, 127(3), 150-154.

Stormwater Manager's Resource Center (2003). http://www.stormwatercenter.net

Strecker, E. W., Quigley, M. M., and Urbonas, B. R., Jones, J. E., Clary, J. K. (2001). "Determining Urban Storm Water BMP Effectiveness." *Journal of Water Resources Planning and Management*, 127(3), 144-149.

STV Inc., (2004). http://www.stvinc.com

Traver, R. G., Chadderton, R. A., (1983). "The Downstream Effects of Storm Water Detention Basins." *1983 International Symposium on Urban Hydrology, Hydraulics and Sediment Control*, University of Kentucky, Lexington, KY.

Traver, R. G., Welker, A., Emerson, C., Kwiatkowski, M., Ladd, T., Kob, L. (2004). "Lessons Learned – Porous Concrete Demonstration Site." *Stormwater* 5(6).

Traver, R. G., Welker, A. (2003). "Quality Assurance – Quality Control Project Plan" Villanova Stormwater Porous Concrete Demonstration Site – A Retrofit.

Thurston, H.W., Goddard, H.C., Szlag, D., and Lemberg, B. (2003). "Controlling Storm-Water Runoff with Tradable Allowances for Impervious Surfaces." *Journal of Water Resources Planning and Management*, 129(5), 409-418.

U.S. Army Corps of Engineers Hydrologic Engineering Center (2001). "Hydrologic Modeling System HEC-HMS User's Manual; Version 2.1." U.S. Army Corps of Engineers Hydrologic Engineering Center, Davis, CA.

U.S. Army Corps of Engineers Hydrologic Engineering Center (2003). "HEC DSS Vue HEC Data Storage System Visual Utility Engine User's Manual; Version 1.0." U.S. Army Corps of Engineers Hydrologic Engineering Center, Davis, CA.

U.S. Environmental Protection Agency (USEPA) (2002). "National Management Measures to Control Nonpoint Source Pollution from Urban Areas".

U.S. Environmental Protection Agency (USEPA) (2003). "National Pollutant Discharge Elimination System." Office of Wastewater Management. http://cfpub2.epa.gov/npdes

Viesmann, W., Lewis, G. L. (1995). "…" Introduction to Hydrology, 4th ed., (1), Addison-Wesley, Boston, MA., 211-213.

Whipple, W. (1991). "Best Management Practices for Storm Water and Infiltration Control." *Water Resources Bulletin*, 27(6), 895-902.

Appendix A – Instrumentation

The first component of the water quantity balance is precipitation. For rainfall measurements a Campbell Scientific (CS) Tipping Bucket TE525WS Rain Gage (Campbell 2000c) was installed. In conjunction with the rain gage, accurate outflow measurements are necessary to properly assess the effectiveness of the BMP for infiltrating runoff. The infiltration storage beds are interconnected and drain to the lower bed as mentioned in previous sections. The lower storage bed is equipped with an Instrumentation Northwest (INW) PS-9805 Pressure/Temperature Transducer which measures the water surface elevation and water temperature in the bed. The probe is located in the junction box in the lower corner of the infiltration bed as discussed previously. An INW PS-9800 Pressure/Temperature Transducer and V-notch weir were installed in the catch basin at the downstream end of the overflow pipe. The transducer, in conjunction with the weir, gives an accurate flow rate measurement of water leaving the site. A CS CR23X Micrologger (Campbell 2000) is used to power the instruments and collect and store data. A CS CR200 Datalogger (Campbell 2003a) is used to collect and store data from the Tipping Bucket Rain Gage. Two CS NL100 Network Link Interfaces (Campbell 2003b) connect the Loggers to the Villanova computer network.

Configuration

The CS CR23X Micrologger is the primary data acquisition device for the majority of the instruments. The CS CR200 is the primary acquisition device for the CS Tipping Bucket Rain Gage. Both Loggers are connected to the Network Link Interfaces (NLI) using standard 9 pin communications cables. The NLIs are in turn connected to the University's 10 Base-T port using twisted pair cables with male RJ-45 plug

connectors. The Campbell Scientific TE525WS Tipping Bucket Rain Gage is connected to the Datalogger using the P_SW Pulse Channel Input and two Ground Terminals. The INW 9805 Pressure/Temperature Transducer is connected to the Micrologger using two Voltage Excitation Channels, two full Differential Channels, one Single Ended Analog Channel, and three Ground Terminals. The INW 9800 Pressure/Temperature Transducer is connected using one 12 Volt Output Channel, one Single Ended Analog Channel, and one Ground Terminal.

LoggerNet software Version 2.1c (Campbell 2002) is used in conjunction with both Loggers. The software allows users to set up, configure, and retrieve data from the Loggers remotely through the University's network. The Edlog program is used for the creation, editing, and documenting of programs for the CR23X Micrologger. The "Short Cut for Windows" program is used for the creation, editing, and documenting of the program for the CR200 Datalogger. Edlog uses a programming language designed specifically for Campbell Scientific Dataloggers. Short Cut uses a programming language similar in structure to the BASIC programming language. Each instrument requires unique instruction commands to function. These instructions are discussed more in the following sections. The time intervals, data format, and storage locations are also set in the program editors. The Loggers' Battery voltages are monitored to prevent any lost of data due to low battery voltage. Table A-1 shows the various measurements, the units in which they are recorded, and the recording time intervals. The complete Edlog program can be found on page 96.

Measurement	Units	Time Increment
Battery Voltages	Volts	1 hour
Rainfall	Inches	5 minutes
Port Water Depth	Inches	5 minutes
Port Temperature	^{o}C	5 minutes
Weir Water Depth	Inches	5 minutes

Table A-1: Measurement units and time increments

The Campbell Scientific TE525WS Tipping Bucket Rain Gage features an eight-inch collector with tips of 0.01 inches per tip. The rain gage has a 6.25 inch overall diameter, a height of 9.5 inches and weighs two and a half pounds. The funnel is a gold anodized spun aluminum knife-edge collector ring and funnel assembly. The funnel collector diameter is 8 inches. The rain gage features a side bracket with clamps for pole mounting. The gage was mounted on the North side of Bartley Hall to a pole on the roof.

The rain gage connector cable is a two-conductor shielded cable. The signal output is a momentary switch closure that is activated by the tipping bucket mechanism. See Table A-2 for the rain gage wiring summary. In the CR200 Datalogger program created by Short Cut, the rain gage functions are programmed using the "PulseCount" command for rainfall measurement. The Pulse Channel, Configuration, and counting method are all set in this command. The multiplier used in the command determines the units in which the rainfall is reported. In this case, the units have been kept in inches using a multiplier of 0.01 inches per tip. The program is set to run one repetition every five minutes thereby recording the number of tips in the previous five minutes. The program then stores the values in the Rainfall table on the Datalogger. The rain gage has

a resolution of one tip. It can function properly in temperatures between 0^{o} and $+50^{o}$C and humidity between 0 and 100%. The complete Short-Cut program can be found on page 102.

Color	Function	Connection
Black	Signal	Pulse Ch. P_SW
White	Signal Return	Ground
Clear	Ground at logger	Ground

Table A-2: Wiring summary for the rain gage

The INW PS-9805 Pressure Transducer is connected to the CR23X Micrologger by a nine conductor vented cable. The cable is run through the wall of the catch basin in a 1.5" diameter electrical conduit directly to the basement of Sullivan Hall where the Micrologger is located. The wiring summary is shown in Table A-3.

Color	Function	Micrologger Connection
White	V(+) excitation (800 mV)	Excitation Ch. EX1
Green	Analog Ground	Ground
Blue	Vr (+)	Differential Ch. 7H
Red	Vr (-)	Differential Ch. 7L
Yellow	Vo (+)	Differential Ch. 8H
Purple	Vo (-)	Differential Ch. 8L
Shield	Ground at logger	Ground
Orange	(T1) temperature excitation	Excitation Ch. EX2
Brown	(T2) temperature out	Single Ended Ch. 18
Black	Temperature analog ground	Ground

Table A-3: Wiring summary for the 9805 Pressure Transducer

In addition to the nine conductors and shield there is also a vent tube in the cable. This vent tube enables the pressure transducer to reference atmospheric pressure as detailed in the Analytical Methods section below. The pressure transducer is programmed using "Instruction 8" in Edlog. "Instruction 8" is an Input/Output Instruction that applies an excitation voltage, delays for a specified amount of time, and then makes a differential voltage measurement (Campbell 2002). The transducer is excited and records a port water depth and port temperature every five minutes. The Micrologger stores this data in arrays 103 and 104 respectively. The complete program can be found in Appendix A.

The INW PS-9800 Pressure Transducer is also connected to the CR23X Micrologger by a nine conductor vented cable. Of the nine conductors, three are in use. A 100-ohm resistor is also used connecting the Single Ended Channel and the Ground

Terminal to complete the voltage loop. The cable is run into Sullivan Hall in the same manner as the INW PS-9805. The wiring summary for this Pressure Transducer is shown below in Table A-4.

Color	Function	Micrologger Connection
Blue	Pressure signal return	Single Ended Ch. 24
White	V (+) pressure	12 Volt Output Channel
Shield	Ground at logger	Ground

Table A-4: Wiring summary for the 9800 Pressure Transducer

As with the INW PS-9805, the PS-9800 also has a vent tube in the cable that enables atmospheric pressure to be referenced. The PS-9800 Pressure Transducer is programmed using "Instruction 1" in Edlog. "Instruction 1" is an Input/Output Instruction that measures the input voltage with respect to ground with the output is measured in millivolts (Edlog On-Line Help). The PS-9800 Transducer is excited and records the water surface elevation behind the weir every five minutes. The Micrologger stores this data in array 105.

Analytical Methods

The INW PS-9805 Pressure Transducer indirectly measures both the absolute pressure and the atmospheric pressure. The difference between these pressures is the hydrostatic pressure created by the depth of ponded water. The depth of water is directly related to the hydrostatic pressure exerted by the water. This relation is shown below:

$$P = g * h \quad \text{(A-1)}$$

Where:

P = pressure in lb/in^2 (psi)

γ = specific weight of water in lb/ft^3

h = height of water in ft

The transducer sends a voltage signal representing each pressure measurement. The CR23X then calculates a ratio (L) of the signals as follows:

$$L = 100 * \frac{V_0}{V_r} \quad \text{(A-2)}$$

Where:

V_o = voltage corresponding to the absolute pressure at the depth of the transducer (mV)

V_r = voltage corresponding to the atmospheric pressure (mV)

The ratio is then converted to a pressure by the following formula:

$$P = m * L + b \quad \text{(A-3)}$$

Where:

P = pressure (psi)

m = calibration constant

b = calibration constant (psi)

The calibration procedure is outlined below in the Instrument Calibration and Frequency section. The pressure is then converted to a depth of water by means of the following equation:

$$h = [P * 2.31 ft \frac{H_2 0}{psi}] * 12 \frac{in}{ft} \quad \text{(A-4)}$$

Where:

h = depth of water (in)

The PS-9800 Pressure Transducer also indirectly measures absolute pressure and atmospheric pressure. Zero pressure, the pressure exerted when the probe is above the surface of the liquid, is converted to a current flow of 4 mA. The increase in current is linear with the increase in liquid depth until a maximum value of 20 mA is reached. From this linear plot, “m” and “b” values can be obtained for the slope and y-intercept of the line. I think these constants take into account unit conversion to inches.

$$h = (m * V) + b \quad \text{(A-5)}$$

Where:

h = depth of water (in)

m = calibration constant

b = calibration constant

V = mA draw

The geometry of the V-notch weir makes it ideal for accurately measuring both low and high flows. The weir was machined from a ¼" 6061 Aluminum plate. This alloy is both easily machined and is resistant to weathering. The weir plate was securely mounted and sealed to a cedar frame. The frame was lug-bolted and caulked into the concrete catch basin. A ½" clear Plexiglas cover was installed over the area of the catch basin upstream of the weir. This cover prevents off-site run-off from being included in outflow measurements. The design, construction, and discharge coefficient of the weir are based on the guidelines set in the ASTM Standard Test for Open-Channel Flow Measurement of Water with Thin-Plate Weirs (ASTM, 1996). The weir is 15" high and 18" wide with an angle of approximately 62 degrees. The INW 9800 Pressure Transducer is securely fastened to the upstream face of the weir. The crest of the weir is 14.82 in above the transducer. Therefore the head on the weir is equal to the depth of water minus 14.82 in. This calculation and the corresponding flow rate calculation are done manually and results are kept in the main data spreadsheet. See the Data Management section below for more information on the data spreadsheets. With a maximum head of 15 inches, the weir can measure flows from 0 to 2.6 cfs as shown in the rating curve in Figure. The equation used to relate depth of water to flow rate for this weir is below.

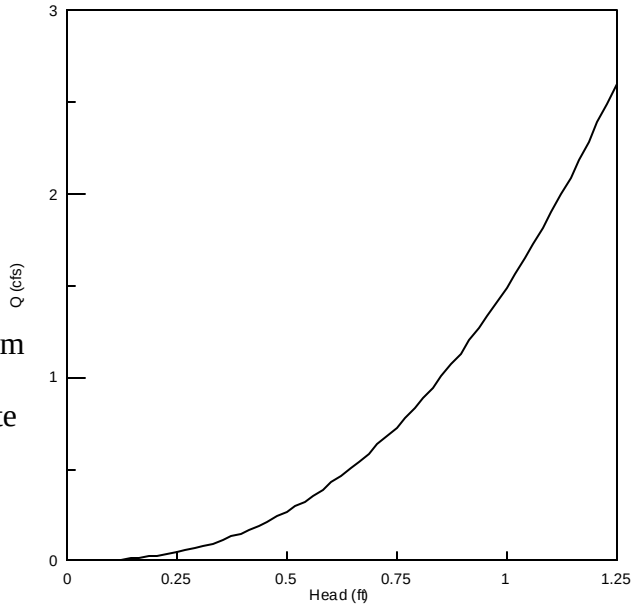

Figure A-1: Weir rating curve

$$Q = (\frac{8}{15})(2 * g)^{\frac{1}{2}} C_{et} \tan(\frac{q}{2})(H + d_{Ht})^{\frac{5}{2}} \quad \text{(A-6)}$$

Where:

g = gravity (ft/s^2)

C_{et} = is the coefficient of discharge, 0.575

q = angle of V-notch (radians), 1.08

H = head on weir (ft)

δ_{Ht} = head correction, 0.004 ft

Quality Control

The data is downloaded and reviewed on a weekly basis. A quality control review is conducted to check the data for erroneous values.

Instrument Testing, Inspection, and Maintenance

The Campbell Scientific CR23X Micrologger is mounted and locked inside a 16" by 18" Campbell Scientific enclosure along with the NL 100 Network Link Interface. The enclosure is mounted to a concrete wall in a closet in the basement of Sullivan Hall, the dormitory building adjacent to the site. The enclosure contains packets of desiccant to protect the equipment from moisture. There is a humidity indicator on the inside panel of the enclosure that is checked on a monthly basis to insure that the desiccant is still effective. The Ground Lug on the Micrologger is connected to a lug on the enclosure, which is in turn connected to the building's ground in an electrical outlet using 12 American Wire Gage (AWG) copper wire as per the manufacturer's instructions. The CS CR200 Datalogger and NL 100 are mounted in a similar fashion inside a 10" by 12" Campbell Scientific enclosure. The enclosure is securely mounted to a metal beam on

the roof of Bartley Hall, the neighboring Commerce and Finance building. Desiccant packets and a humidity indicator are also contained in the enclosure. The Ground Lug on the Datalogger is connected to a lug on the enclosure, which is in turn connected to a metal support beam using 12 AWG copper wire.

The Campbell Scientific Tipping Bucket TE525WS Rain Gage requires minimal maintenance. There is a bubble level inside the gage to insure the gage is properly leveled. The rain gage debris filter, funnel, and the bucket reservoirs should be kept clean. Common causes of inaccurate rainfall measurements are birds and other wildlife. To prevent birds and other wildlife from tampering with the gage, a ring of Nixalite Model S bird control wire was installed around the funnel of the rain gage. The bird wire consists of a series of stainless steel needles set at various angles. "The deliberate pattern creates a barrier that keeps birds and other climbing animals off of surfaces and structures" according to the company's website. To this date, the bird wire has been successful and no problems with birds or other animals have been encountered.

The accuracy of the gage varies depending on the rainfall rate. With a rainfall rate of up to one inch per hour, the gage is accurate to within ± 1%. For a rainfall rate between one to two inches per hour, the accuracy of the gage is between 0 and -2.5%. For rainfalls over two inches per hour, the accuracy is between 0 and -3.5%. The Rain Gage is located in close proximity to the site as recommended by the EPA manual Urban Stormwater BMP Performance Monitoring. There are two other data logging rain gages located within a quarter-mile used to verify the rainfall data collected at the site.

The INW pressure transducers and V-notch weir are inspected on a monthly basis. Visual observations are compared to recorded data for quality control purposes. The

pressure transducers' vent tubes have desiccant tubes that are located on the Micrologger end of the cables. The desiccant is checked at least once every two months as per the manufacturer's specifications. The desiccant should be bright blue, as moisture is absorbed the desiccant becomes lighter in color and will need to be replaced. If viable desiccant is not maintained permanent damage may occur to the transducers.

Instrument Calibration and Frequency

The Campbell Scientific TE525WS Tipping Bucket Rain Gage is calibrated in the factory and should not require field calibration. However, Campbell Scientific includes a calibration check in the TE525WS Tipping Bucket Rain Gage Instruction Manual. They recommend this check, which is described below, every 12 months.

> Secure a metal can with a capacity of at least one quart of water. Punch a very small hole in the bottom of the can. Place the can in the top funnel and pour 16 fluid ounces of water into the can. If it takes less than forty-five minutes for the water to run out, the hole in the can is too large. For the TE525WS Rain Gage, 57 ± 2 tips should occur. If adjustment is required, adjusting screws are located on the bottom of the gage adjacent to the large center drain hole. Adjust both screws the same number of turns. Rotation in the clockwise direction increases the number of tips while counterclockwise rotation decreases the number of tips. One half turn of both screws causes a 2-3% change. After adjustment, check and re-level the rain gage lid. If factory recalibration is required, contact Campbell Scientific.

The calibration constants for the pressure transducers are determined by a simple calibration procedure. For the PS-9805 Pressure Transducer, the probe is first left unsubmerged and Voltage readings are taken. The probe is then submerged under known depths of water with calculated hydrostatic pressures and corresponding readings are taken. L is plotted versus P as illustrated in Figure A-2 below. The slope of the line is the 'm' calibration constant and the y-intercept is the 'b' constant. For the 9805 Pressure Transducer, SN#2233005, the 'm' and 'b' constants are 0.263 and 0.139 psi respectively. For the 9800 Pressure Transducer, the procedure is the same with readings taken in mA instead of Volts. For the probe, SN#2206014, the "m" and "b" constants are 0.00868 and -36.026 respectively. These values are based on a calibration curve of mA plotted against water height in inches. The pressure transducers were factory calibrated at the time of shipment. As per the manufacturer's recommendations, the transducers are recalibrated every six months.

The weir calibration will be verified every 12 months by a manual flow rate measurement taken with a graduated cylinder and stopwatch.

Data Management

The data management goals for both the water quantity and quality aspect of this project are based on the guidelines set in the EPA manual Urban Stormwater BMP Performance Monitoring. The database should be one that is easy to "…store, retrieve, and transfer data…" (EPA, 2002)

Data is downloaded from the CR23X Micrologger and CR200 Datalogger once a week or more often as needed to a computer located in the laboratory. The files obtained from the loggers are *.dat data files. The file name of the data file is the date range for

which the data applies to followed by the letters “pc” to denote that the data file is for the porous concrete site. For example a data file from December 10th 2002 to January 3rd 2003 would be labeled as “12-10-02 to 01-03-03pc.dat”. Rainfall data files follow the same labeling scheme, with the word “rainfall” added after the “pc.” For the CR23X Micrologger, each data file is associated with an *.fsl file. The *.fsl is a final storage label file that is created when the program is compiled in Edlog. It contains all of the column headings for each of the arrays. In each array the following column headings are found: array number and individual columns for year, day, hour, minute, and second that the measurement represents. Since a single program is used, the *.fsl file for all data files is the same. The data files are then opened in Excel and converted into *.xls spreadsheets. The readings from the different sensors are stored in the arrays as prescribed in the Edlog program as seen in Table A-5 below. Array 102 is reserved for instrumentation not associated with this aspect of the BMP study. For more information on the programs see CR23X Micrologger and CR200 Datalogger sections and the program printouts in Appendix A. When converted, the arrays are all located in a single worksheet. Creating an individual worksheet for each array within the Excel file then separates the data. Copies of both the original data files and the Excel spreadsheets are kept locally on the laboratory computer and backed-up on a weekly basis to the University’s network.

The pressure transducer measurements for weir water depth are stored in array 105. Additional columns are added to the Excel spreadsheets, which convert the height of the water in the chamber to head on the weir. That head is then converted to a flow rate using the weir equation for flow over a triangular weir as discussed previously.

Array Number/Table	Instrument	Measurement
101	Micrologger	Battery Voltage
103	9805 Pressure Transducer	Port Water Depth
104	9805 Pressure Transducer	Port Water Temperature
105	9800 Pressure Transducer	Weir Water Depth
Table 1	Rain Gage	Rainfall

Table A-5: Array / Measurement Table

Edlog Program for CR23X Micrologger and Attached Instruments

```
;{CR23X}
;
;Tells the CR23X to run the program in Table 1 every five minutes.
*Table 1 Program
  01: 300       Execution Interval (seconds)

;Instruction that reads the Battery Voltage of the CR23X.
;"Loc 1" Temporarily store the voltage reading in Loc 1.
1:  Batt Voltage (P10)
 1: 1       Loc [ BattVolt  ]

;Do the following set of instructions.
2:  Do (P86)
 1: 41      Set Port 1 High

;Instruction 138 measures the period of the CS616 Water Content Reflectometer.
;There are 4 of these instructions. Each one operates 3 of the CS616s.
;Note: This instruction does not output the Moisture content (see Polynomial p55)
;"3 Reps" Run this instruction 3 times. 4 instructions * 3 reps = 12 CS616s
;"1 SE Channel" SE port 1 on the CR23X (Green wire) the instruction will iterate SE
ports.
```

;"1 C1 ...Control Port" This port enables the CS616s, all 3 CS616s will be attached here (Orange wires)
;"1.0 Mult" No multiplier.
;"0.0 Offset" No offset.

```
   3:  CS616 Water Content Reflectometer (P138)
    1: 3        Reps
    2: 1        SE Channel
    3: 11       All reps use C1
    4: 3        Loc [ A11Period ]
    5: 1.0      Mult
    6: 0.0      Offset

   4:  CS616 Water Content Reflectometer (P138)
    1: 3        Reps
    2: 4        SE Channel
    3: 12       All reps use C2
    4: 6        Loc [ A21Period ]
    5: 1.0      Mult
    6: 0.0      Offset

   5:  CS616 Water Content Reflectometer (P138)
    1: 3        Reps
    2: 7        SE Channel
    3: 13       All reps use C3
    4: 9        Loc [ B11Period ]
    5: 1.0      Mult
    6: 0.0      Offset

   6:  CS616 Water Content Reflectometer (P138)
    1: 3        Reps
    2: 10       SE Channel
    3: 14       All reps use C4
    4: 12       Loc [ B21Period ]
    5: 1.0      Mult
    6: 0.0      Offset
```

;This instruction converts the period from P138 to a Moisture Content.
;"12 Reps" Instruction must convert 12 readings.
;"3 X Loc [MM1Period]" This is the first stored period reading. Iterate from location 3 - 14.
;"15 F(X) Loc [MM1_VWC]" This is the first stored converted value. Iterate from loc. 15 - 26.
;The following coefficients are listed in the CS616 Manual; C0 through C5.

```
   7:  Polynomial (P55)
    1: 12       Reps
    2: 3        X Loc [ A11Period ]
```

```
   3: 15      F(X) Loc [ A11_VWC   ]
   4: -0.358  C0
   5: 0.0173  C1
   6: 0.000156 C2
   7: 0.0     C3
   8: 0.0     C4
   9: 0.0     C5

;This instruction turns the probes off.
   8:  Do (P86)
   1: 51      Set Port 1 Low

;This is the section of code that we're having trouble with.  There are 2 sections, 1 for
;each pressure transducer.  Both are connected following the wiring diagram in the book.
;The first is hooked to Diff channels 7 and 8 (SE 13-16) for the voltages and SE channel
17
;for the temp.
;The white and orange excitation are hooked to EX 1 and 2 respectively.  We decided not
to
;store the L value, the D is depth in inches.
;The second is in Diff channels 10 and 11 and SE channel 23.
;The white and orange for these are in EX 3 and 4.
;Lines 26-43 deal with storing the data.  I'm sure we have some extra lines but it gets us
the
;data the way that we want it.  We put an instruction 71(average), for the differential
;voltages and then instruction 70(sample) for the temps.  Is this right?  We just used what
we
;had for our moisture meters since there were no storage examples in the PS9805 book.
;When we download the data, we're getting -6999 for both Vr's and for both temps.

;Serial #:2233005
;m=0.263, b=0.139

   9:  Ex-Del-Diff (P8)
   1: 2       Reps
   2: 22      50 mV, 60 Hz Reject, Slow Range
   3: 7       DIFF Channel
   4: 1       Excite all reps w/Exchan 1
   5: 1       Delay (0.01 sec units)
   6: 800     mV Excitation
   7: 27      Loc [ Vr1       ]
   8: 1.0     Mult
   9: 0.0     Offset

L1=100*(Vo1/Vr1)
```

```
P1=0.263*L1+0.139

PortDepth=(P1*2.31)*12

    10:  Temp (107) (P11)
     1: 1        Reps
     2: 17       SE Channel
     3: 2        Excite all reps w/E2
     4: 34       Loc [ PortTemp  ]
     5: 1.0      Mult
     6: 0.0      Offset

;Serial #: 2206014
;m=0.0868, b=-36.026

    11:  Volt (SE) (P1)
     1: 1        Reps
     2: 24       1000 mV, 60 Hz Reject, Slow Range
     3: 24       SE Channel
     4: 32       Loc [ Voltage   ]
     5: 1.0      Mult
     6: 0.0      Offset
WeirDepth=((0.0868*Voltage)-36.026)

;These 4 instructions (10 - 13) actually write the battery voltage each hour.
;Instruction (P80) Place the written data in the final storage area 1 in array 101.
;Instruction (P77) Time stamp.
;Instruction (P71) AVERAGE the voltage readings from each program interval.

    12:  If time is (P92)
     1: 0000     Minutes (Seconds --) into a
     2: 60       Interval (same units as above)
     3: 10       Set Output Flag High (Flag 0)

    13:  Set Active Storage Area (P80)
     1: 1        Final Storage Area 1
     2: 101      Array ID

    14:  Real Time (P77)
     1: 1221     Year,Day,Hour/Minute,Seconds (midnight = 2400)

    15:  Average (P71)
     1: 1        Reps
     2: 1        Loc [ BattVolt  ]

;These 4 instructions (18 - 21) actually write the moisture meter data every 30 minutes.
```

```
;Instruction (P80) Write data in the final storage area 1 in array 103.
;Instruction (P77) Time stamp.
;Instruction (P71) Average moisture content over the given program interval.

   16:  If time is (P92)
    1: 0000     Minutes (Seconds --) into a
    2: 15       Interval (same units as above)
    3: 10       Set Output Flag High (Flag 0)

   17:  Set Active Storage Area (P80)
    1: 1        Final Storage Area 1
    2: 102      Array ID

   18:  Real Time (P77)
    1: 1221     Year,Day,Hour/Minute,Seconds (midnight = 2400)

   19:  Average (P71)
    1: 12       Reps
    2: 15       Loc [ A11_VWC   ]

   20:  If time is (P92)
    1: 0000     Minutes (Seconds --) into a
    2: 5        Interval (same units as above)
    3: 10       Set Output Flag High (Flag 0)

   21:  Set Active Storage Area (P80)
    1: 1        Final Storage Area 1
    2: 103      Array ID

   22:  Real Time (P77)
    1: 1221     Year,Day,Hour/Minute,Seconds (midnight = 2400)

   23:  Average (P71)
    1: 2        Reps
    2: 27       Loc [ Vr1       ]

   24:  Sample (P70)
    1: 2        Reps
    2: 30       Loc [ P1        ]

   25:  If time is (P92)
    1: 0000     Minutes (Seconds --) into a
    2: 5        Interval (same units as above)
    3: 10       Set Output Flag High (Flag 0)

   26:  Set Active Storage Area (P80)
```

```
 1: 1        Final Storage Area 1
 2: 104      Array ID
27:  Real Time (P77)
 1: 1221     Year,Day,Hour/Minute,Seconds (midnight = 2400)

28:  Average (P71)
 1: 1        Reps
 2: 34       Loc [ PortTemp  ]

29:  If time is (P92)
 1: 0000     Minutes (Seconds --) into a
 2: 5        Interval (same units as above)
 3: 10       Set Output Flag High (Flag 0)

30:  Set Active Storage Area (P80)
 1: 1        Final Storage Area 1
 2: 105      Array ID

31:  Real Time (P77)
 1: 1221     Year,Day,Hour/Minute,Seconds (midnight = 2400)

32:  Average (P71)
 1: 2        Reps
 2: 32       Loc [ Voltage   ]

End Program

Input Locations

1     [ BattVolt  ]  RW--   1      1     ----- ------ ---
2     [ _________ ]  ----   0      0     ----- ------ ---
3     [ A11Period ]  RW--   1      1     Start ------ ---
4     [ A12Period ]  RW--   1      1     ----- Member ---
5     [ A13Period ]  RW--   1      1     ----- ------ End
6     [ A21Period ]  RW--   1      1     Start ------ ---
7     [ A22Period ]  RW--   1      1     ----- Member ---
8     [ A23Period ]  RW--   1      1     ----- ------ End
9     [ B11Period ]  RW--   1      1     Start ------ ---
10    [ B12Period ]  RW--   1      1     ----- Member ---
11    [ B13Period ]  RW--   1      1     ----- ------ End
12    [ B21Period ]  RW--   1      1     Start ------ ---
13    [ B22Period ]  RW--   1      1     ----- Member ---
14    [ B23Period ]  RW--   1      1     ----- ------ End
15    [ A11_VWC   ]  RW--   1      1     Start ------ ---
16    [ A12_VWC   ]  RW--   1      1     ----- Member ---
17    [ A13_VWC   ]  RW--   1      1     ----- Member ---
```

```
18    [ A21_VWC   ] RW--   1      1      ----- Member ---
19    [ A22_VWC   ] RW--   1      1      ----- Member ---
20    [ A23_VWC   ] RW--   1      1      ----- Member ---
21    [ B11_VWC   ] RW--   1      1      ----- Member ---
22    [ B12_VWC   ] RW--   1      1      ----- Member ---
23    [ B13_VWC   ] RW--   1      1      ----- Member ---
24    [ B21_VWC   ] RW--   1      1      ----- Member ---
25    [ B22_VWC   ] RW--   1      1      ----- Member ---
26    [ B23_VWC   ] RW--   1      1      ----- ------ End
27    [ Vr1       ] RW--   1      1     Start ------ ---
28    [ Vo1       ] RW--   1      1      ----- ------ End
29    [ L1        ] ----   0      0     ----- ------ ---
30    [ P1        ] R---   1      0     ----- ------ ---
31    [ PortDepth ] R---   1      0     ----- ------ ---
32    [ Voltage   ] RW--   1      1     ----- ------ ---
33    [ WeirDepth ] R---   1      0     ----- ------ ---
34    [ PortTemp  ] RW--   1      1     ----- ------ ---
```

Short Cut Program for CR200 Datalogger and TE525 Rain Gage

```
'CR200 Series
'Created by SCWIN (Version 2.0 (Beta))
Public Flag(8)
Public Batt_Volt
Public Rain_in
DataTable(Rainfall,True,-1)
  DataInterval(0,5,Min)
  Totalize(1,Rain_in,0)
EndTable
DataTable(Table2,True,-1)
  DataInterval(0,1440,Min)
  Minimum(1,Batt_Volt,0,0)
EndTable
BeginProg
Scan(5,Min)
' Code for datalogger Battery Voltage measurement, Batt_Volt:
  Battery(Batt_Volt)
' Code for Rain measurement, Rain_in:
  PulseCount(Rain_in,P_SW,2,0,0.01,0)
CallTable(Rainfall)
CallTable(Table2)
NextScan
EndProg
```

Appendix B – Infiltration Bed Calculations

Upper Infiltration Bed Volumne Calculations				
Depth (ft)	Area (ft^2)	Volume (ft^3)	Porosity	Volume of Pore Space (ft^3)
0	1635.62	0.00	0.4	0.00
0.1	2046.61	184.11	0.4	73.64
0.2	2085.51	390.72	0.4	156.29
0.3	2124.65	601.23	0.4	240.49
0.4	2164.03	815.66	0.4	326.26
0.5	2203.65	1034.04	0.4	413.62
0.6	2243.51	1256.40	0.4	502.56
0.7	2283.61	1482.76	0.4	593.10
0.8	2323.94	1713.13	0.4	685.25
0.9	2364.52	1947.56	0.4	779.02
1	2405.34	2186.05	0.4	874.42
1.1	2446.40	2428.64	0.4	971.46
1.2	2487.70	2675.34	0.4	1070.14
1.3	2529.24	2926.19	0.4	1170.48
1.4	2571.02	3181.20	0.4	1272.48
1.5	2613.04	3440.41	0.4	1376.16
1.6	2655.30	3703.82	0.4	1481.53
1.7	2697.80	3971.48	0.4	1588.59
1.8	2740.53	4243.39	0.4	1697.36
1.9	2783.51	4519.60	0.4	1807.84
2	2826.73	4800.11	0.4	1920.04
2.1	2870.19	5084.95	0.4	2033.98
2.2	2913.89	5374.16	0.4	2149.66
2.3	2957.83	5667.74	0.4	2267.10
2.4	3002.01	5965.74	0.4	2386.29
2.5	3046.43	6268.16	0.4	2507.26
2.6	3091.09	6575.03	0.4	2630.01
2.7	3135.99	6886.39	0.4	2754.56
2.8	3181.12	7202.24	0.4	2880.90
2.9	3226.50	7522.63	0.4	3009.05
3	3272.12	7847.56	0.4	3139.02
3.1	3317.98	8177.06	0.4	3270.82
3.2	3364.08	8511.16	0.4	3404.47
3.3	3410.42	8849.89	0.4	3539.96
3.4	3457.00	9193.26	0.4	3677.30
3.5	3503.82	9541.30	0.4	3816.52
3.6	3550.88	9894.04	0.4	3957.61
3.7	3598.18	10251.49	0.4	4100.60
3.8	3645.71	10613.68	0.4	4245.47
3.9	3693.49	10980.64	0.4	4392.26
4	3741.51	11352.39	0.4	4540.96

Middle Infiltration Bed Volume Calculations				
Depth (ft)	Area (ft^2)	Volume (ft^3)	Porosity	Volume of Pore Space (ft^3)
0	3742.94	0.00	0.4	0.00
0.1	5198.51	447.07	0.4	178.83
0.2	5249.76	969.49	0.4	387.79
0.3	5301.25	1497.04	0.4	598.81
0.4	5352.98	2029.75	0.4	811.90
0.5	5404.96	2567.65	0.4	1027.06
0.6	5457.17	3110.75	0.4	1244.30
0.7	5509.62	3659.09	0.4	1463.64
0.8	5562.31	4212.69	0.4	1685.08
0.9	5615.24	4771.57	0.4	1908.63
1	5668.41	5335.75	0.4	2134.30
1.1	5721.82	5905.26	0.4	2362.10
1.2	5775.47	6480.12	0.4	2592.05
1.3	5829.36	7060.37	0.4	2824.15
1.4	5883.49	7646.01	0.4	3058.40
1.5	5937.87	8237.08	0.4	3294.83
1.6	5992.48	8833.59	0.4	3533.44
1.7	6047.33	9435.58	0.4	3774.23
1.8	6102.42	10043.07	0.4	4017.23
1.9	6157.75	10656.08	0.4	4262.43
2	6213.32	11274.63	0.4	4509.85
2.1	6269.13	11898.76	0.4	4759.50
2.2	6325.18	12528.47	0.4	5011.39
2.3	6381.47	13163.80	0.4	5265.52
2.4	6438.00	13804.78	0.4	5521.91
2.5	6494.78	14451.42	0.4	5780.57
2.6	6551.79	15103.75	0.4	6041.50
2.7	6609.04	15761.79	0.4	6304.71
2.8	6666.53	16425.57	0.4	6570.23
2.9	6724.26	17095.10	0.4	6838.04
3	6782.23	17770.43	0.4	7108.17
3.1	6840.44	18451.56	0.4	7380.63
3.2	6898.89	19138.53	0.4	7655.41
3.3	6957.58	19831.35	0.4	7932.54
3.4	7016.51	20530.06	0.4	8212.02
3.5	7075.69	21234.67	0.4	8493.87
3.6	7135.10	21945.21	0.4	8778.08
3.7	7194.75	22661.70	0.4	9064.68
3.8	7254.64	23384.17	0.4	9353.67
3.9	7314.77	24112.64	0.4	9645.06
4	7375.14	24847.13	0.4	9938.85

Lower Infiltration Bed Volume Calculations				
Depth (ft)	Area (ft^2)	Volume (ft^3)	Porosity	Volume of Pore Space (ft^3)
0	1060.83	0.00	0.4	0.00
0.1	1450.97	125.59	0.4	50.24
0.2	1477.68	272.02	0.4	108.81
0.3	1504.64	421.14	0.4	168.46
0.4	1531.83	572.96	0.4	229.18
0.5	1559.27	727.52	0.4	291.01
0.6	1586.94	884.83	0.4	353.93
0.7	1614.86	1044.92	0.4	417.97
0.8	1643.01	1207.81	0.4	483.12
0.9	1671.41	1373.53	0.4	549.41
1	1700.04	1542.10	0.4	616.84
1.1	1728.92	1713.55	0.4	685.42
1.2	1758.03	1887.90	0.4	755.16
1.3	1787.39	2065.17	0.4	826.07
1.4	1816.98	2245.39	0.4	898.15
1.5	1846.82	2428.58	0.4	971.43
1.6	1876.89	2614.76	0.4	1045.90
1.7	1907.21	2803.97	0.4	1121.59
1.8	1937.76	2996.21	0.4	1198.49
1.9	1968.56	3191.53	0.4	1276.61
2	1999.59	3389.94	0.4	1355.98
2.1	2030.87	3591.46	0.4	1436.58
2.2	2062.38	3796.12	0.4	1518.45
2.3	2094.14	4003.95	0.4	1601.58
2.4	2126.13	4214.96	0.4	1685.98
2.5	2158.37	4429.19	0.4	1771.67
2.6	2190.84	4646.65	0.4	1858.66
2.7	2223.56	4867.37	0.4	1946.95
2.8	2256.51	5091.37	0.4	2036.55
2.9	2289.71	5318.68	0.4	2127.47
3	2323.14	5549.32	0.4	2219.73
3.1	2356.82	5783.32	0.4	2313.33
3.2	2390.73	6020.70	0.4	2408.28
3.3	2424.89	6261.48	0.4	2504.59
3.4	2459.28	6505.69	0.4	2602.27
3.5	2493.92	6753.35	0.4	2701.34
3.6	2528.79	7004.48	0.4	2801.79
3.7	2563.91	7259.12	0.4	2903.65
3.8	2599.26	7517.28	0.4	3006.91
3.9	2634.86	7778.98	0.4	3111.59
4	2670.69	8044.26	0.4	3217.70

Appendix C – Sample Elevation-Storage-Outflow Calculation Tables

Elevation-Storage-Outflow Tables 9/27 Storm Event - Storm Specific Infiltration Rate				
Lower Bed				
Elevation (ft)	Storage (ac-ft)	Infiltration (cfs)	Outflow (cfs)	Outflow + Infiltration (cfs)
0	0	0	0	0
0.1	0.001153418	0.0011	0	0.0011
0.2	0.002498252	0.0011	0	0.0011
0.3	0.003867731	0.0011	0	0.0011
0.4	0.005262076	0.0011	0	0.0011
0.5	0.006681507	0.0011	0	0.0011
0.6	0.008126245	0.0011	0	0.0011
0.7	0.009596509	0.0011	0	0.0011
0.8	0.011092521	0.0011	0	0.0011
0.9	0.012614501	0.0011	0	0.0011
1	0.014162669	0.0011	0	0.0011
1.1	0.015737245	0.0011	0	0.0011
1.2	0.01733845	0.0011	0	0.0011
1.3	0.018966505	0.0011	0	0.0011
1.4	0.02062163	0.0011	0	0.0011
1.5	0.022304045	0.0011	0	0.0011
1.6	0.024013971	0.0011	1.6956	1.6967
1.7	0.025751627	0.0011	1.9782	1.9793
1.8	0.027517235	0.0011	2.2608	2.2619
1.9	0.029311016	0.0011	2.5434	2.5445
2	0.031133188	0.0011	2.8260	2.8271
2.1	0.032983973	0.0011	3.1086	3.1097
2.2	0.034863592	0.0011	3.3912	3.3923
2.3	0.036772264	0.0011	3.6738	3.6749
2.4	0.03871021	0.0011	3.9564	3.9575
2.5	0.04067765	0.0011	4.2390	4.2401
2.6	0.042674805	0.0011	4.5216	4.5227
2.7	0.044701896	0.0011	4.8042	4.8053
2.8	0.046759142	0.0011	5.0868	5.0879
2.9	0.048846764	0.0011	5.3694	5.3705
3	0.050964983	0.0011	5.6520	5.6531

Middle Bed				
Elevation (ft)	Storage (ac-ft)	Infiltration (cfs)	Outflow (cfs)	Outflow + Infiltration (cfs)
0	0	0	0	0
0.1	0.004105915	0.0011	0.0298	0.0308
0.2	0.008903762	0.0011	0.0843	0.0853
0.3	0.013748789	0.0011	0.1548	0.1558
0.4	0.018641215	0.0011	0.2030	0.2040
0.5	0.023581261	0.0011	0.2426	0.2437
0.6	0.028569148	0.0011	0.2766	0.2777
0.7	0.033605095	0.0011	0.3069	0.3079
0.8	0.038689324	0.0011	0.3344	0.3355
0.9	0.043822054	0.0011	0.3598	0.3609
1	0.049003506	0.0011	0.3836	0.3846
1.1	0.054233901	0.0011	0.4059	0.4070
1.2	0.059513458	0.0011	0.4271	0.4282
1.3	0.064842399	0.0011	0.4473	0.4484
1.4	0.070220944	0.0011	0.4666	0.4677
1.5	0.075649312	0.0011	0.4852	0.4862
1.6	0.081127726	0.0011	0.5031	0.5041
1.7	0.086656404	0.0011	0.5203	0.5214
1.8	0.092235567	0.0011	0.5370	0.5381
1.9	0.097865437	0.0011	0.5532	0.5543
2	0.103546232	0.0011	0.5689	0.5700
2.1	0.109278174	0.0011	0.5842	0.5853
2.2	0.115061483	0.0011	0.5992	0.6002
2.3	0.12089638	0.0011	0.6137	0.6148
2.4	0.126783084	0.0011	0.6279	0.6290
2.5	0.132721817	0.0011	0.6418	0.6429
2.6	0.138712798	0.0011	0.6555	0.6565
2.7	0.144756249	0.0011	0.6688	0.6698
2.8	0.150852389	0.0011	0.6819	0.6829
2.9	0.157001439	0.0011	0.6947	0.6957
3	0.163203619	0.0011	0.7073	0.7083
3.1	0.16945915	0.0011	0.7197	0.7207
3.2	0.175768253	0.0011	0.7318	0.7329
3.3	0.182131147	0.0011	0.7438	0.7448
3.4	0.188548053	0.0011	0.8449	0.8460
3.5	0.195019191	0.0011	1.0199	1.0210
3.6	0.201544782	0.0011	1.2429	1.2440
3.7	0.208125047	0.0011	1.5048	1.5058
3.8	0.214760205	0.0011	1.8001	1.8011
3.9	0.221450477	0.0011	2.1253	2.1263
4	0.228196084	0.0011	2.4778	2.4788

Upper Bed				
Elevation (ft)	Storage (ac-ft)	Infiltration (cfs)	Outflow (cfs)	Outflow + Infiltration (cfs)
0	0	0	0	0
0.1	0.000002296	0.0011	0	0.0011
0.2	0.000004592	0.0011	0	0.0011
0.3	0.000006888	0.0011	0	0.0011
0.4	0.000009184	0.0011	0	0.0011
0.5	0.00001148	0.0011	0	0.0011
0.6	0.000013776	0.0011	0	0.0011
0.7	0.000016072	0.0011	0	0.0011
0.8	0.000018368	0.0011	0	0.0011
0.9	0.000020664	0.0011	0	0.0011
1	0.00002296	0.0011	0	0.0011
1.1	0.000025256	0.0011	0	0.0011
1.2	0.000027552	0.0011	0	0.0011
1.3	0.000029848	0.0011	0	0.0011
1.4	0.000032144	0.0011	0	0.0011
1.5	0.00003444	0.0011	0	0.0011
1.6	0.000036736	0.0011	0	0.0011
1.7	0.000039032	0.0011	0	0.0011
1.8	0.000041328	0.0011	0	0.0011
1.9	0.000043624	0.0011	0	0.0011
2	0.00004592	0.0011	0	0.0011
2.1	0.000048216	0.0011	0	0.0011
2.2	0.000050512	0.0011	0	0.0011
2.3	0.000052808	0.0011	0	0.0011
2.4	0.000055104	0.0011	0	0.0011
2.5	0.0000574	0.0011	0	0.0011
2.6	0.000059696	0.0011	0	0.0011
2.7	0.000061992	0.0011	0	0.0011
2.8	0.000064288	0.0011	0	0.0011
2.9	0.000066584	0.0011	0	0.0011
3	0.00006888	0.0011	0	0.0011
3.1	0.000071176	0.0011	0	0.0011
3.2	0.000073472	0.0011	0	0.0011
3.3	0.000075768	0.0011	0	0.0011
3.4	0.000078064	0.0011	0	0.0011
3.5	0.00008036	0.0011	0.0894	0.0904
3.6	0.000082656	0.0011	0.2528	0.2538
3.7	0.000084952	0.0011	0.4644	0.4654
3.8	0.000087248	0.0011	0.7149	0.7160
3.9	0.000089544	0.0011	0.9991	1.0002
4	0.00009184	0.0011	1.3134	1.3145

Elevation-Storage-Outflow Tables 9/12 Storm Event - Storm Specific Infiltration Rate				
Lower Bed				
Elevation (ft)	Storage (ac-ft)	Infiltration (cfs)	Outflow (cfs)	Outflow + Infiltration (cfs)
0	0	0	0	0
0.1	0.001153418	0.0020	0	0.0020
0.2	0.002498252	0.0023	0	0.0023
0.3	0.003867731	0.0025	0	0.0025
0.4	0.005262076	0.0028	0	0.0028
0.5	0.006681507	0.0031	0	0.0031
0.6	0.008126245	0.0034	0	0.0034
0.7	0.009596509	0.0037	0	0.0037
0.8	0.011092521	0.0039	0	0.0039
0.9	0.012614501	0.0042	0	0.0042
1	0.014162669	0.0045	0	0.0045
1.1	0.015737245	0.0048	0	0.0048
1.2	0.01733845	0.0051	0	0.0051
1.3	0.018966505	0.0053	0	0.0053
1.4	0.02062163	0.0056	0	0.0056
1.5	0.022304045	0.0059	0	0.0059
1.6	0.024013971	0.0062	1.6956	1.7018
1.7	0.025751627	0.0065	1.9782	1.9847
1.8	0.027517235	0.0067	2.2608	2.2675
1.9	0.029311016	0.0070	2.5434	2.5504
2	0.031133188	0.0073	2.8260	2.8333
2.1	0.032983973	0.0076	3.1086	3.1162
2.2	0.034863592	0.0079	3.3912	3.3991
2.3	0.036772264	0.0081	3.6738	3.6819
2.4	0.03871021	0.0084	3.9564	3.9648
2.5	0.04067765	0.0087	4.2390	4.2477
2.6	0.042674805	0.0090	4.5216	4.5306
2.7	0.044701896	0.0093	4.8042	4.8135
2.8	0.046759142	0.0095	5.0868	5.0963
2.9	0.048846764	0.0098	5.3694	5.3792
3	0.050964983	0.0101	5.6520	5.6621

Middle Bed				
Elevation (ft)	Storage (ac-ft)	Infiltration (cfs)	Outflow (cfs)	Outflow + Infiltration (cfs)
0	0	0	0	0
0.1	0.004105915	0.0020	0.0298	0.0318
0.2	0.008903762	0.0023	0.0843	0.0865
0.3	0.013748789	0.0025	0.1548	0.1573
0.4	0.018641215	0.0028	0.2030	0.2058
0.5	0.023581261	0.0031	0.2426	0.2457
0.6	0.028569148	0.0034	0.2766	0.2800
0.7	0.033605095	0.0037	0.3069	0.3105
0.8	0.038689324	0.0039	0.3344	0.3383
0.9	0.043822054	0.0042	0.3598	0.3640
1	0.049003506	0.0045	0.3836	0.3881
1.1	0.054233901	0.0048	0.4059	0.4107
1.2	0.059513458	0.0051	0.4271	0.4322
1.3	0.064842399	0.0053	0.4473	0.4527
1.4	0.070220944	0.0056	0.4666	0.4723
1.5	0.075649312	0.0059	0.4852	0.4911
1.6	0.081127726	0.0062	0.5031	0.5092
1.7	0.086656404	0.0065	0.5203	0.5268
1.8	0.092235567	0.0067	0.5370	0.5437
1.9	0.097865437	0.0070	0.5532	0.5602
2	0.103546232	0.0073	0.5689	0.5762
2.1	0.109278174	0.0076	0.5842	0.5918
2.2	0.115061483	0.0079	0.5992	0.6070
2.3	0.12089638	0.0081	0.6137	0.6219
2.4	0.126783084	0.0084	0.6279	0.6364
2.5	0.132721817	0.0087	0.6418	0.6505
2.6	0.138712798	0.0090	0.6555	0.6644
2.7	0.144756249	0.0093	0.6688	0.6780
2.8	0.150852389	0.0095	0.6819	0.6914
2.9	0.157001439	0.0098	0.6947	0.7045
3	0.163203619	0.0101	0.7073	0.7174
3.1	0.16945915	0.0104	0.7197	0.7300
3.2	0.175768253	0.0107	0.7318	0.7425
3.3	0.182131147	0.0109	0.7438	0.7547
3.4	0.188548053	0.0112	0.8449	0.8561
3.5	0.195019191	0.0115	1.0199	1.0314
3.6	0.201544782	0.0118	1.2429	1.2547
3.7	0.208125047	0.0121	1.5048	1.5168
3.8	0.214760205	0.0123	1.8001	1.8124
3.9	0.221450477	0.0126	2.1253	2.1379
4	0.228196084	0.0129	2.4778	2.4907

Upper Bed				
Elevation (ft)	Storage (ac-ft)	Infiltration (cfs)	Outflow (cfs)	Outflow + Infiltration (cfs)
0	0	0	0	0
0.1	0.000002296	0.0020	0	0.0020
0.2	0.000004592	0.0023	0	0.0023
0.3	0.000006888	0.0025	0	0.0025
0.4	0.000009184	0.0028	0	0.0028
0.5	0.00001148	0.0031	0	0.0031
0.6	0.000013776	0.0034	0	0.0034
0.7	0.000016072	0.0037	0	0.0037
0.8	0.000018368	0.0039	0	0.0039
0.9	0.000020664	0.0042	0	0.0042
1	0.00002296	0.0045	0	0.0045
1.1	0.000025256	0.0048	0	0.0048
1.2	0.000027552	0.0051	0	0.0051
1.3	0.000029848	0.0053	0	0.0053
1.4	0.000032144	0.0056	0	0.0056
1.5	0.00003444	0.0059	0	0.0059
1.6	0.000036736	0.0062	0	0.0062
1.7	0.000039032	0.0065	0	0.0065
1.8	0.000041328	0.0067	0	0.0067
1.9	0.000043624	0.0070	0	0.0070
2	0.00004592	0.0073	0	0.0073
2.1	0.000048216	0.0076	0	0.0076
2.2	0.000050512	0.0079	0	0.0079
2.3	0.000052808	0.0081	0	0.0081
2.4	0.000055104	0.0084	0	0.0084
2.5	0.0000574	0.0087	0	0.0087
2.6	0.000059696	0.0090	0	0.0090
2.7	0.000061992	0.0093	0	0.0093
2.8	0.000064288	0.0095	0	0.0095
2.9	0.000066584	0.0098	0	0.0098
3	0.00006888	0.0101	0	0.0101
3.1	0.000071176	0.0104	0	0.0104
3.2	0.000073472	0.0107	0	0.0107
3.3	0.000075768	0.0109	0	0.0109
3.4	0.000078064	0.0112	0	0.0112
3.5	0.00008036	0.0115	0.0894	0.1009
3.6	0.000082656	0.0118	0.2528	0.2645
3.7	0.000084952	0.0121	0.4644	0.4764
3.8	0.000087248	0.0123	0.7149	0.7273
3.9	0.000089544	0.0126	0.9991	1.0118
4	0.00009184	0.0129	1.3134	1.3263

Appendix D – Storm List Spreadsheet

Storm Event	Rainfall Start	Rainfall End	Rainfall Duration (hrs)	Max 1 Hour Precip (in)	Rainfall (in)	Intensity (in/hr)	Staying on site (in/area)	Antecedant Dry Time (hrs)
9/12/03	9/12/03 11:10 PM	9/15/03 6:45 PM	67.58	0.52	2.3	0.03	1.89	N/A
9/18/03	9/18/03 2:25 PM	9/19/03 2:55 AM	12.50	0.40	1.27	0.10	1.04	67.67
9/22/03	9/22/03 8:35 PM	9/23/03 12:00 PM	15.42	0.52	0.93	0.06	0.76	65.67
9/27/03	9/27/03 2:15 PM	9/28/03 6:55 AM	16.67	0.54	0.7	0.04	0.57	98.25
10/14/03	10/14/03 8:10 PM	10/15/03 4:25 AM	8.25	0.62	1.35	0.16	1.11	242.58
11/4/03	11/4/03 9:00 PM	11/6/03 10:20 PM	49.33	0.16	0.78	0.02	0.64	150.50
11/12/03	11/12/03 12:20 AM	11/12/03 7:10 AM	6.83	0.12	0.44	0.06	0.36	122.00
11/19/03	11/19/03 5:05 AM	11/20/03 3:40 AM	22.58	0.68	1.64	0.07	1.34	165.92
11/28/03	11/28/03 7:50 AM	11/29/03 2:00 AM	18.17	0.32	0.84	0.05	0.69	79.67
12/9/03	12/9/03 2:50 PM	12/11/03 1:15 PM	46.42	0.26	1.56	0.03	1.28	252.83
12/14/03	12/14/03 12:30 PM	12/14/03 10:35 PM	10.08	0.26	1.06	0.11	0.87	71.25
12/24/03	12/24/03 1:55 AM	12/24/03 3:50 PM	13.92	0.53	1.81	0.13	1.48	152.50
1/4/04	1/4/04 6:20 PM	1/5/04 11:00 PM	28.67	0.12	0.55	0.02	0.45	266.50
4/2/04	4/2/04 11:40 AM	4/3/04 5:35 AM	17.92	0.11	0.84	0.05	0.69	24.00
4/12/04	4/12/04 12:15 PM	4/15/04 2:25 AM	61.83	0.21	2.1	0.03	1.72	20.50
4/23/04	4/23/04 6:10 PM	4/23/04 11:15 PM	5.08	0.43	0.77	0.15	0.63	207.75

Storm Event	Flow Start	Flow End	Outflow Volume (ft^3)	Flow (in/area)	Max Port Depth (in)
9/12/03	9/13/03 8:45 AM	9/15/03 5:50 PM	4.64	0.00	9.81
9/18/03	9/18/03 9:15 PM	9/19/03 3:15 AM	12.57	0.00	11.89
9/22/03	9/23/03 6:20 AM	9/23/03 9:55 AM	7.37	0.00	5.80
9/27/03	9/28/03 12:35 AM	9/28/03 1:35 AM	2.39	0.00	2.83
10/14/03	10/14/03 9:00 PM	10/15/03 3:25 AM	24.92	0.01	8.21
11/4/03	11/5/03 5:30 PM	11/6/03 11:25 PM	4.96	0.00	1.97
11/12/03	11/12/03 1:55 AM	11/12/03 8:20 AM	1.60	0.00	0.92
11/19/03	11/19/03 4:05 PM	11/20/03 4:25 AM	50.55	0.01	11.98
11/28/03	11/28/03 6:15 PM	11/29/03 12:35 AM	19.51	0.00	4.53
12/9/03	12/9/03 2:50 PM	12/11/03 4:05 PM	215.02	0.04	15.86
12/14/03	12/14/03 2:45 PM	12/15/03 4:10 AM	92.22	0.02	12.20
12/24/03	12/24/03 3:40 AM	12/24/03 9:15 PM	137.22	0.03	15.17
1/4/04	1/5/04 3:45 AM	1/5/04 7:00 PM	10.97	0.00	1.08
4/2/04	4/2/04 12:25 PM	4/3/04 1:20 PM	60.39	0.01	8.11
4/12/04	4/12/04 4:05 PM	4/15/2004 7:15	157.11	0.03	13.28
4/23/04	4/23/04 6:40 PM	4/24/04 12:55 AM	24.31	0.01	2.89

Appendix E – Sample Infiltration Rate Calculation Spreadsheets

	Storm Specific Infiltration Rate Calculations for 9/22 Storm Event				
Time	Port Water Height (in)	Port Water Height (ft)	Volume (ft^3)	dV/dt (ft^3/5 min)	Infiltration Outflow (cfs)
0	0.195	0.016	7.926	0	0
5	0.244	0.020	10.194	-2.268	-0.008
10	0.195	0.016	7.926	2.268	0.008
15	0.195	0.016	7.926	0	0
20	0.195	0.016	7.926	0	0
25	0.195	0.016	7.926	0	0
30	0.195	0.016	7.926	0	0
35	0.195	0.016	7.926	0	0
40	0.195	0.016	7.926	0	0
45	0.195	0.016	7.926	0	0
50	0.194	0.016	7.879	0.046	0.000
55	0.194	0.016	7.879	0	0
60	0.243	0.020	10.148	-2.268	-0.008
65	0.194	0.016	7.879	2.268	0.008
70	0.194	0.016	7.879	0	0
75	0.194	0.016	7.879	0	0
80	0.194	0.016	7.879	0	0
85	0.243	0.020	10.148	-2.268	-0.008
90	0.194	0.016	7.879	2.268	0.008
95	0.194	0.016	7.879	0	0
100	0.194	0.016	7.879	0	0
105	0.194	0.016	7.879	0	0
110	0.194	0.016	7.879	0	0
115	0.194	0.016	7.879	0	0
120	0.194	0.016	7.879	0	0
125	0.194	0.016	7.879	0	0
130	0.194	0.016	7.879	0	0
135	0.194	0.016	7.879	0	0
140	0.194	0.016	7.879	0	0
145	0.194	0.016	7.879	0	0
150	0.242	0.020	10.101	-2.222	-0.007
155	0.192	0.016	7.787	2.314	0.008
160	0.193	0.016	7.833	-0.046	0.000
165	0.193	0.016	7.833	0	0
170	0.193	0.016	7.833	0	0
175	0.193	0.016	7.833	0	0
180	0.193	0.016	7.833	0	0
185	0.193	0.016	7.833	0	0
190	0.194	0.016	7.879	-0.046	0.000
195	0.193	0.016	7.833	0.046	0.000
200	0.193	0.016	7.833	0	0
205	0.193	0.016	7.833	0	0
210	0.193	0.016	7.833	0	0
215	0.194	0.016	7.879	-0.046	0.000
220	0.194	0.016	7.879	0	0
225	0.194	0.016	7.879	0	0
230	0.194	0.016	7.879	0	0
235	0.194	0.016	7.879	0	0
240	0.194	0.016	7.879	0	0
245	0.194	0.016	7.879	0	0
250	0.193	0.016	7.833	0.046	0.000
255	0.194	0.016	7.879	-0.046	0.000
260	0.194	0.016	7.879	0	0
265	0.193	0.016	7.833	0.046	0.000
270	0.242	0.020	10.101	-2.268	-0.008
275	0.242	0.020	10.101	0	0
280	0.242	0.020	10.101	0	0
285	0.242	0.020	10.101	0	0
290	0.193	0.016	7.833	2.268	0.008
295	0.242	0.020	10.101	-2.268	-0.008
300	0.242	0.020	10.101	0	0
305	0.242	0.020	10.101	0	0
310	0.242	0.020	10.101	0	0
315	0.193	0.016	7.833	2.268	0.008
320	0.193	0.016	7.833	0	0
325	0.193	0.016	7.833	0	0

	Storm Specific Infiltration Rate Calculations for 9/12 Storm Event				
Time	Port Water Height (in)	Port Water Height (ft)	Volume (ft^3)	dV/dt (ft^3/5 min)	Infiltration Outflow (cfs)
0	0.176	0.015	7.025	0	0
5	0.176	0.015	7.025	0	0
10	0.176	0.015	7.025	0	0
15	0.176	0.015	7.025	0	0
20	0.176	0.015	7.025	0	0
25	0.176	0.015	7.025	0	0
30	0.176	0.015	7.025	0	0
35	0.176	0.015	7.025	0	0
40	0.176	0.015	7.025	0	0
45	0.176	0.015	7.025	0	0
50	0.176	0.015	7.025	0	0
55	0.176	0.015	7.025	0	0
60	0.176	0.015	7.025	0	0
65	0.174	0.015	6.957	0.069	0.000
70	0.173	0.014	6.888	0.069	0.000
75	0.233	0.019	9.681	-2.793	-0.009
80	0.174	0.015	6.957	2.724	0.009
85	0.174	0.015	6.957	0	0
90	0.174	0.015	6.957	0	0
95	0.234	0.020	9.748	-2.792	-0.009
100	0.176	0.015	7.025	2.723	0.009
105	0.176	0.015	7.025	0	0
110	0.234	0.020	9.748	-2.723	-0.009
115	0.176	0.015	7.025	2.723	0.009
120	0.176	0.015	7.025	0	0
125	0.176	0.015	7.025	0	0
130	0.176	0.015	7.025	0	0
135	0.176	0.015	7.025	0	0
140	0.234	0.020	9.748	-2.723	-0.009
145	0.234	0.020	9.748	0	0
150	0.234	0.020	9.748	0	0
155	0.236	0.020	9.816	-0.068	0.000
160	0.177	0.015	7.094	2.722	0.009
165	0.177	0.015	7.094	0	0
170	0.236	0.020	9.816	-2.722	-0.009
175	0.236	0.020	9.816	0	0
180	0.177	0.015	7.094	2.722	0.009
185	0.177	0.015	7.094	0	0
190	0.240	0.020	10.018	-2.924	-0.010
195	0.180	0.015	7.231	2.787	0.009
200	0.180	0.015	7.231	0	0
205	0.237	0.020	9.883	-2.652	-0.009
210	0.179	0.015	7.162	2.721	0.009
215	0.179	0.015	7.162	0	0
220	0.179	0.015	7.162	0	0
225	0.179	0.015	7.162	0	0
230	0.179	0.015	7.162	0	0
235	0.237	0.020	9.883	-2.721	-0.009
240	0.237	0.020	9.883	0	0
245	0.179	0.015	7.162	2.721	0.009
250	0.179	0.015	7.162	0	0
255	0.179	0.015	7.162	0	0
260	0.237	0.020	9.883	-2.721	-0.009
265	0.179	0.015	7.162	2.721	0.009
270	0.179	0.015	7.162	0	0
275	0.179	0.015	7.162	0	0
280	0.179	0.015	7.162	0	0
285	0.179	0.015	7.162	0	0
290	0.179	0.015	7.162	0	0
295	0.237	0.020	9.883	-2.721	-0.009
300	0.179	0.015	7.162	2.721	0.009
305	0.179	0.015	7.162	0	0
310	0.179	0.015	7.162	0	0
315	0.179	0.015	7.162	0	0
320	0.179	0.015	7.162	0	0
325	0.237	0.020	9.883	-2.721	-0.009

Appendix F - Linear Storm Event Graphs and Sample Data Set

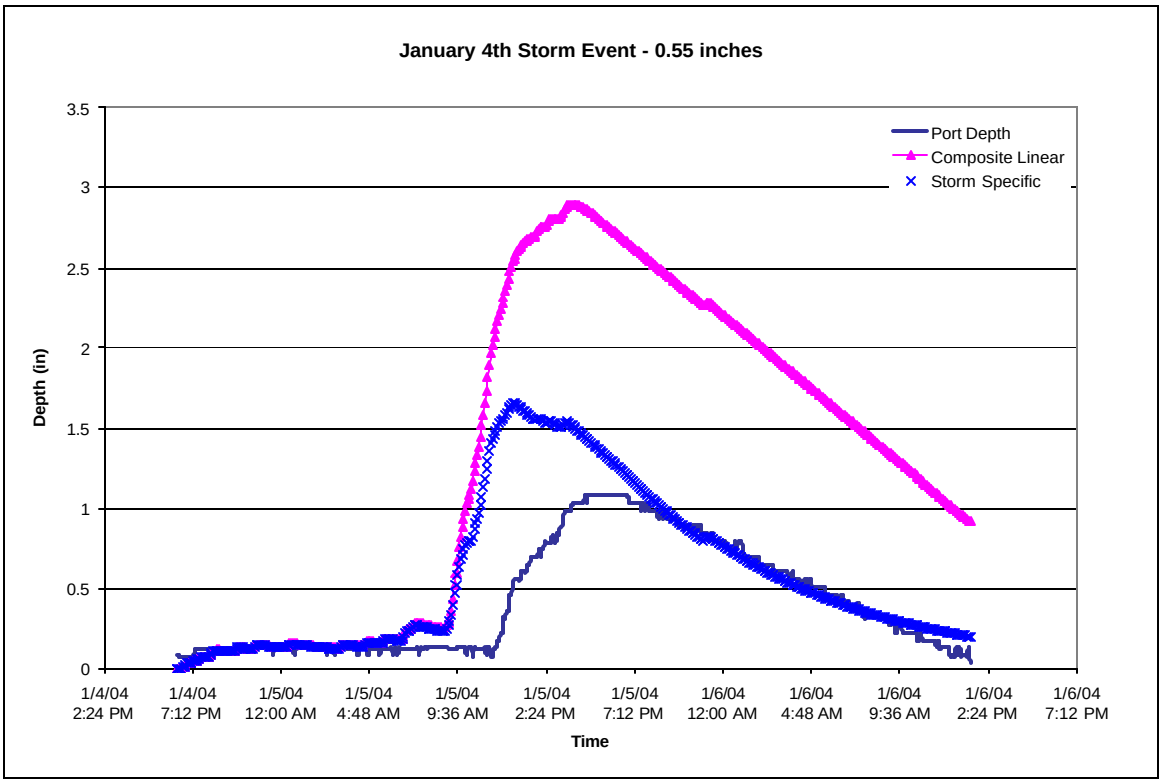

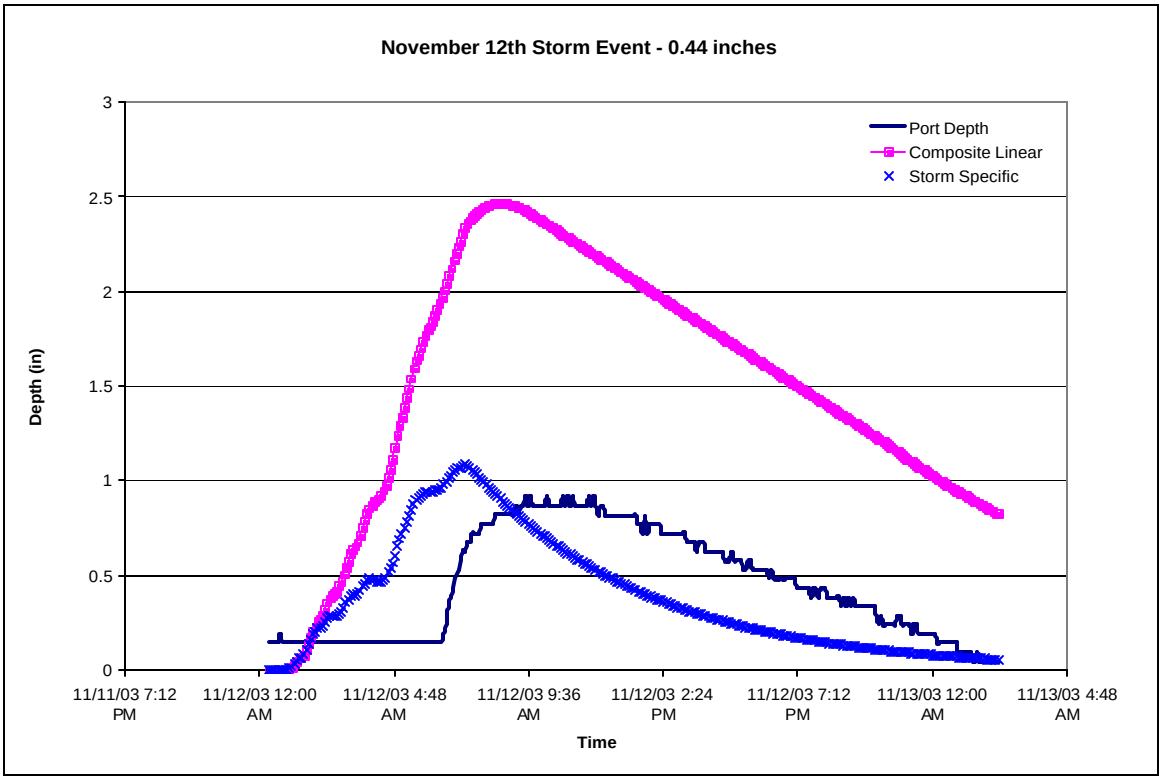

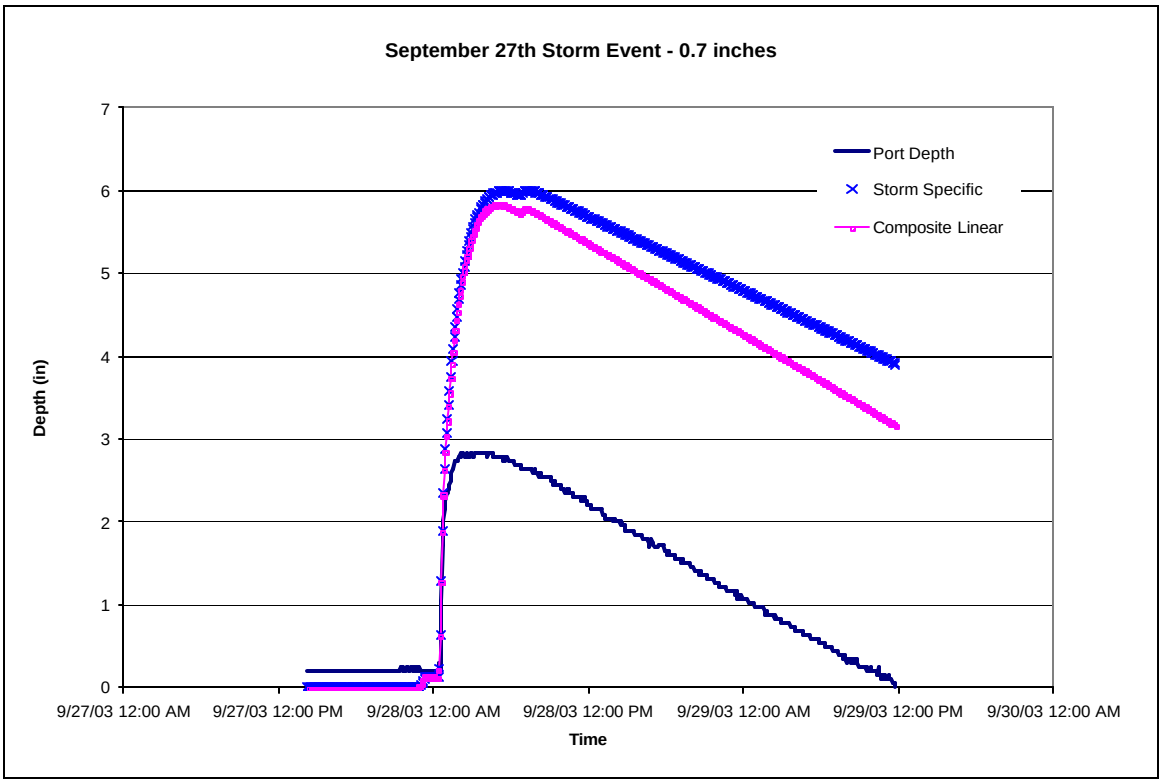
September 27th Storm Event - 0.7 inches
Depth (in)
0
1
2
3
4
5
6
7
9/27/03 12:00 AM
9/27/03 12:00 PM
9/28/03 12:00 AM
9/28/03 12:00 PM
9/29/03 12:00 AM
9/29/03 12:00 PM
9/30/03 12:00 AM
Time
Port Depth
Storm Specific
Composite Linear

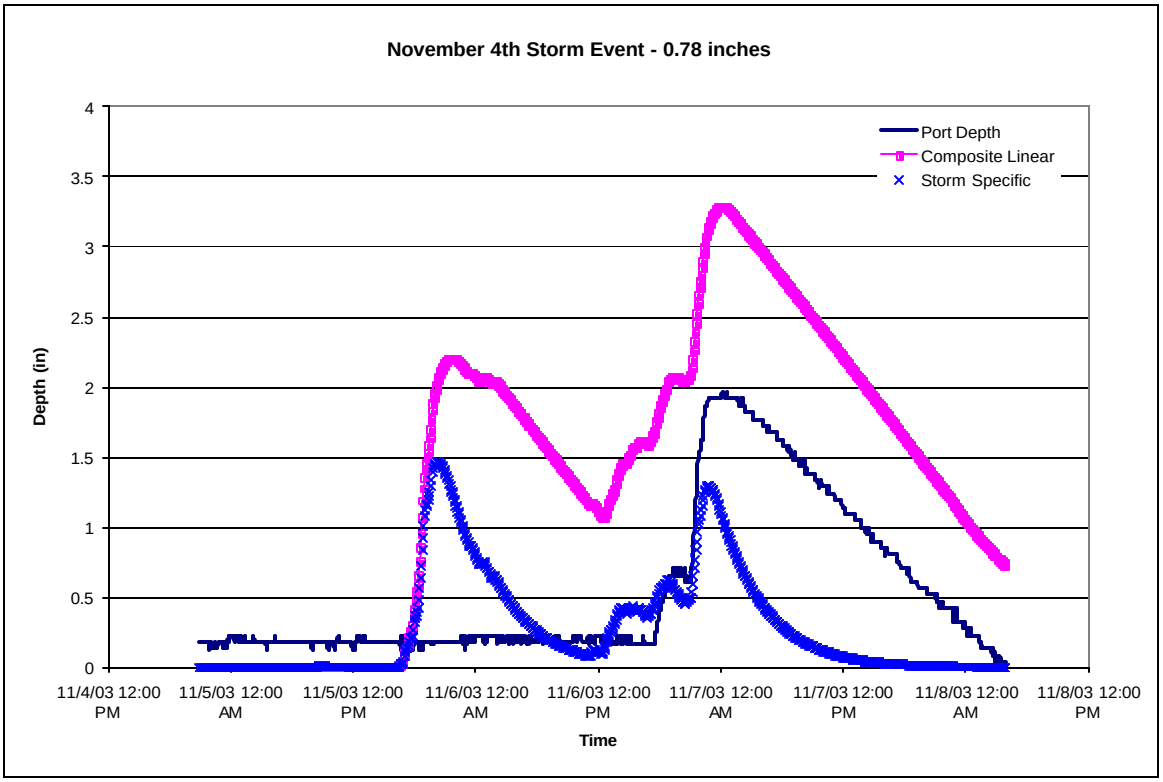
November 4th Storm Event - 0.78 inches
Depth (in)
0
0.5
1
1.5
2
2.5
3
3.5
4
11/4/03 12:00 PM
11/5/03 12:00 AM
11/5/03 12:00 PM
11/6/03 12:00 AM
11/6/03 12:00 PM
11/7/03 12:00 AM
11/7/03 12:00 PM
11/8/03 12:00 AM
11/8/03 12:00 PM
Time
Port Depth
Composite Linear
Storm Specific

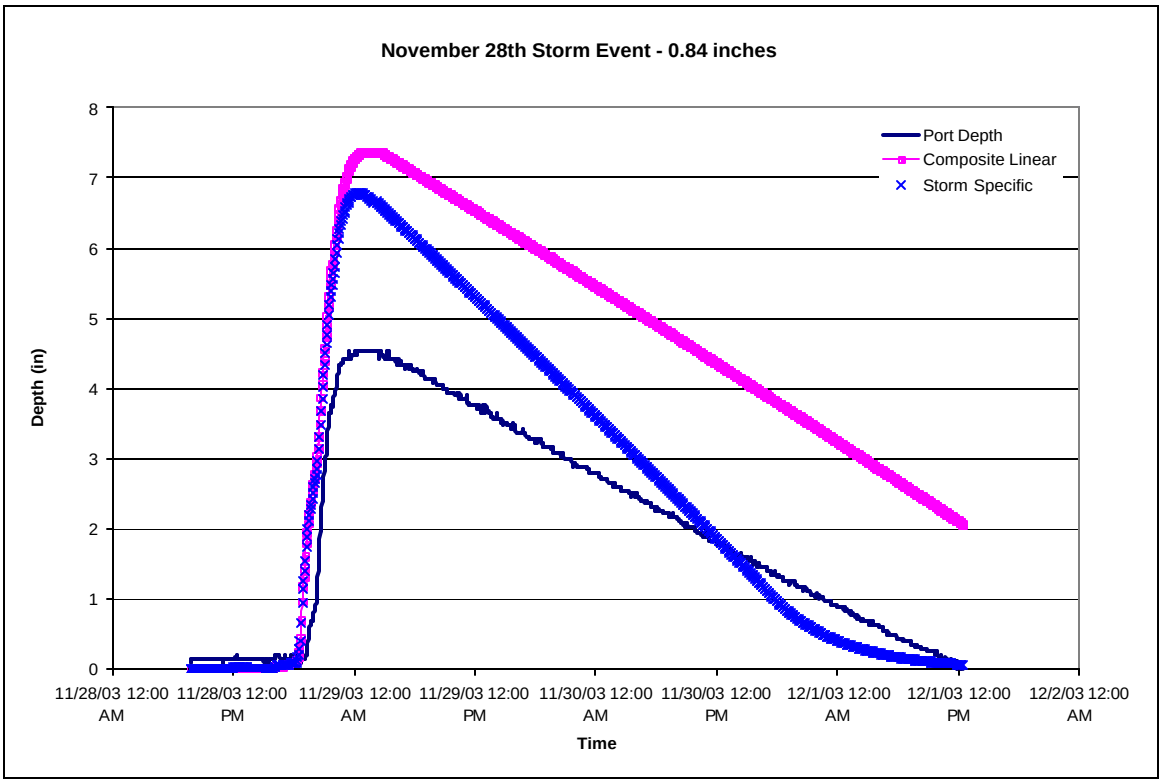
November 28th Storm Event - 0.84 inches
Depth (in)
0
1
2
3
4
5
6
7
8
11/28/03 12:00 AM
11/28/03 12:00 PM
11/29/03 12:00 AM
11/29/03 12:00 PM
11/30/03 12:00 AM
11/30/03 12:00 PM
12/1/03 12:00 AM
12/1/03 12:00 PM
12/2/03 12:00 AM
Time
Port Depth
Composite Linear
Storm Specific

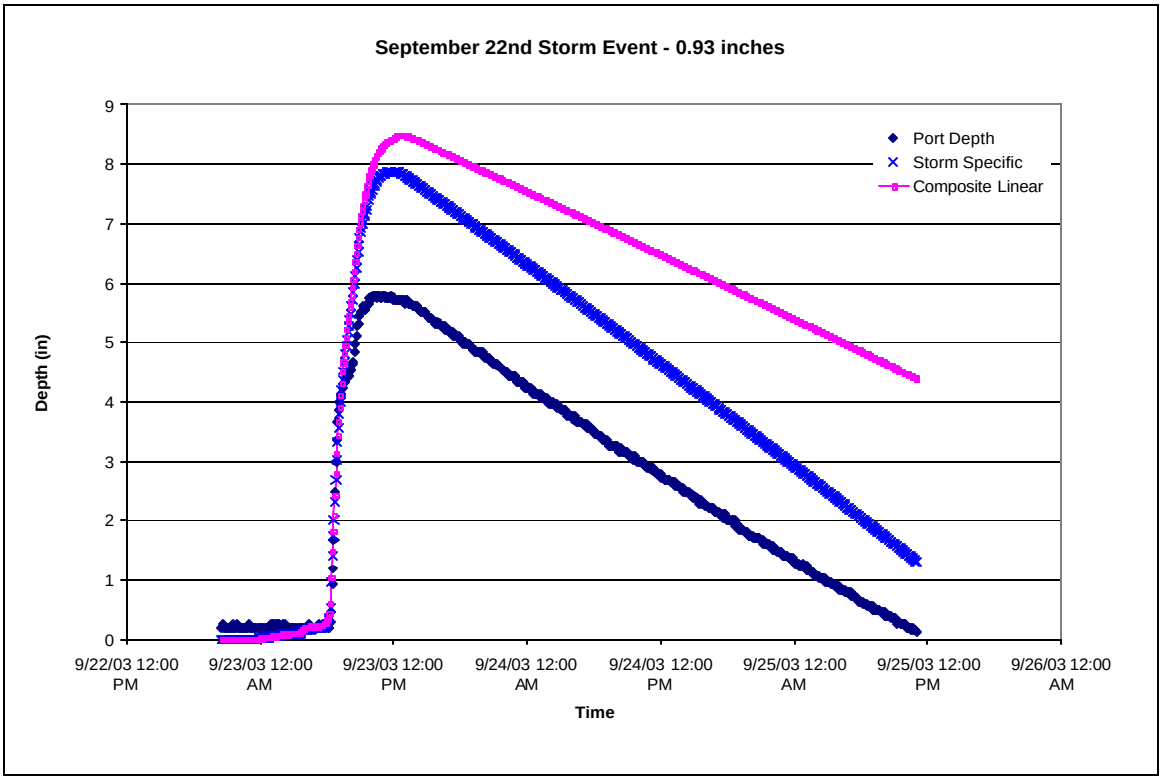
September 22nd Storm Event - 0.93 inches
Depth (in)
0
1
2
3
4
5
6
7
8
9
9/22/03 12:00 PM
9/23/03 12:00 AM
9/23/03 12:00 PM
9/24/03 12:00 AM
9/24/03 12:00 PM
9/25/03 12:00 AM
9/25/03 12:00 PM
9/26/03 12:00 AM
Time
Port Depth
Storm Specific
Composite Linear

Appendix G - Polynomial Storm Event Graphs and Sample Data Set

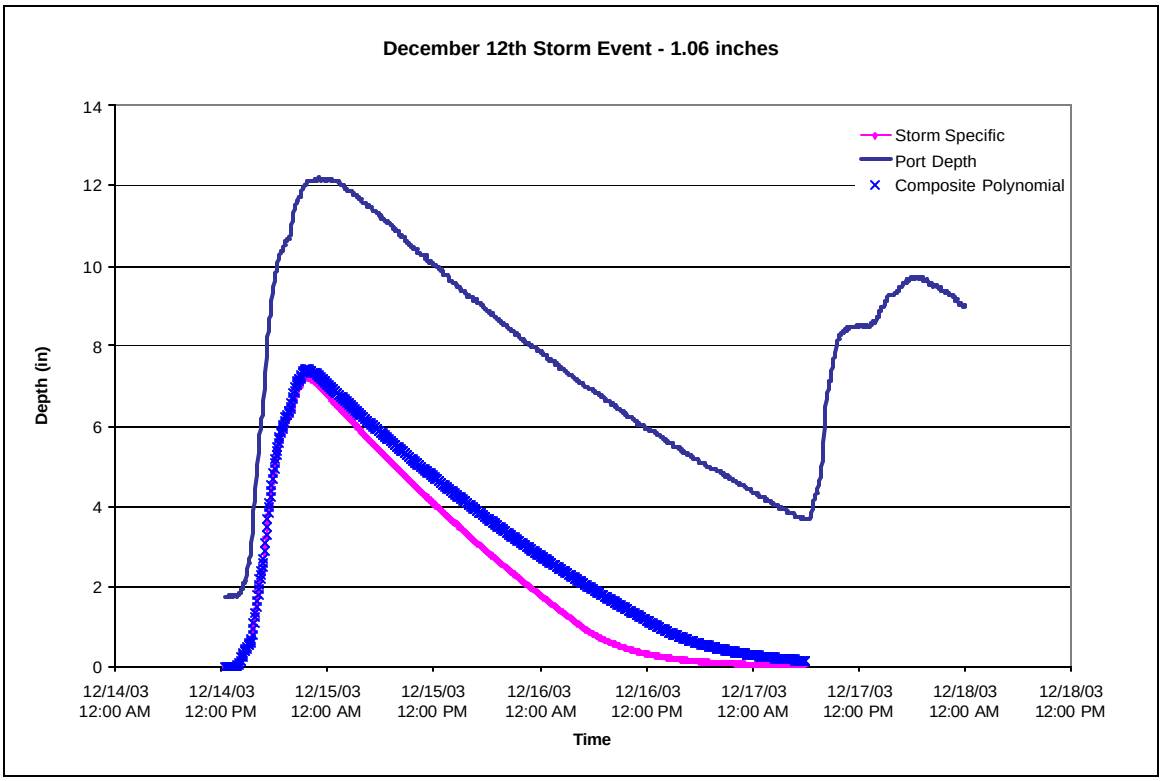

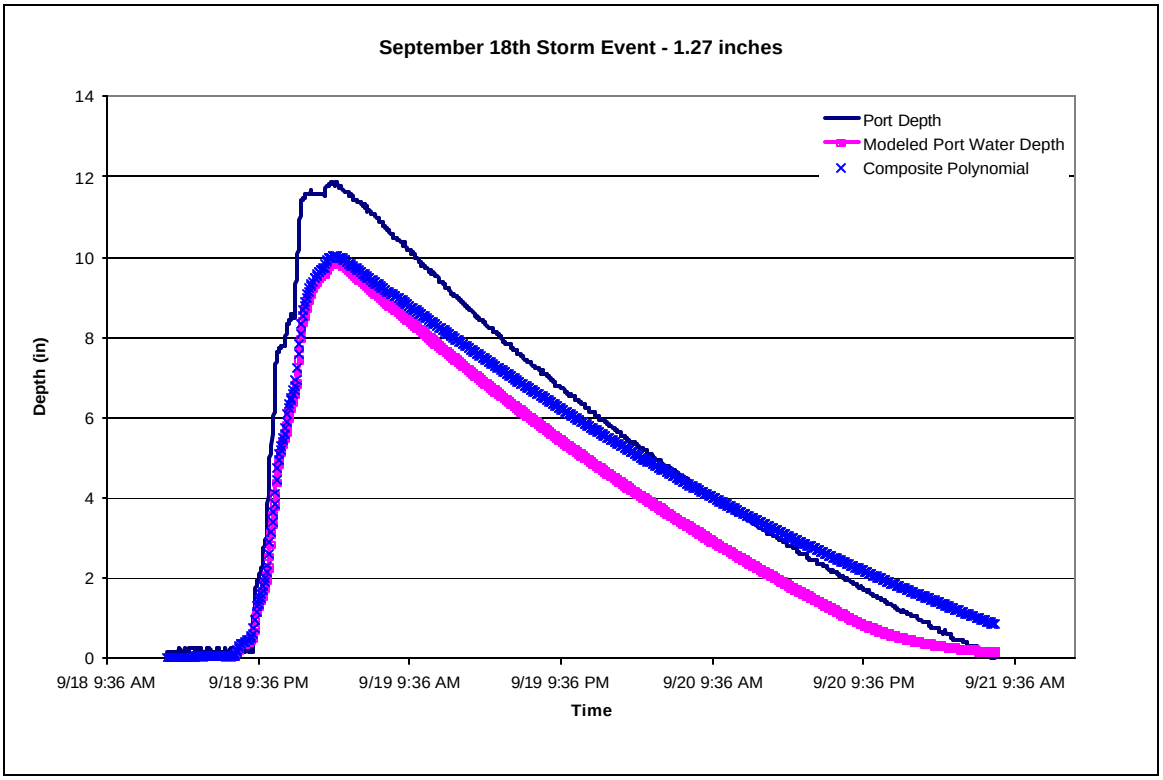

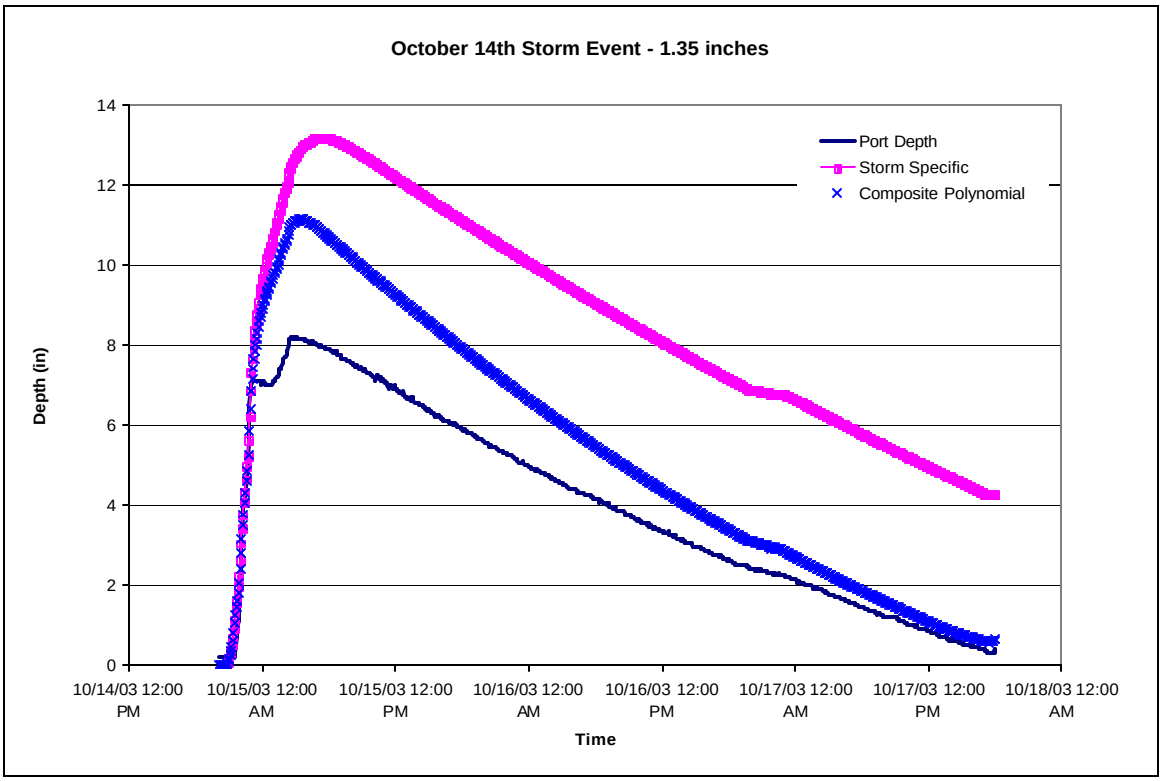
October 14th Storm Event - 1.35 inches
Depth (in)
0
2
4
6
8
10
12
14
10/14/03 12:00 PM
10/15/03 12:00 AM
10/15/03 12:00 PM
10/16/03 12:00 AM
10/16/03 12:00 PM
10/17/03 12:00 AM
10/17/03 12:00 PM
10/18/03 12:00 AM
Time
Port Depth
Storm Specific
Composite Polynomial

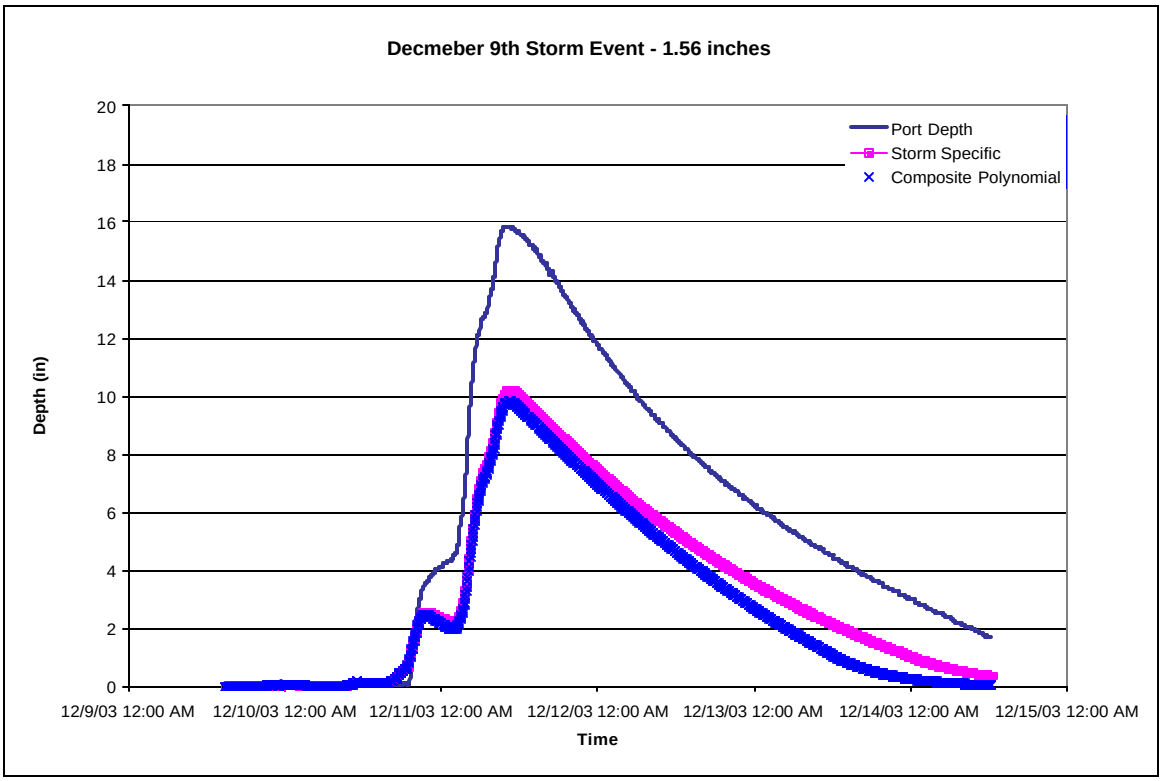
Decmeber 9th Storm Event - 1.56 inches
Depth (in)
0
2
4
6
8
10
12
14
16
18
20
12/9/03 12:00 AM
12/10/03 12:00 AM
12/11/03 12:00 AM
12/12/03 12:00 AM
12/13/03 12:00 AM
12/14/03 12:00 AM
12/15/03 12:00 AM
Time
Port Depth
Storm Specific
Composite Polynomial

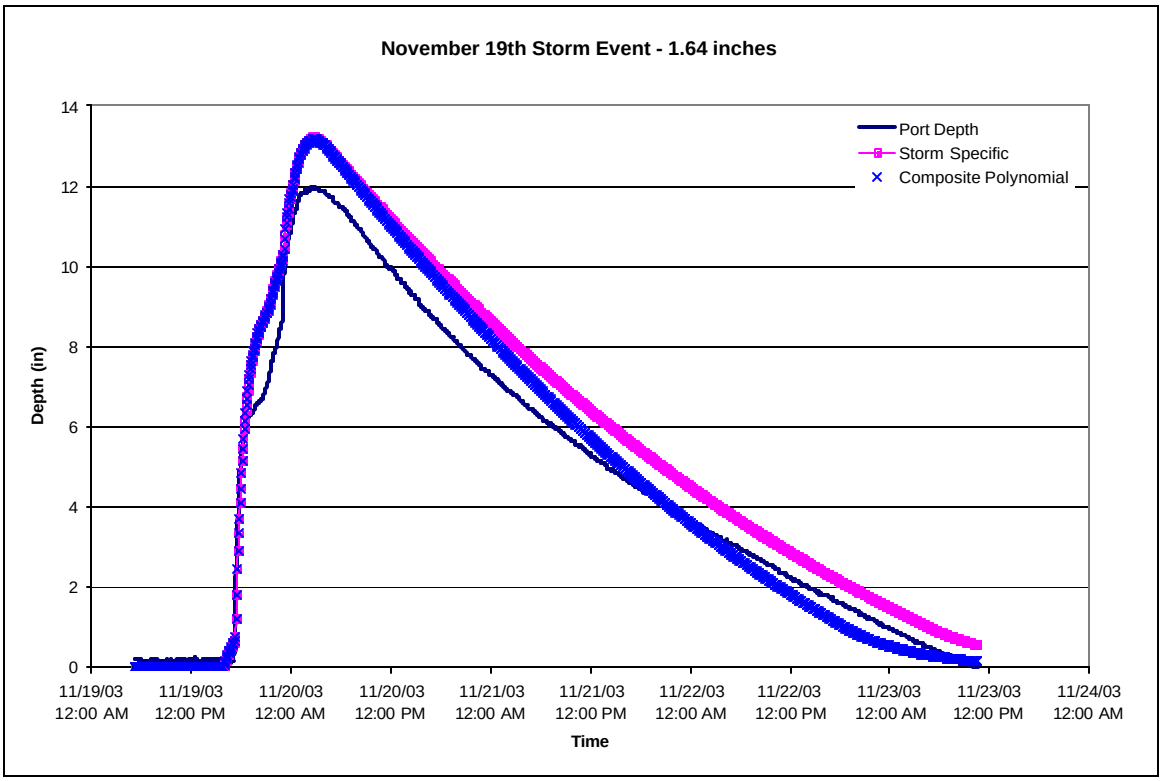
November 19th Storm Event - 1.64 inches
Port Depth
Storm Specific
Composite Polynomial
Depth (in)
0
2
4
6
8
10
12
14
11/19/03 12:00 AM
11/19/03 12:00 PM
11/20/03 12:00 AM
11/20/03 12:00 PM
11/21/03 12:00 AM
11/21/03 12:00 PM
11/22/03 12:00 AM
11/22/03 12:00 PM
11/23/03 12:00 AM
11/23/03 12:00 PM
11/24/03 12:00 AM
Time

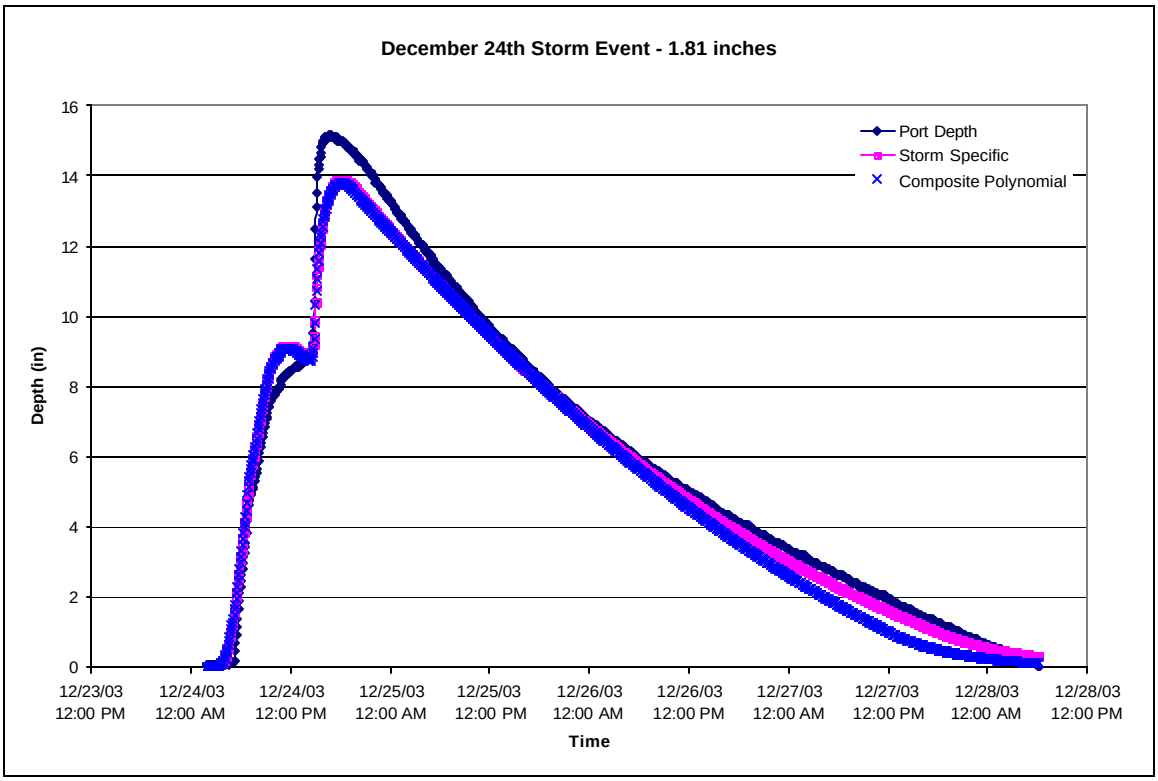
December 24th Storm Event - 1.81 inches
Port Depth
Storm Specific
Composite Polynomial
Depth (in)
0
2
4
6
8
10
12
14
16
12/23/03 12:00 PM
12/24/03 12:00 AM
12/24/03 12:00 PM
12/25/03 12:00 AM
12/25/03 12:00 PM
12/26/03 12:00 AM
12/26/03 12:00 PM
12/27/03 12:00 AM
12/27/03 12:00 PM
12/28/03 12:00 AM
12/28/03 12:00 PM
Time

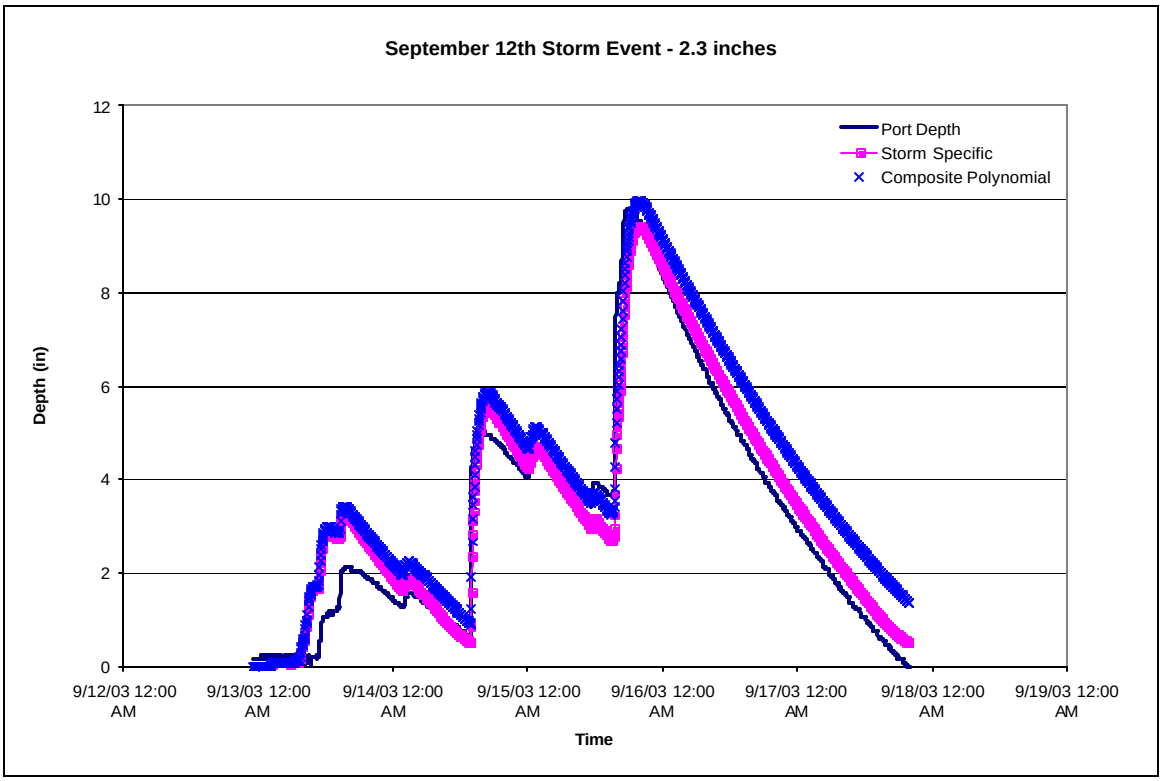
September 12th Storm Event - 2.3 inches
Depth (in)
12
10
8
6
4
2
0
Port Depth
Storm Specific
Composite Polynomial
9/12/03 12:00 AM
9/13/03 12:00 AM
9/14/03 12:00 AM
9/15/03 12:00 AM
9/16/03 12:00 AM
9/17/03 12:00 AM
9/18/03 12:00 AM
9/19/03 12:00 AM
Time